NATIONAL TRANSPORTATION SAFETY BOARD
Office of Aviation Safety
Washington, D.C. 20594

July 3, 2017

<u>**POWERPLANT GROUP CHAIRMAN'S FACTUAL REPORT**</u>

NTSB No: DCA17FA021

A.   ACCIDENT

Location: Chicago O'Hare International Airport, Chicago, Illinois

Date: October 28, 2016

Time: 14:32 central daylight time (CDT)

Aircraft: American Airlines, Boeing 767-323, registration number N345AN, flight number 383

B.   POWERPLANT GROUP

Safety Board Powerplant Group Chairman: Jean-Pierre Scarfo
                                             Powerplant Lead Engineer
                                             Washington D.C.

General Electric Member: Dan Kemme
                                             Consulting Engineer -Aviation Safety Lead
                                             Cincinnati, Ohio

Boeing Member: Van Winters
                                             Propulsion Safety
                                             Seattle, Washington

Federal Aviation Administration Member: Herman Mak
                                             Aerospace Engineer
                                             Burlington, Massachusetts

American Airlines Member: Daniel Morgan
                                             Engineer – CF6-80C2 Powerplants Engineering
                                             Tulsa, Oklahoma

ATI Specialty Materials Member: Anthony Banik
                                             Vice President of Technology and R&D
                                             Monroe, North Carolina

C.   SUMMARY

On October 28, 2016, at about 14:32 central daylight time, an American Airlines (AA) flight number 383, a Boeing B767-300, registration number N345AN, powered by two General Electric (GE) CF6-80C2B6 turbofan engines, experienced a right engine (No. 2) uncontained high pressure turbine failure and subsequent fire during the takeoff ground roll on runway 28R at the Chicago O'Hare International Airport (ORD), Chicago, Illinois. The flightcrew aborted the takeoff, stopped the aircraft on runway 28R with about 3,700 feet of runway remaining, and evacuated the airplane. The right engine, the right wing, and portions of the right fuselage experienced fire damage and impact damage from exiting engine debris. Aircraft rescue and firefighting (ARFF) extinguished the fire after the evacuation started; according to ARFF, the first foam application was within two minutes and 51 seconds after notification. Of the 161 passengers and 9 crew members onboard, one passenger received serious injuries during the evacuation and the airplane was substantially damaged as a result of the fire. A piece of the high pressure turbine stage 2 disk penetrated through the inboard section of the right wing and was recovered in a United Parcel Service (UPS) warehouse about 2,935 feet away. The flight was operating under the provisions of 14 *Code of Federal Regulations* (CFR) Part 121 flight from ORD to Miami International Airport (MIA).

Examination of the right engine revealed that the high pressure turbine stage 2 disk, serial number MUNBB592, experienced a rotor burst/separation. Fragments of the ruptured high pressure turbine stage 2 disk as well as blade and vane fragments: 1) penetrated through the high pressure turbine case and right engine nacelle structure, 2) one disk segment impacted and penetrated through the right wing creating two distinct holes, 3) small fragments impacted the right side of the fuselage, 4) small fragments impacted right and left landing gear doors, 5) small fragments impacted and penetrated the left engine nacelle with no engine damage observed, and 6) one disk segment along with smaller fragments created multiple impact scars and gouges into runway 28R. The high pressure turbine stage 2 disk ruptured/separated into four pieces and about 96% of the entire disk was recovered. Three of the four disk fragments were recovered on the airport property north (outboard of the right engine) of runway 28R between 475-feet to 1,365-feet from the location of the airplane on the runway when the engine failure occurred. The larger and heavier pieces travelled the farthest away. The fourth fragment, which was also the second largest weighing approximately 58 pounds and representing almost 40% of the entire disk, was recovered on the airport property at the UPS warehouse. This disk fragment penetrated through the UPS building roof; no persons were injured.

The NTSB Materials Laboratory in Washington D.C. as well the GE Aviation Materials Laboratory facility in Evendale, Ohio conducted a metallurgical examination of the high pressure turbine stage 2 disk fragments. The results of the metallurgical examination revealed a subsurface production material anomaly located near the bore of the disk from which multiple cracks initiated; cracks propagated in a manner consistent with low-cycle fatigue, both radially inward toward the disk bore, as well as radially outward toward the disk blade slots. Metallographic examination indicated no apparent voids/cracks between the anomaly and the rest of the parent material matrix. The NTSB and GE conducted striation density estimates, a technique to estimate the approximate number of stress cycles from crack initiation to failure on the various cracks initiating and propagating from the production material anomaly. A review of the maintenance records indicated that American Airlines had inspected the event disk using an eddy current inspection technique 3,057 cycles prior to the event; eddy current inspection is essentially a surface and near-surface inspection. Since the crack initiation was subsurface, the various cracks propagated in different and opposite directions from the material anomaly, and with the initiation times for each crack unknown, it could not be positively determined when any of the cracks breached the disk surface. Evaluation of the cracks revealed a steep decrease in striation density as the cracks progressed away from the origin, which GE stated was consistent with higher alternating stress, low-cycle fatigue crack propagation mechanisms. The fracture surface beyond the striated region had a dimpled morphology, consistent with tensile overload.

The high pressure turbine stage 2 disk was made of Inconel® alloy 718; bulk chemistry and hardness traverses confirmed that the parent material met the chemistry and hardness requirements. Additional analysis of the material anomaly identified it as a 'discrete white spot' that is associated with a step in the ingot production process. The material anomaly was further classified as a 'discrete dirty white spot' due to its composition; 'discrete dirty white spots' are associated with clusters of micron-sized oxide, nitride, and/or carbonitride particulates. The disk was produced using a triple-melt process that incorporated vacuum induction melting (this first process is often referred to as the Master Heat), electroslag remelting, and vacuum arc remelting in that order to create the ingot. The ingot went through a mechanical and thermal conversion process to create the billet; it is from the billet that the final forged disk was produced. Historical production and testing results on the triple-melt process indicate that the 'discrete dirty white spot' is an inherent infrequent characteristic of the vacuum arc remelting process.

TDY Industries, LLC, doing business as ATI Specialty Materials, was the melter (supplier) that created the ingot/billet from which the event high pressure turbine stage 2 disk was forged. From Master Heat FA94, five ingots/billets were produced and identified as FA94-1, FA94-2, FA94-3, FA94-4, and FA94-5; FA94-2 was the ingot/billet from which the event disk was manufactured. Review of the ATI production records for Master Heat FA94 did not reveal or identify any material anomalies or deviations from the approved process. GE conducted a review of ATI production records for other Master Heats created at the same time as the event Master Heat FA94 and found no evidence to suggest that the event Master Heat FA94 was processed any differently to account for the 'dirty white spot'. A review of the production records for FA94-2 did not reveal or identify any anomalies or deviations from the approved process nor any anomalies in the material.

Thirty-six parts, including the failed event disk, serial number MUNBB592, were produced from Master Heat FA94. Eight parts (not including the failed disk) from Master Heat FA94 were either in flying status, available for installation into an engine/airplane, or were scrapped but not yet destroyed; all eight were sent to GE for inspection. GE performed high-resolution ultrasonic inspections on all eight parts and found no defects. The high-resolution ultrasonic inspection technique employed by GE has a greater detection sensitivity than what was available at the time the event billet and disk were produced. The remaining 27 pieces (not including the event disk) produced from Master Heat FA94 were either scrapped (19 prior to the event) or in industrial power generation applications and were not removed for inspection (8).

Based on this event, GE plans to issue two service bulletins: Service Bulletin 72-1562 for the CF6-80C2 engine model and Service Bulletin 72-0869 for the CF6-80A engine model. Service Bulletin 72-1562 calls for an ultrasonic inspection of all CF6-80C2 high pressure turbine stage 1 and 2 disks produced before the year 2000. Since HPT stage 2 disks used in the CF6-80C2 engine can also be used on the CF6-80A (dual certificated), Service Bulletin 72-0869 will incorporate the same inspection requirements (ultrasonic inspection) and subpopulation (disks produced before the year 2000) as planned for Service Bulletin 72-1572. Service Bulletins 72-1562 and Service Bulletin 72-0869 are anticipated to be released by the end of June 2017 and August 2017, respectively. The Federal Aviation Administration has indicated that it may issue Airworthiness Directives mandating the intent of the service bulletins to ultrasonically inspect all CF6-80C2 high pressure turbine stage 1 and 2 disks produced before the year 2000 and CF6-80A high pressure turbine stage 2 disks produced before the year 2000. Two criteria defined this subset of Inconel® alloy 718 parts subjected to the ultrasonic inspection. One, GE performed an extensive study of ultrasonic inspection indication rates from the mid-1990s to 2016 from their suppliers of Inconel® alloy 718 and concluded that there were noticeable improvements in product cleanliness (fewer indications) in the year 2000 and later due to process improvements implemented prior to that timeframe. Two, a stress/volume assessment

showed that the CF6-80C2 high pressure stage 1 and 2 disks have similar stress/volume characteristics, so GE decided to inspect the stage 1 disk in addition to the stage 2 disk. Additionally, both disks are exposed at shop visit facilitating their inspection.

TABLE OF CONTENTS

TABLE OF PHOTOS

TABLE OF FIGURES

TABLE OF TABLES

TABLE OF CHARTS

TABLE OF ACRONYMS

°C	TEMPERATURE IN DEGREE CELSIUS
AA	AMERICAN AIRLINES
AC	ADVISORY CIRCULAR
AC	AIR CONDITIONING
AC	ALTERNATING CURRENT
ACC	ACTIVE CLEARANCE CONTROL
AD	AIRWORTHINESS DIRECTIVE
AIA	AEROSPACE INDUSTRIES ASSOCIATION
ALF	AFT LOOKING FORWARD
ALS	AIRWORTHINESS LIMITATION SECTION
AMOC	ALTERNATE MEANS OF COMPLIANCE
AOW	ALL OPERATORS WIRE
ARFF	AIRCRAFT RESCUE AND FIRE FIGHTING
ASM	AMERICAN SOCIETY FOR METALS
ASNT	AMERICAN SOCIETY OF NON-DESTRUCTIVE TESTING
ATI	ALLEGHENY TECHNOLOGIES INCORPORATED
CAAM	CONTINUED AIRWORTHINESS ASSESSMENT METHODOLOGIES
CDT	CENTRAL DAYLIGHT TIME
CFR	CODE OF FEDERAL REGULATIONS
CRF	COMPRESSOR REAR FRAME
CSN	CYCLES SINCE NEW
DAC	DISTANCE-AMPLITUDE CORRECTION
DC	DIRECT CURRENT
DDWS	DISCRETE DIRTY WHITE SPOT OR DIRTY DISCRETE WHITE SPOT
DM	DOUBLE-MELT
DWS	DIRTY WHITE SPOT
ECI	EDDY CURRENT INSPECTION
ECO	ENGINE CERTIFICATION OFFICE
ECS	ENVIRONMENTAL CONTROL SYSTEM
EHM	ENGINE HEAVY MAINTENANCE
EM	ENGINE MANUAL
ESM	ENGINE SHOP MANUAL
ESN	ENGINE SERIAL NUMBER
ESR	ELECTROSLAG REMELTING
ETC	ENGINE TITANIUM CONSORTIUM
FAA	FEDERAL AVIATION ADMINISTRATION
FBH	FLAT BOTTOM HOLE
FDR	FLIGHT DATA RECORDER
FOD	FOREIGN OBJECT DEBRIS
FPI	FLUORESCENT PENETRANT INSPECTION
FSH	FULL SCREEN HEIGHT
GE	GENERAL ELECTRIC
GFM	GESELLSCHAFT FÜR FERTIGUNGSTECHNIK UND MASCHINENBAU
GPS	GLOBAL POSITIONING SATELLITE
HMU	HYDROMECHANICAL UNIT
HPC	HIGH PRESSURE COMPRESSOR
HPSOV	HIGH PRESSURE SHUTOFF VALVE
HPT	HIGH PRESSURE TURBINE
HRC	ROCKWELL HARDNESS "C" SCALE
HSC	HOT SECTION/COMPRESSOR
ICA	INSTRUCTIONS FOR CONTINUED AIRWORTHINESS
IDG	INTEGRATED DRIVE GENERATOR
LCF	LOW-CYCLE FATIGUE
LE	LEADING EDGE

LPC	LOW PRESSURE COMPRESSOR
LPT	LOW PRESSURE TURBINE
MHz	MEGAHERTZ
MIA	MIAMI INTERNATIONAL AIRPORT
MIL-STD	MILITARY STANDARD
mm	MILLIMETER
MOM	MULTI-OPERATOR MESSAGE
MRB	MATERIAL REVIEW BOARD
MTU	MOTOREN-UND TURBINEN-UNION GMBH
N1	FAN/LOW ROTOR SPEED
N2	HIGH-ROTOR SPEED
NAS	NATIONAL AEROSPACE STANDARD
NDI	NON-DESTRUCTIVE INSPECTION
NDT	NON-DESTRUCTIVE TESTING
NTSB	NATIONAL TRANSPORTATION SAFETY BOARD
OEM	ORIGINAL EQUIPMENT MANUFACTURER
OJT	ON THE JOB
ORD	CHICAGO O'HARE INTERNATIONAL AIRPORT
PAUT	PHASED ARRAY ULTRASONIC INSPECTION
PN	PART NUMBER
PRSOV	PRESSURE REGULATING AND SHUTOFF VALVE
RIP	RELIABILITY IMPROVEMENT PROGRAM
RISC	ROTOR INTEGRITY STEERING COMMITTEE
ROMAN	ROTOR MANUFACTURING
SB	SERVICE BULLETIN
SN	SERIAL NUMBER
SPM	STANDARD PRACTICES MANUAL
SPMC	SPECIALTY METAL PROCESS CONSORTIUM
TCDS	TYPE CERTIFICATE DATA SHEET
TE	TRAILING EDGE
TI	TECHNICAL INSTRUCTION
TM	TRIPLE-MELT
TR	THRUST REVERSER
TRF	TURBINE REAR FRAME
TSLSV	TIME SINCE LAST SHOP VISIT
TSN	TIME SINCE NEW
UPS	UNITED PARCEL SERVICE
UT	ULTRASONIC TEST
UTI	ULTRASONIC TEST INSPECTION
VAR	VACUUM ARC REMELTING
VIM	VACUUM INDUCTION MELTING
WDS	WAVELENGTH DISPERSIVE X-RAY SPECTROSCOPY
WG	WYMAN-GORDON
WS	WHITE SPOT

TABLE OF DEFINITIONS

Definitions are from the FAA advisory circular (AC) 33.15-2 *Manufacturing Process for Premium Quality Nickel Alloy for Engine Rotating Parts* dated February 4, 2011 unless otherwise cited.

CONVERSION	The hot working of a case ingot to refine the grain structure and provide an intermediate shape (billet or bar) which becomes input material for subsequent forging.
COUPLANT	A substance, usually a liquid or gel, that is applied to the transducer match layer to facilitate the transmission of the acoustic wave from the transducer to the material being inspected.
CRITICAL ROTATING PARTS	Rotor structural parts (such as disks, spools, spacers, hubs, and shafts), the failure of which could result in a hazardous engine condition. In this context, a hazardous engine condition should be interpreted as the conditions described in FAR Part 33.75. The FAA considers such parts as Priority Parts for the purposes of production certification and surveillance. (Aerospace Industries Association Rotor Manufacturing Project (RoMan) Report October 24, 2002) (DOT/FAA/AR-06/3 February 2006)
CRITICAL ROTATING PARTS	Rotating parts whose primary failure is identified by FMEA as immediately leading to a potential hazardous engine condition should be designated as CRITICAL or some other suitable designation such as FLIGHT SAFETY PART or LIFE CONTROLLED PART. This designation should be conveyed to all parties involved in the processing of the part. (DOT/FAA/AR-06/3 February 2006)
ELECTRO SLAG REMELTING	A remelting process comprised of a conditioned consumable electrode, an electrical resistance heated refining slag, and a solidifying ingot contained in a water-cooled crucible. The ingot may be an intermediate form for subsequent VAR or a final form for conversion to product.
ELECTRODE	The consumable feedstock form for ESR or VAR.
MACROETCH	Chemical treatment of a metal surface to accentuate structural details and anomalies for visual observation. Macroetch surfaces are usually reviewed and rated visually with no magnification.
MASTER ALLOY	Refined product used for some raw materials to aid in VIM melting. For example, a high melting point metal such as niobium may be alloyed with nickel to produce a nickel-niobium master alloy with a melting point near that of the superalloy being produced.
SEGREGATION	Region in the alloy product containing an abnormal content of alloying elements.
SLAG/FLUX	A precisely defined mixture of metal oxides and fluorides used in the ESR process. The composition is selected for a combination of melting point, viscosity, electrical resistivity, refining capability and ability to produce a uniform ingot surface.
VACUUM ARC REMELTING	Process comprised of a conditioned consumable electrode and a solidifying ingot in an enclosed water-cooled crucible with an applied vacuum. An electrical arc generates the heat that melts the electrode.
VACUUM INDUCTION MELTING	Process used to melt, homogenize and refine raw materials and convert them to cast consumable electrodes for subsequent remelting by the ESR or VAR processes.
WHITE SPOT	Region of negative alloy segregation during the remelting process-often defined as a characteristic light etching spot during the macroetching process. Such area may be detrimental to properties, especially if they contain concentrations of inclusions.

D.   DETAILS OF THE INVESTIGATION

1.0   ENGINE AND AIRPLANE INFORMATION

1.1   ENGINE DESCRIPTION

Two GE CF6-80C2B6 turbofan engines (**FIGURE 1**) powered the accident airplane. The CF6-80C2B6 is a dual-rotor, variable stator, high bypass ratio turbofan engine. Main bearings in three frames support the dual coaxial rotor design. The frames are interconnected by stator cases for structural support. The low-speed rotor (N1) consists of the large diameter fan and four low pressure compressor (LPC) booster stages, interconnected to a five-stage low pressure turbine (LPT) rotor by a tubular fan mid shaft turning coaxially inside the high-speed rotor cavity. The high-speed rotor (N2), consisting of a fourteen-stage high pressure compressor (HPC) and a two-stage high pressure turbine (HPT), is located between the fan rotor and the LPT rotor. According to the engine's FAA Type Certificate Data Sheet (TCDS) E13NE, Revision 26, dated September 11, 2014, the CF6-80C2B6 has a maximum takeoff thrust rating of 60,070 pounds and a maximum continuous thrust rating of 56,100 pounds, with the maximum thrust flat-rated[1] to 77°F (25°C) and maximum continuous thrust flat-rated to 86°F (30°C).

FIGURE 1: GENERIC GE CF6-80C2 TURBOFAN ENGINE

FIGURE COURTESY OF GE

---

[1] Flat-rated to a specific temperature indicates that the engine can attain the rated thrust level up to that specified inlet temperature.

All directional references to front and rear; left and right; top and bottom; and clockwise and counterclockwise are made aft looking forward (ALF), as is the convention. All numbering is in the circumferential direction starting with the No. 1 position at the 12:00 o'clock position or immediately clockwise from the 12:00 o'clock position, and progressing sequentially clockwise ALF. The direction of rotation of the engine is clockwise ALF.

1.2 ENGINE HISTORY

The right engine installed on the accident airplane was a General Electric (GE) CF6-80C2B6 turbofan engine, engine serial number (ESN) 690-373 (PHOTO 1). At the time of the accident, ESN 690-373 had accumulated 68,785 hours time since new (TSN), 10,984 cycles since new (CSN), 19,139 hours time since last shop visit (TSLSV), and 3,057 cycles since last shop visit (CSLSV). The last engine shop visit occurred in January 2011 at the AA engine maintenance facility in Tulsa, Oklahoma. With rare exception, all AA CF6-80C2 engine shop visits occurred at the Tulsa maintenance facility.

PHOTO 1: RIGHT ENGINE DATA PLATE

1.3 HIGH PRESSURE TURBINE ROTOR AND HIGH PRESSURE TURBINE STAGE 2 DISK DESCRIPTION

The function of the HPT rotor is to drive the HPC rotor by converting the combustor exhaust gas flow into mechanical force. The HPT rotor is a two-stage air-cooled turbine (FIGURE 2). The HPT rotor assembly consists of an integral stage 1 turbine disk shaft, a conical vaned impeller spacer (there are 24 impeller spacer-to-HPT stage 2 disk bolts) with cover, thermal shield, and stage 2 disk. Forward and aft rotating air seals are assembled to the HPT rotor shaft and provide air-cooled cavities about the rotor system. An integral coupling nut and pressure tube seals and forms the internal cavity. A continuous flow of compressor discharge air is directed to the internal cavity of the rotor through diffuser vanes, which are part of the diffuser assembly, to cool the stage 1 and 2 disks and the stage 1 blades through holes in the dovetails. The remaining air is centrifuged through the stage 2 blade dovetails and cools the stage 2 blade airfoils. The HPT stage 2 disk, which is made of Inconel® alloy 718[2], incorporates a flange on the forward side for transmitting torque to the stage 1 disk. An aft flange supports the aft air seal and the integral coupling nut and pressure tube. The HPT stage 2 blades[3] fit in axial dovetail slots in the HPT stage 2 disk. The HPT stage 2 retainer is bolted to the aft face of the disk to retain the blades; the forward retainer is the thermal shield. The aft retainer incorporates a seal wire to seal the blade air delivery system.

---

[2] Inconel® alloy 718 is a wrought precipitation hardenable nickel base alloy.
[3] There are 74 HPT stage 2 blades; therefore, the disk has 74 blade retaining blade posts.
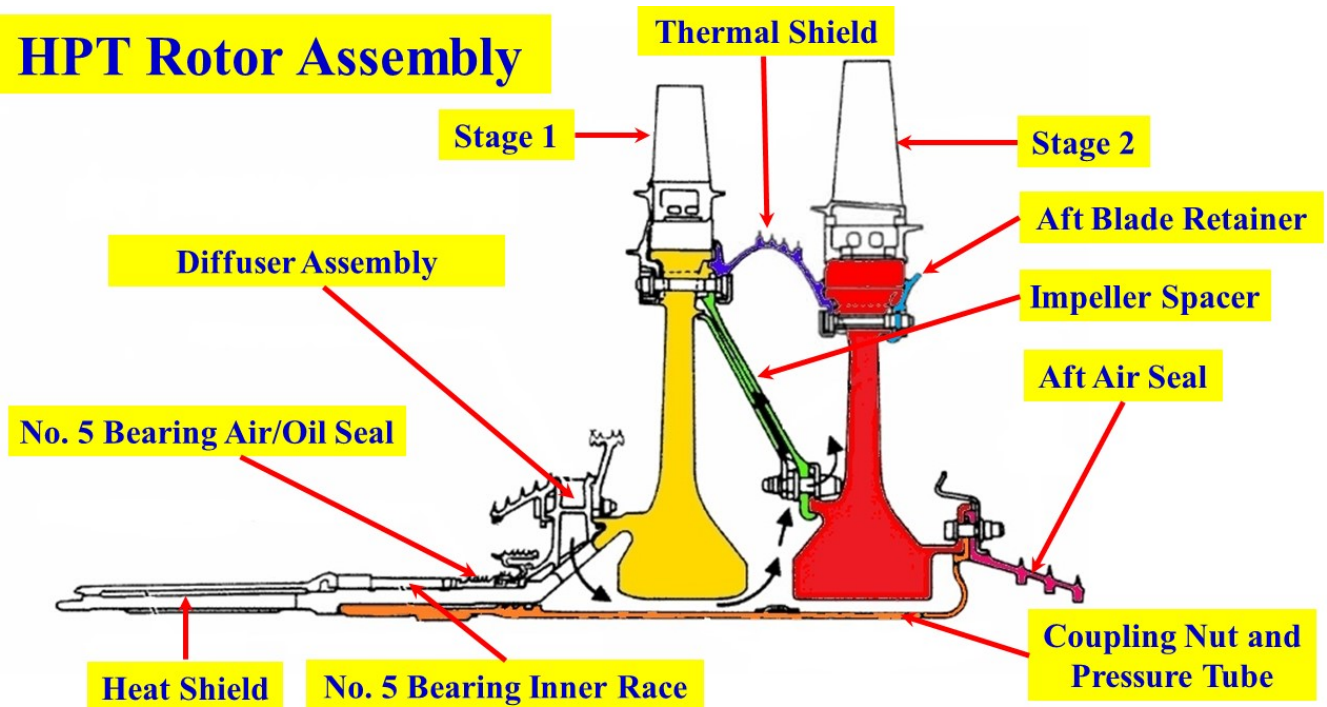
FIGURE 2: CF6-80C2 HIGH PRESSURE TURBINE SCHEMATIC

FIGURE COURTESY OF GE

1.4   HIGH PRESSURE TURBINE STAGE 2 DISK HISTORY

According to the AA maintenance records, the HPT stage 2 disk installed on the event engine ESN 690-373 was part number (PN) 9362M43P04 and serial number (SN) MUNBB592. This was confirmed when disk fragment identified as "B" (See Section 2.7 *HPT Stage 2 Disk Fragment Documentation* for details) was recovered (**PHOTO 2**). At the time of accident, the HPT stage 2 disk had accumulated 68,785 hours TSN and 10,984 CSN. See **TABLE 1** for timeline history.

PHOTO 2: PART MARKING ON THE HPT STAGE 2 DISK LOCATED ON TOP OF DISK POST FRAGMENT 'B' – PN ON LEFT AND SN ON RIGHT

PHOTO COURTESY OF GE

GE delivered the event engine, ESN 690-373, new to AA with the event HPT stage 2 disk, SN MUNBB592 (new), installed[4]. On April 30, 1998, Boeing delivered airplane N392AN to AA with ESN 690-373 installed in the left engine position (position 1) where it remained until March 2007.

---

[4] The delivery paperwork for the engine indicated that it had 6 hours TSN and 8 CSN when received by AA.

The FAA issued AD 2002-07-12 *Airworthiness Directives; General Electric Company CF6–80A, CF6–80C2, and CF6–80E1 Series Turbofan Engines* with an effective date of May 15, 2002 which required revising the Airworthiness Limitation Section (ALS) of the manufacturer's Instructions for Continued Airworthiness (ICA) and for air carrier operations to revise their approved continuous airworthiness maintenance program to include a set of mandatory inspections. These inspections required eddy current inspection (ECI) and/or fluorescent penetrant inspection (FPI) of engine rotating life-limited parts. AD 2002-07-12 required that: "Within the next 30 days after the effective date of this AD, revise the manufacturer's Life Limits Section of the Instructions[5] for Continued Airworthiness (ICA), and for air carrier operations revise the approved continuous airworthiness maintenance program, by adding ''MANDATORY INSPECTIONS''. For the CF6-80C2 HPT stage 2 disk the following inspections were required: 72-53-06 Paragraph 3 Fluorescent-Penetrant Inspection, 72-53-06 Paragraph 6 Eddy Current Inspection of Rim Boltholes for Cracks, and 72-53-06 Paragraph 7 Disk Bore Area Eddy Current Inspection.

On March 25, 2007, AA removed ESN 690-373 from airplane N392AN and sent it to the AA Tulsa facility for a hot section/compressor (HSC)[6] workscope; the HPT stage 2 disk (and engine) had accumulated 36,732 hours TSN and 5,818 CSN at that time. AA added the mandatory inspection requirements in accordance with AD 2002-07-12 to their maintenance program and upon removal of HPT stage 2 disk from the engine it was cleaned and inspected per CF6-80C2 Engine Shop Manual (ESM) GEK92451 Section 72-00-53 – *Inspection*; Section 72-00-53 does not require dimensional inspection of the HPT stage 2 disk. To satisfy the mandatory AD HPT stage 2 disk inspection requirements, AA performed the following inspections: Fluorescent penetrant inspection (FPI) per TASK 72-53-06-200-000-002, Eddy Current Inspection (ECI) of the HPT Stage 2 Rim Boltholes per TASK 72-53-06-200-000-006, Eddy Current Inspection of the Disk Bore per TASK 72-53-06-200-000-007. In addition, AA performed Eddy Current Inspection of the Disk Slot Bottoms per TASK 72-53-06-200-802; this inspection is not a mandatory inspection per the AD. Initial FPI revealed indications in the boltholes; AA repaired the boltholes per ESM Section 72-53-06. Follow-up FPI revealed no indications or anomalies on the entire disk. AA reinstalled the HPT stage 2 disk back into the same engine, ESN 690-373. Then on September 16, 2007, AA installed ESN 690-373 on the left engine position of airplane N386AA, where it remained until January 2011.

On January 15, 2011, AA removed the engine from airplane N386AA and sent it to the AA Tulsa facility for an engine heavy maintenance (EHM) workscope; the HPT stage 2 disk had accumulated 49,646 hours TSN and 7,927 CSN at that time. AA removed the HPT stage 2 disk from the engine and inspected it in accordance with CF6-80C2 ESM GEK92451 Section 72-53-06 – *Inspection*, which includes all mandatory inspections, visual inspections, and dimensional inspections. AD 2009-04-10 superseded AD 2002-07-12; AA complied with AD 2009-04-10 during this shop visit. As it pertains to the CF6-80C2 HPT stage 2 disks, AD 2009-04-10 did not change any inspection requirements from what was mandated in AD 2002-07-12. AA documented no anomalies. AA reinstalled the HPT stage 2 disk back into the same engine, ESN 690-373. Then on May 12, 2011, AA installed the engine on the right engine position of airplane N345AN, where it remained until November 2013.

On November 11, 2013, AA removed the engine for reliability improvement program (RIP) tasks; HPT stage 2 disk had accumulated 59,787 hours TSN and 9,533 CSN at that time. During this shop visit, AA did not disassemble the HPT module, and therefore did not inspect the HPT stage 2 disk. Then on December 4, 2013, AA reinstalled the engine on the right engine position of airplane N345AN, where it remained until the accident. At the time of the accident, the HPT stage 2 disk had accumulated 68,785 hours

---

[5] The Life Limits Section and the Airworthiness Limitations Section (ALS) both refer to the same Chapter 5 Section of the engine manual (EM).

[6] The HSC workscope is designed to restore HPT module clearances and engine performance. Parts are removed and repaired only as necessary to facilitate serviceability of the module unless otherwise specified.

TSN, 10,984 CSN, 19,139 hours TSLSV and 3,057 CSLSV. The event disk, PN 9362M43P04, has a life limit of 15,000 cycles when installed on the CF6-80C2B6 application[7]. Therefore, at the time of the accident the HPT stage 2 disk had 4,016 cycles of serviceable life remaining before required removal.

AA's service bulletin (SB) records showed three tracked SBs for the event HPT stage 2 disk; GE SB 72-1133 R2, GE SB 72-1141, and SB AA1519 R1. GE SB 72-1133 is a category 7 SB[8] that provided rework instructions for the HPT stage 2 disk forward flange arm and required a PN change when accomplished. AA accomplishes this SB on an "As Required" basis; AA did not accomplish this SB on the event HPT stage 2 disk nor was it required. GE SB 72-1141 introduced a redesigned HPT stage 2 disk to meet the 15,000-cycle limit for all applications (See **FOOTNOTE 7** for additional details). AA accomplishes SB 72-1141 on an attrition basis; AA did not accomplish this SB on the event HPT stage 2 disk because it was still serviceable and it was not required. AA created SB AA1519 to track the accomplishment of the ECI of the HPT stage 2 disk boltholes (TASK 72-53-06-200-000-006). In 2004, AA cancelled SB AA1519 and tracked the ECI on shop orders.

AA requested an Alternate Means of Compliance (AMOC) for AD 2009-04-10. The FAA approved the AMOC on February 24, 2009, which allowed the use of a UniWest ETC-2000 System for the HPT stage 2 disk bore ECI. AA Technical Instructions (TI) GEC2-1251 authorized the use of UniWest ETC-2000 ECI system per the approved AMOC. AA accomplished the ECI inspections at both shop visits (2007 and 2011) using US-450 desktop or production ECI instrument and probe PN PPE1078R2, SN 106046 (this probe is only used for the bore inspection). The GE standard practice manual (SPM) provides a list of specifications and equipment to perform the HPT stage 2 disk ECIs. SPM 70-32-10 lists PN PPE1078R2 as an approved probe. AA non-destructive testing (NDT) instruments used to make airworthiness determinations are periodically calibrated/certified at intervals not to exceed one year.

TABLE 1: HIGH PRESSURE TURBINE STAGE 2 DISK SN MUNBB592 HISTORY	
6/17/1997	Billet certified by melter (ATI Specialty Materials)
8/8/1997	Forging certified by forger (Wyman-Gorman)
2/3/1998	Disk completed by Motoren-und Turbinen-Union GmbH (MTU) - finished machining and disk deemed acceptable
4/30/1998	Airplane N392AN with engine SN 690-373 delivered to American Airlines with event disk installed
3/25/2007	Engine removed for overhaul - Disk eddy current and fluorescent penetrant inspection – AD 2002-07-12 complied with; 36,732 hours TSN & 5,818 CSN
9/16/2007	Event disk reinstalled in engine SN 690-373 and engine installed on American Airlines N386AA
1/15/2011	Engine removed – AD 2009-04-10 was complied with; 49,646 hours TSN & 7,927 CSN
5/12/2011	Event disk reinstalled in engine SN 690-373 and engine installed on American Airlines N345AN
10/28/2016	Uncontained event disk; 68,785 hours TSN, 10,984 CSN, and 3,057 cycles since last ECI

1.5   DESCRIPTION OF ENGINE NACELLE

The engine nacelle is comprised of the following fixed and hinged components; inlet cowl (includes the inlet lip), fan cowl, thrust reverser (TR), core cowl, turbine exhaust sleeve/nozzle, and turbine exhaust plug/centerbody (**FIGURE 3** and **PHOTO 3**). The fixed components include the inlet cowl, turbine exhaust sleeve/nozzle, and turbine exhaust plug/centerbody; while the hinged components include the fan cowl, TR, and core cowl. The inlet cowl is bolted to the engine fan case "A"-flange, the turbine exhaust sleeve/nozzle is bolted to the outer portion of the turbine rear frame (TRF), and the turbine exhaust plug/centerbody is bolted to the inner portion of the TRF. The fan cowl, TR, and core cowl are each

---

[7] When PN 9362M43P04 disk is installed on a CF6-80C2B5F or -80C2B7F, the life limit is reduced from 15,000 CSN to 9,000 CSN due to the higher thrust rating. The event disk was never installed in any engine model except for the CF6-80C2B6.
[8] GE recommends accomplishment at customer convenience.

comprised of two halves hinged on either side of the strut and joined by three latch hooks on the lower bifurcation centerline. Boeing provides all the nacelle hardware, including the TR, and GE supplies the engine.
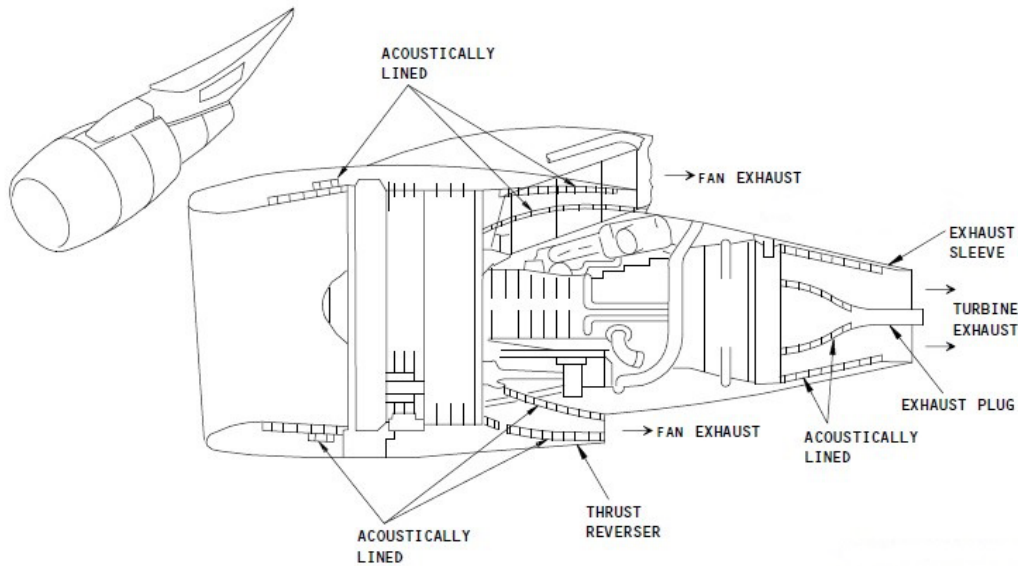
FIGURE 3: BOEING 767-300/GE CF6-80C2 INSTALLATION NACELLE NOMENCLATURE AND LOCATION
FIGURE COURTESY OF BOEING

PHOTO 3: BOEING 767-300/GE CF6-80C2 INSTALLATION NACELLE NOMENCLATURE AND LOCATION
PICTURE IS OF THE SISTER ENGINE (LEFT) ON THE EVENT AIRPLANE

2.0 ON-SITE EXAMINATION OF ENGINES STILL INSTALLED ON THE AIRPLANE

The Powerplant Group, comprised of members from GE, Boeing, AA, the Federal Aviation Administration (FAA), and the National Transportation Safety Board (NTSB) convened at ORD on October 29, 2016 to perform a detailed examination of the accident engine and airplane and completed its work on November 3, 2016.

According to witness statements of airport personnel, video tape evidence, flight data recorder (FDR) data, and global positioning satellite (GPS) data, the accident flight started its takeoff roll on runway 28R at the intersection of taxiway N5. The airplane experienced a right engine HPT failure and subsequent fire about 6,550 feet from runway 28R takeoff threshold, and came to a full stop just east of taxiway DD, about 9,225 feet from runway 28R takeoff threshold.

2.1 HPT STAGE 2 DISK FRAGMENT SEARCH AND RUNWAY IMPACT DAMAGE DOCUMENTATION

On October 29, 2016, a group comprised of persons from Boeing, GE, FAA, AA, airport personnel, and NTSB walked from where the airplane stopped (just east of taxiway DD, about 9,500 feet from the takeoff end of runway 28R), south along runway 10C-28C east to taxiway 'P6', then north to up to taxiway 'T10', and all areas in between (**FIGURE 4**). Most of the collected engine cowling and smaller pieces of engine debris were recovered at or near the engine failure initiation site; larger engine pieces were recovered some distance away (**FIGURE 5**). The runway gouge depicted in **FIGURES 4 – 6** and **PHOTOS 4** and **5** is where some of the HPT stage 2 disk fragments exited the engine and impacted runway 28R.
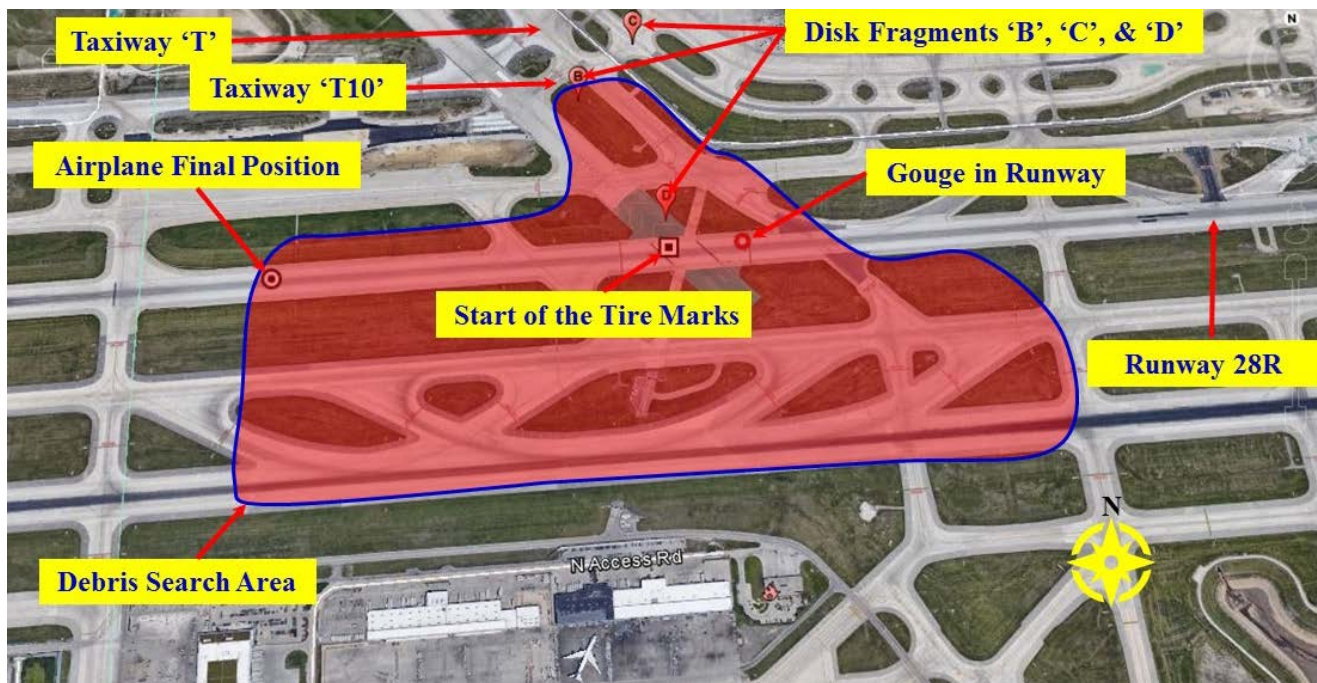
FIGURE 4: HPT STAGE 2 DISK FRAGMENT SEARCH AREA
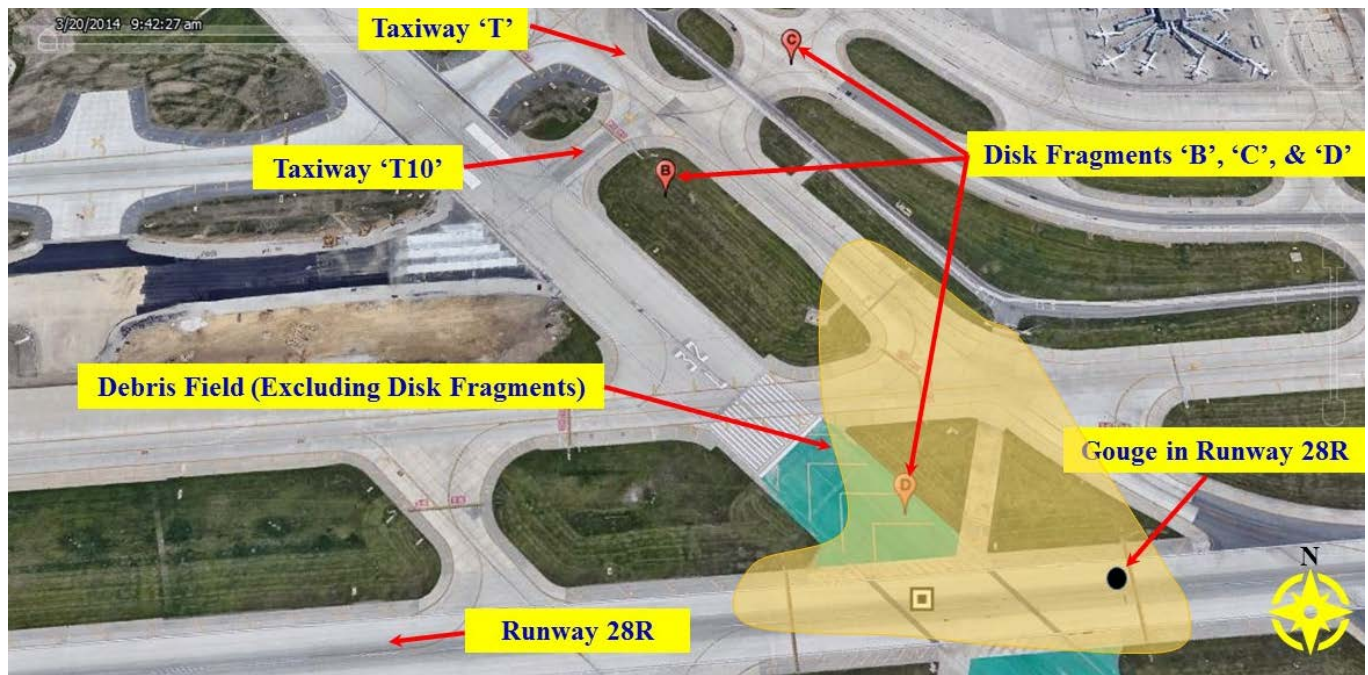
FIGURE 5: DEBRIS FIELD LOCATION

Runway 28R, about 31.5-feet to the right of the runway centerline (midpoint of gouge to midpoint of centerline) just east of the intersection of runway 28R and taxiway 'T', exhibited an impact ground scar/gouge consistent with impact from exiting HPT stage 2 disk fragment(s). The gouge was oriented about 30° forward (direction of airplane travel) relative to the HPT stage 2 plane of rotation (**PHOTO 4**) and in the general direction where three separate fragments of the HPT stage 2 disk were discovered north (right) of runway 28R. The gouge measured approximately 33-inches lengthwise, 8-inches at its widest, and 2-inches at its deepest. Additional smaller runway impacts marks were observed forward and aft of the initial impact scar (**PHOTO 5**).
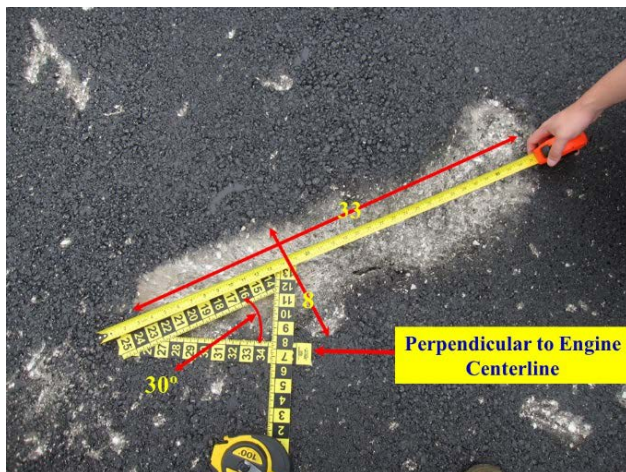
PHOTO 4: HPT STAGE 2 DISK GROUND IMPACT

PHOTO 5: GENERAL DIRECTION OF GROUND IMPACT AND RECOVERED FRAGMENTS

Three HPT stage 2 disk fragments (arbitrarily labeled as 'B' 'C' and 'D') were found during the search of the 28R runway and surrounding area. One HPT stage 2 disk fragment (arbitrarily labeled as 'A') penetrated through the roof of the UPS cargo facility south of runway 28R-10L (still on the airport property), about 2,935 feet (See **FIGURE 6**) from where the engine failure occurred (initial ground scar/gouge). AA personnel recovered fragment 'A' before the investigative group had arrived on scene. Fragment 'A' is thought to have penetrated through the inboard right wing and remained airborne until it struck and penetrated through the roof of the UPS building. Fragments 'B', 'C' and 'D' were recovered north of runway 28R at distance of 1,365-feet, 1,500-feet, and 475-feet from the initial ground scar/gouge respectively.
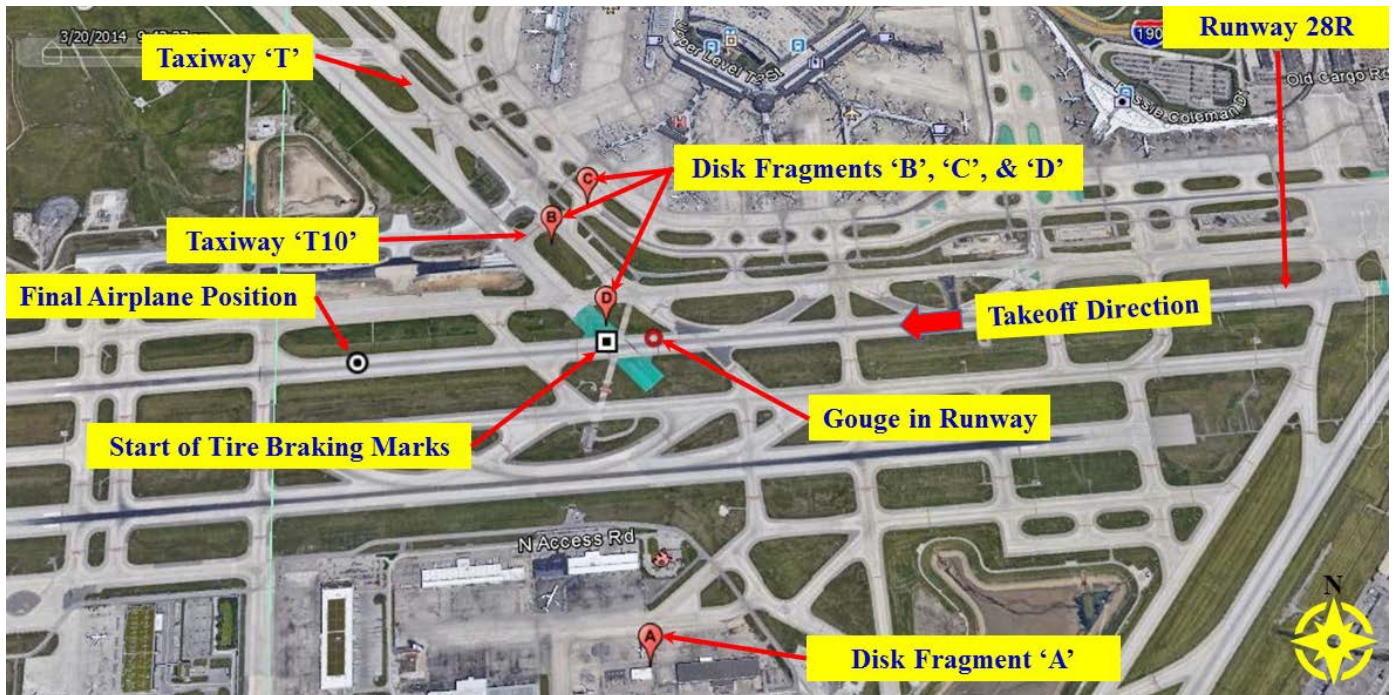
FIGURE 6: RECOVERED HIGH PRESSURE TURBINE STAGE 2 DISK FRAGMENT LOCATIONS

2.2 LEFT ENGINE (ESN 690-409) NACELLE DAMAGE

Examination of the left engine, No. 1, revealed small fragment impact marks along the inboard nacelle (**PHOTOS 6** and **7**); 2 impact marks in the fan cowl, 4 in the TR translating sleeve, 2 in the TR inner wall, and 1 in the core exhaust nozzle. The impact marks were arbitrarily labeled to facilitate documentation. **TABLE 2** provides the impact damage locations and descriptions; locations in red are those that were penetration thru-holes in the cowling structure.

PHOTO 6: EXHAUST NOZZLE DAMAGE
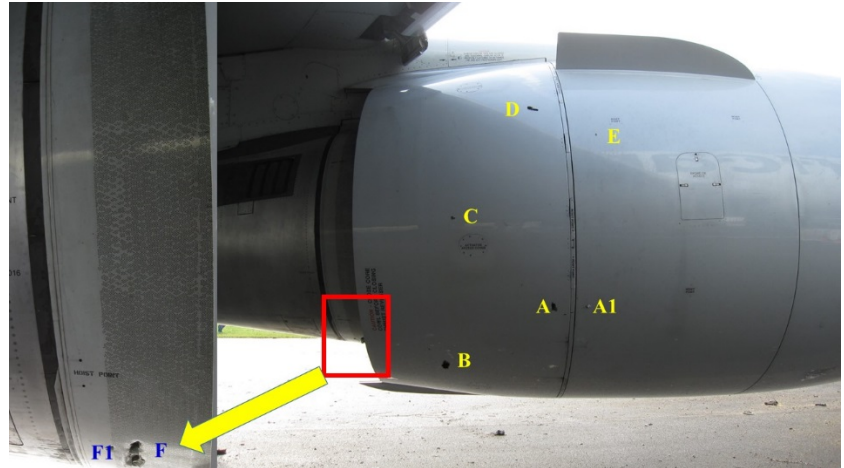
PHOTO 7: DAMAGE FAN COWL, TR, AND CORE COWL

TABLE 2: LEFT ENGINE NACELLE DAMAGE DOCUMENTATION					
IDENTIFIER	COWL	LOCATION	IMPACT/HOLE DIMENSIONS	TYPE OF IMPACT	PHOTOS
A (PHOTO 8)	TR Translation Cowl (transcowl)	4:00 o'clock 3.25-inches aft of transcowl leading edge (LE) and 65-inches circumferential from the TR split line at the 6:00 o'clock position	1.25-inch axial x 2.5-inches circumferential	Puncture of outer skin but not a thru-hole	PHOTO 8: IMPACTS 'A' AND 'A1' (OUTBOARD)
A1 (PHOTO 8)	Fan Cowl	4:00 o'clock 3.75-inches forward of fan cowl trailing edge (TE) and 66-inches circumferential from the fan cowl split line at the 6:00 o'clock position	1.125-inches axial x 0.75-inches circumferential	Puncture of outer skin but not a thru-hole	
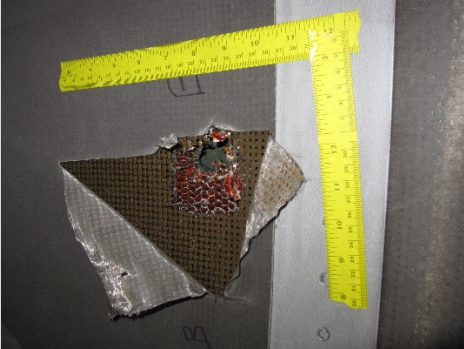
IDENTIFIER	COWL	LOCATION	IMPACT/HOLE DIMENSIONS	TYPE OF IMPACT	PHOTOS
TABLE 2: LEFT ENGINE NACELLE DAMAGE DOCUMENTATION					
B (**PHOTO 9**)	**TR Transcowl**	**5:00 o'clock 31-inches aft of the transcowl LE and 42-inches circumferential from the TR split line at the 6:00 o'clock position**	**2.25-inches axial x 4.25-inches circumferential**	**A pass-thru penetration – in line with a blade fragment imbedded in the TR lower bifurcation side wall**	**PHOTO 9: BLADE FRAGMENT THRU-HOLE 'B' (OUTBOARD)**
B (**fan flow path side**) (**PHOTO 10**)	**TR Transcowl**	**5:00 o'clock 31-inches aft of the transcowl LE**	**2.25-inches axial x 1.00-inches circumferential**	**Puncture thru-hole**	**PHOTO 10: BLADE FRAGMENT THRU-HOLE 'B'(INBOARD)**
B1 (**PHOTOS 11** and **12**)	TR Lower Bifurcation Side Wall	6:00 o'clock	3.0-inches axial x 1.25-inches radially Blade fragment weighed 5.455 ounces	HPT stage 2 blade fragment embedded in the structure	**PHOTO 11: HPT STAGE 2 BLADE FRAGMENT EMBEDDED IN BIFURCATION PANEL (OUTBOARD)**

TABLE 2: LEFT ENGINE NACELLE DAMAGE DOCUMENTATION					
IDENTIFIER	**COWL**	**LOCATION**	**IMPACT/HOLE DIMENSIONS**	**TYPE OF IMPACT**	**PHOTOS**
					PHOTO 12: HPT STAGE 2 BLADE FRAGMENT EMBEDDED IN BIFURCATION PANEL (INBOARD)
C (**PHOTO 13**)	**TR Transcowl**	**3:00 o'clock 27.5-inches aft of the transcowl LE and 84-inches circumferential from the TR split line at the 6:00 o'clock position**	**1.125-inches axial x 0.625-inches circumferential**	**Puncture thru-hole**	**PHOTO 13: IMPACT THRU-HOLE 'C' (OUTBOARD)**
C (**fan flow path side**) (**PHOTO 14**)	**TR Transcowl**	**3:00 o'clock 27.5-inches aft of the transcowl LE**	**2.5-inches axial x 1.0-inches circumferential**	**Puncture thru-hole**	**PHOTO 14: IMPACT THRU-HOLE 'C' (INBOARD)**
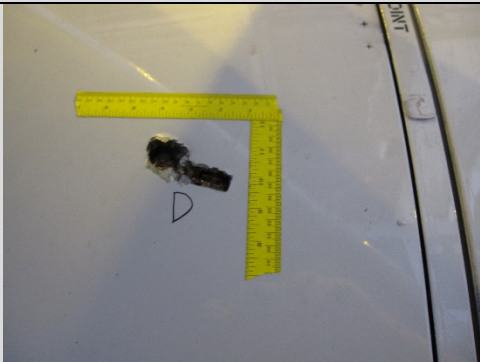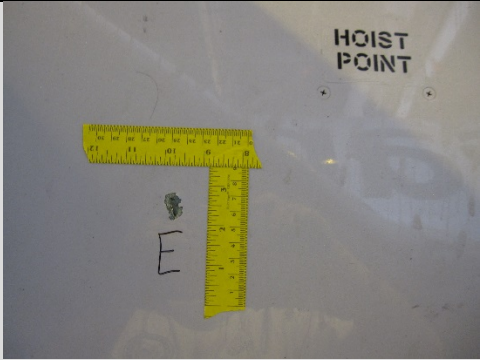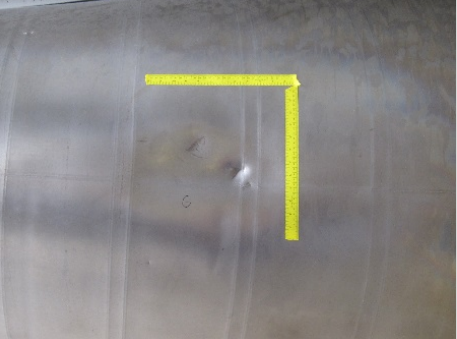
TABLE 2: LEFT ENGINE NACELLE DAMAGE DOCUMENTATION					
IDENTIFIER	COWL	LOCATION	IMPACT/HOLE DIMENSIONS	TYPE OF IMPACT	PHOTOS
D (PHOTO 15)	TR Transcowl	2:00 o'clock 5.75-inches aft of transcowl LE and 65-inches circumferential below the chine	3.0-inches axial x 1.75-inches circumferential	Puncture of outer panel but not through blocker door	**PHOTO 15: IMPACT DAMAGE 'D' (OUTBOARD)**
E (PHOTO 16)	Fan Cowl	2:30 o'clock 6.875-inches forward of fan cowl TE and 28-inches circumferential below the chine	0.5-inches axial x 0.75-inches circumferential	Puncture of outer skin but not a thru-hole	**PHOTO 16: IMPACT DAMAGE 'E' (OUTBOARD)**
F (PHOTO 17)	TR Inner Wall	5:30 o'clock 7.5-inches forward of TR inner wall TE and 13-inches to the bottom of the lower impact and 19-inches to the top of the upper impact circumferential from the TR lower centerline	2.5-inches axial x 7.25-inches circumferential	Puncture thru-hole	**PHOTO 17: IMPACTS 'F' AND 'F1' – 'F' THRU-HOLE (OUTBOARD)**

TABLE 2: LEFT ENGINE NACELLE DAMAGE DOCUMENTATION					
IDENTIFIER	COWL	LOCATION	IMPACT/HOLE DIMENSIONS	TYPE OF IMPACT	PHOTOS
F (core compartment side) (PHOTO 18)	TR Inner Wall	5:30 o'clock 7.5-inches forward of TR inner wall TE	0.75-inches axial x 0.75-inches circumferential	Puncture thru-hole	PHOTO 18: 'F' THRU-HOLE (INBOARD)
F1 (PHOTO 17)	TR Inner Wall	5:30 o'clock 5.0-inches forward of TR inner wall TE	0.875-inches x 1.125-inches circumferential	Puncture of outer skin but not a thru-hole	
G (PHOTO 19)	Core Exhaust Nozzle	3:00 o'clock 31-inches from TE of core exhaust nozzle and forward most impact was 1.5-inches and the rearmost was 2.5-inches from the 3:00 o'clock split line-weld seam	Overall impact area is 11-inches axial x 14-inches circumferential	Multiple surface impact marks in this area– none of which are penetrations	PHOTO 19: SCUFF MARKS 'G' (OUTBOARD)

With the fan cowl and TR opened, the outside of the engine was exposed and a visual examination revealed no debris impact damage. Looking through the left engine inlet, no impact damage was noted on the fan blades.

2.3   RIGHT ENGINE (ESN 690-373) NACELLE & STRUT/PYLON DAMAGE

2.3.1   Inlet Cowl

The inlet cowl was intact and attached to the engine 'A'-flange.   The inlet lip exhibited no significant thermal distress and the outer skin exhibited light sooting while the inner skin was blackened and more sooted than the outer skin.   At the 11:30-12:30 o'clock position, the inner inlet lip skin was buckled and wavy.

The inlet cowl inner barrel (airflow area) exhibited evidence of thermal distress and was blackened and sooted.   The upper section of the inner barrel from 7:30 to 3:30 o'clock position exhibited missing outer perforated acoustic liner skin.   The first layer of the honeycomb ply beneath the acoustic liner outer skin from the 9:00 to 3:00 o'clock (180° arc) was missing.   In this same 180° arc, the second layer of honeycomb was cracked, buckled, and exhibited thermal distress.   The lower section of the inner barrel from the 3:30 to 7:30 o'clock exhibited thermal distress, was blackened and sooted, but the perforated acoustic liner skin remained intact (**PHOTO 20**).

PHOTO 20: INLET COWL DAMAGE – MISSING ACOUSTIC LINER AND DAMAGED HONEYCOMB

2.3.2   Fan Cowl

Both inboard (left side) and outboard (right side) fan cowls were intact and sooted on their external surfaces.   The inboard fan cowl had significant thermal distress on the aft portion between the 6:00 to 7:30 clock position; the skin was charred, paint bubbled, and had lost its structural integrity.   The pressure relief door, which is located on the inboard cowl, was secured and latched (**PHOTO 21**).   The inboard chine was intact and sooted on most of its surface.   The outboard fan cowl exhibited thermal distress centered on the aft area of the cowl between the 3:00 to 6:00 o'clock position; the skin was charred, the paint bubbled, and from the 4:00 to 5:00 o'clock position, the skin had delaminated and lost its structural integrity (**PHOTO 22**).   The oil access door, which is located on the outboard cowl, was secured and latched. All three fan cowl latches were in the CLOSED and LOCKED (latched) position.

PHOTO 21: INBOARD FAN COWL

PHOTO 22: OUTBOARD FAN COWL

2.3.3 Thrust Reverser Cowl

The TR translating sleeve was heavily sooted and exhibited significant thermal distress consisting of delamination to the extent that multiple graphite plies were exposed below the fiberglass nomex exterior. Approximately the aft 15-inches of both the inboard and outboard translating sleeves were missing/consumed from the pylon down to lower bifurcation panel. The TR inner wall was missing an approximately 16-inch axial section from the 3:00 o'clock position to the pylon. The remaining intact inner wall was significantly thermally distressed and delaminated (PHOTOS 23 and 24). All three TR latches were in the CLOSED and LOCKED (latched) position.
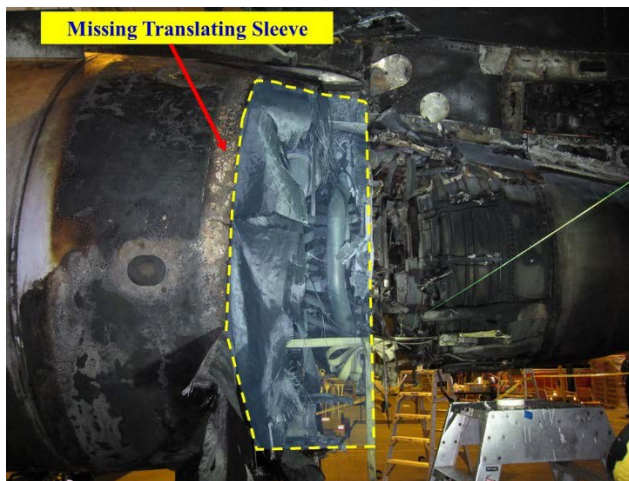
PHOTO 23: INBOARD TRANSCOWL SLEEVE DAMAGE

PHOTO 24: OUTBOARD TRANSCOWL SLEEVE DAMAGE

2.3.4 Core Cowl

Much of the inboard core cowl was missing, with only a small portion of the cowl remaining intact and still attached to the upper hinge fittings. The remaining inboard core cowl was pie-shaped and measured 10-inches circumferentially at the forward end, 15-inches circumferentially at the rear end and the overall length was 37-inches (**PHOTO 25**).

Much of the outboard cowling was also missing with only a small portion of the cowling remaining intact and attached to the upper hinge fittings; the remaining piece was 'L'-shaped and measured as follows: forward piece measured 18-inches circumferentially by 27-inches axial and the rear piece measured 31-inches circumferentially by 15-inches axially (**PHOTO 26**).
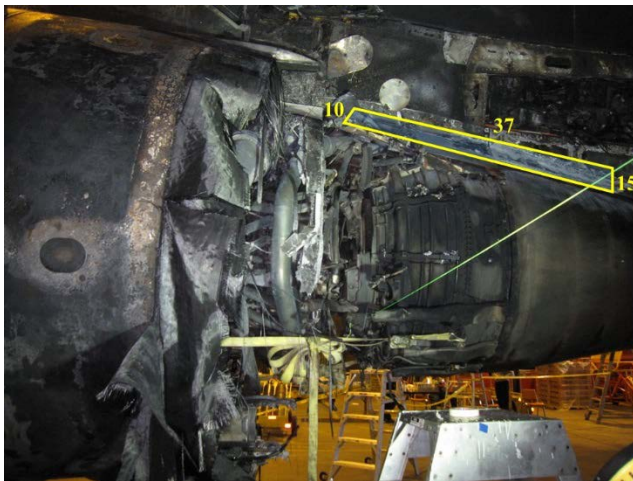
PHOTO 25: INBOARD CORE COWL DAMAGE
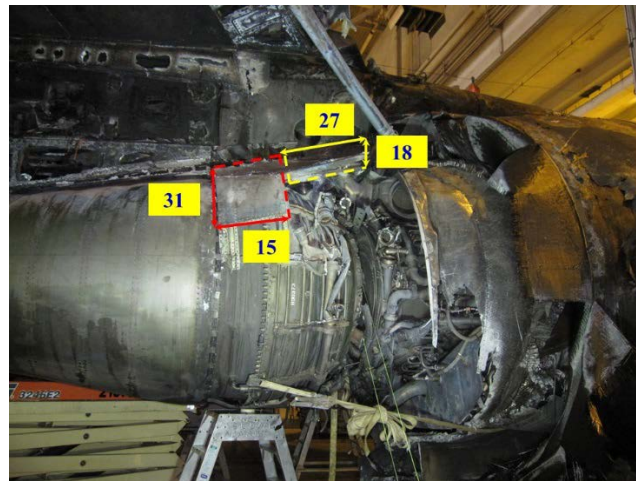
PHOTO 26: OUTBOARD CORE COWL DAMAGE

2.3.5 Core Exhaust Nozzle and Aft Centerbody

The core exhaust nozzle was intact; the aft part of the nozzle was buckled from about the 6:00 to 3:00 o'clock position (**PHOTO 27**) and impact damaged at about the 5:00 o'clock position near the forward edge. All the bolts that secure it to the TRF outer flange were in place, secured, and intact. The aft centerbody was intact, secure, and all the centerbody-to-TRF bolts were intact and in place.

2.3.6 Strut/Pylon

FIGURE 7 provides the nomenclature and location of strut/pylon components. This section documents the external damage found on the strut-to-wing interface fairings. All fairing panels, which include the forward, reverser, underwing, aft access panel, and trailing edge, had significant thermal distress, delamination, and missing material in most of the panel locations (**PHOTOS 28** and **29**). The aft strut fairing heat shield remained intact.

PHOTO 27: BUCKLED CORE EXHAUST NOZZLE
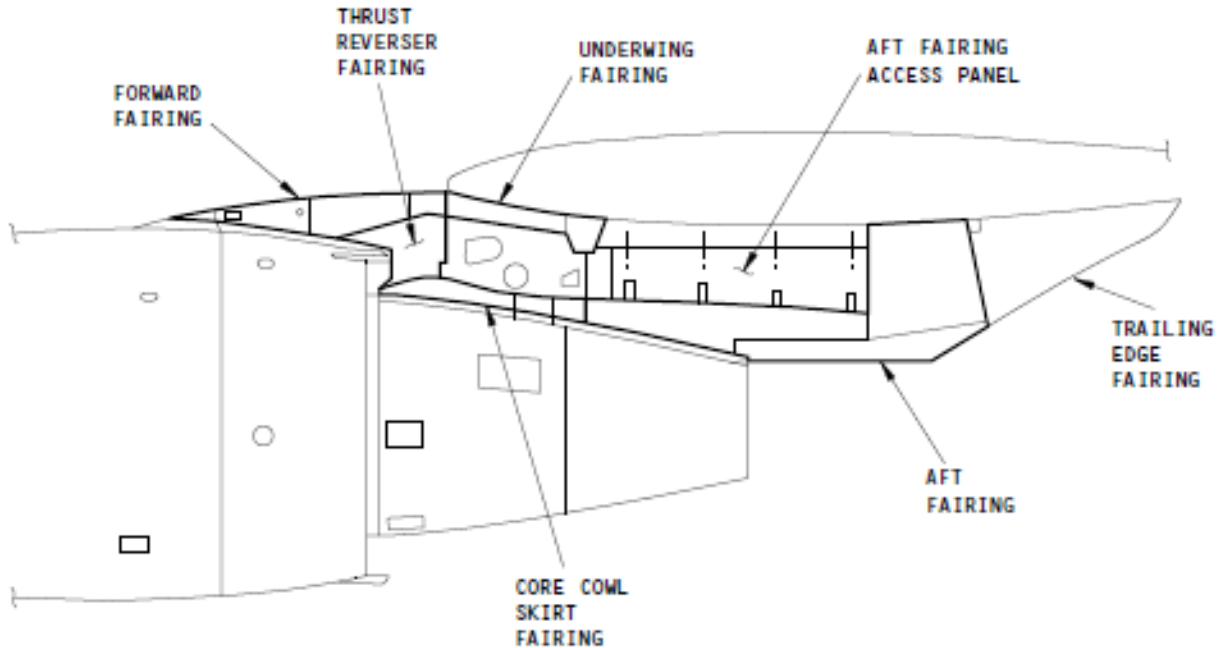
FIGURE 7: PYLON/STRUT NOMENCLATURE

FIGURE COURTESY OF BOEING

PHOTO 28: INBOARD PYLON/STRUT THERMAL DAMAGE

PHOTO 29: OUTBOARD PYLON/STRUT DAMAGE

2.4   RIGHT WING & FUSELAGE IMPACT DAMAGE AND TRAJECTORY

No airplane impact damage was observed outboard of the right engine pylon from exiting HPT stage 2 disk or engine debris; all impact damage was located inboard of the pylon. Examination of the bottom of the wing inboard of the right engine pylon revealed two thru-hole penetrations (**PHOTOS 30** and **31**, holes labeled ❶ and ❷) through the lower and upper skins of the wing. Hole ❶ was located forward of the front spar in the fixed-wing leading edge panel (**PHOTOS 32** and **33**). Hole ❷ was located aft of the wing front spar between wing rib No. 6 and 9 (**PHOTOS 30**, **32**, and **33**).
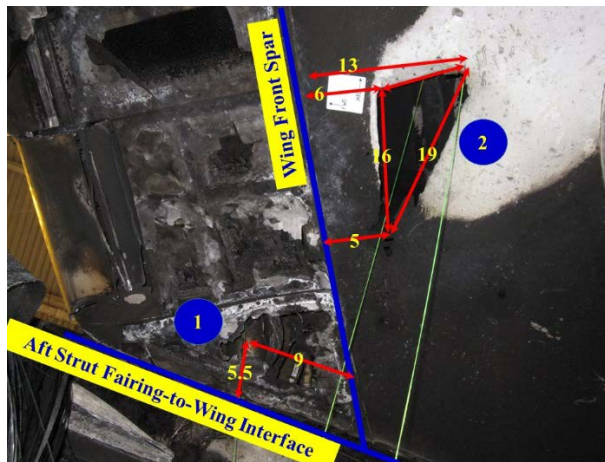
PHOTO 30: RIGHT WING INBOARD OF PYLON LOWER WING SKIN THRU-HOLE PENETRATIONS – ALL MEASUREMENTS ARE IN INCHES
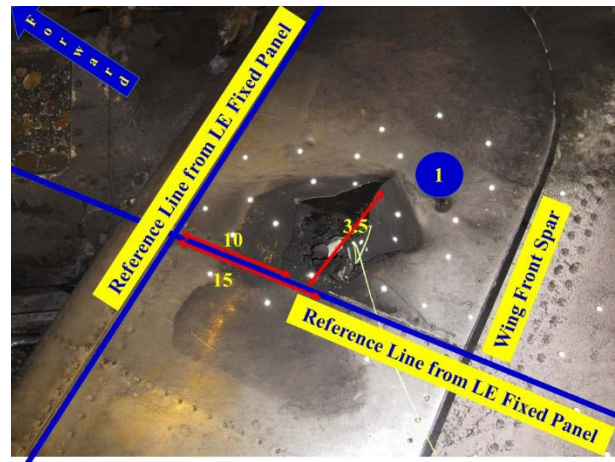
PHOTO 31: RIGHT WING INBOARD OF PYLON UPPER WING SKIN THRU-HOLE PENETRATION – HOLE ❶, ALL MEASUREMENTS ARE IN INCHES

PHOTO 32: RIGHT WING INBOARD OF PYLON UPPER WING SKIN THRU-HOLE PENETRATION – HOLE ❷
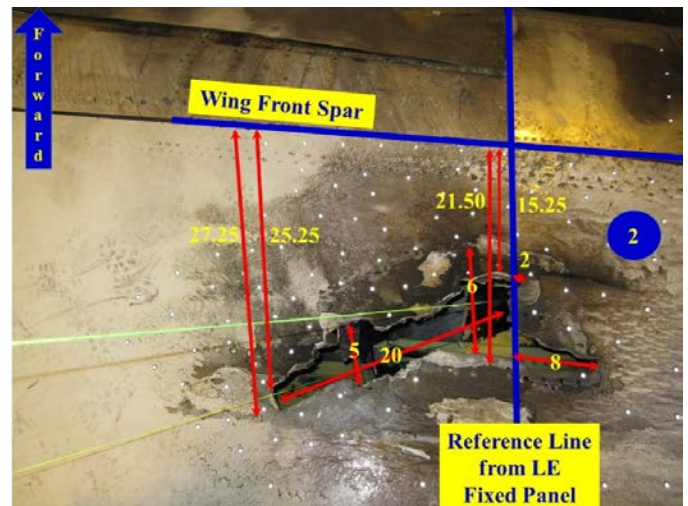
PHOTO 33: RIGHT WING INBOARD OF PYLON UPPER WING SKIN THRU-HOLE PENETRATION – HOLE ❷, ALL MEASUREMENTS IN INCHES

To represent the trajectory area of the exiting HPT stage 2 disk fragments, strings were attached close to the fan mid shaft and on the HPT case representing the inner and outer HPT stage 2 disk diameters and connected to either puncture through holes or ground scar/gouge. Looking through hole ❶, the trajectory of the engine debris that passed through the hole did not impact the front spar and continued upward and exited the top of the fixed-wing leading edge panel (**PHOTOS 34** and **35**). Looking through hole ❷, the trajectory of the HPT stage 2 disk fragment first entered the dry bay though the lower wing skin, severed the main engine fuel feed line, severed rib No. 6 (which is part of the inboard dry bay boundary) and continued through the upper wing skin.
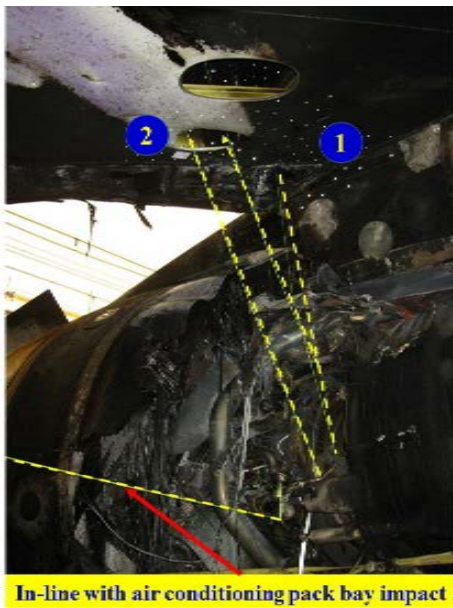
PHOTO 34: INBOARD TRAJECTORY – LOOKING FORWARD
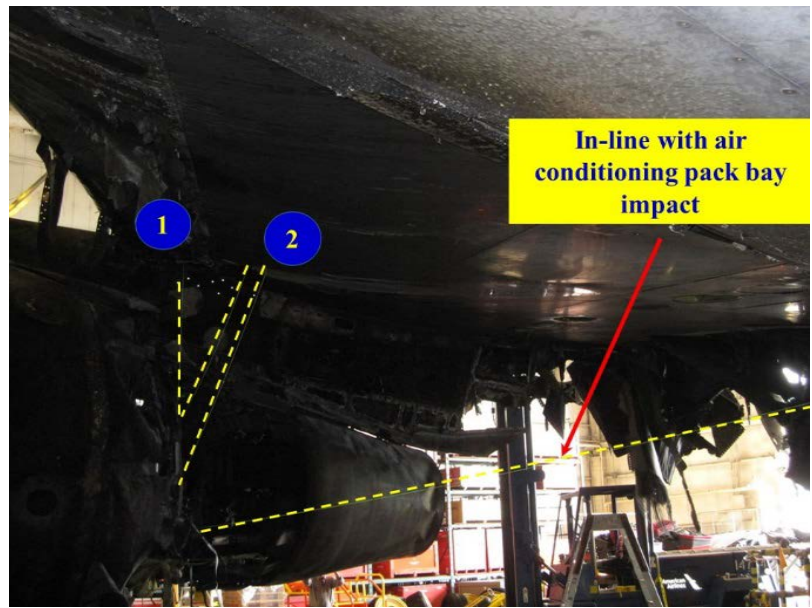
PHOTO 35: INBOARD TRAJECTORY – LOOKING AFT

A mark was made on the hangar floor 31.5-feet from the centerline of the airplane and in-line with the rotational plane of the HPT stage 2 disk to represent the initial impact ground scar/gouge that was observed at runway 28R (PHOTOS 36 and 37).

PHOTO 36: OUTBOARD TRAJECTORY – LOOKING AFT

PHOTO 37: OUTBOARD TRAJECTORY – LOOKING FORWARD

Impact damage from exiting engine debris was evident on:

1) the upper and lower right wing skins,
2) right upper and lower wing ribs (Nos. 5 to 7),
3) upper and lower forward stringers,
4) wing front spar lower chord,
5) right and left wing-to-body fairing panels,
6) right and left landing gear doors,
7) right air conditioning (AC) pack,
8) right and left main landing gear tires,
9) right fuselage skin (**PHOTOS 38** and **39**),
10) right stabilizer leading edge, and
11) the left engine nacelle (See Section 2.2 *Left Engine (ESN 690-409) Nacelle Damage* for details of the left engine nacelle damage).

Engine debris was found inside the right wing dry bay, right wheel well, left nacelle, and right AC bay.

PHOTO 38: DEBRIS IMPACT MARK ON RIGHT SIDE OF FUSELAGE NEAR THE OVERWING DOORS
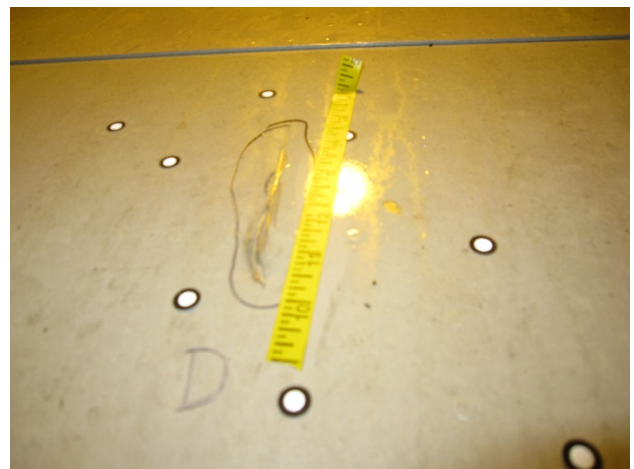
PHOTO 39: CLOSE-UP OF IMPACT MARK – SLIGHTLY WORSE THAN TYPICAL OBSERVED IMPACT

2.5   RIGHT ENGINE – ESN 690-373

2.5.1   Borescope Inspection

The engine was borescope inspected while still installed on the airplane. No attempt to rotate the fan or the core was made; therefore, all findings are what could be easily observed using a flexible borescope. The combustor, HPT stage 1 nozzles, HPT stage 1 blades, LPT stages 1 and 2 rotor and stators, and fan mid shaft in the general area of the HPT stage 2 disk were all visually inspected. No significant damage or distress beyond what was considered normal operational condition was observed, except for LPT secondary impact damage to the airfoils. The fan mid shaft was inspected approximately 3-feet forward and 1-foot aft of the normal HPT stage 2 disk location with no signs of a shaft fracture; scoring was noted on the bumper bearings which is consistent with contact with the HPC rotor. No evidence of LPT rotor/stator clashing was observed.

2.5.2 External Engine Inspection

Looking through the inlet cowl, the fan blades and the inner flow path of the fan case were visible. All the fan blades were present, intact, sooted, and exhibited no impact or thermal distress. The fan case flow path exhibited thermal distress but no impact damage or breaches. With the fan cowl open, the outside of the fan case and the attaching hardware were visible; no sooting or thermal distress was noted. Looking through the core exhaust nozzle, the LPT stage 5 blades were visible; all the blades were present, full length, and intact. From what was visible of the rear engine mount, without removing what remained of the core cowl, the two rear mount links appeared undamaged and were secured to the TRF and the rear engine mount hanger.

The LPT case exhibited a 360° circumferential breach in-plane with the HPT stage 2 hardware; all hardware in the radial plane of the breach was severed. The entire rear flange of the HPT case and the front flange of the LPT case were missing except for a joined/bolted HPT-LPT case flange segment located between the 3:00 and 6:00 o'clock position that was pushed outwards (**PHOTO 40**). The HPT case rear flange segment measured about 30-inches in length and the LPT case segment was shorter, about 22-inches in length. The breach in the LPT case was measured at several locations around the circumference and the gap measured between 3.0-inches and 7.5-inches wide. The remainder of the HPT case forward of the rear flange appeared to be intact underneath the HPT active clearance control (ACC) manifold. The HPT ACC manifold was intact, secure, and exhibited some impact damage and deformation.
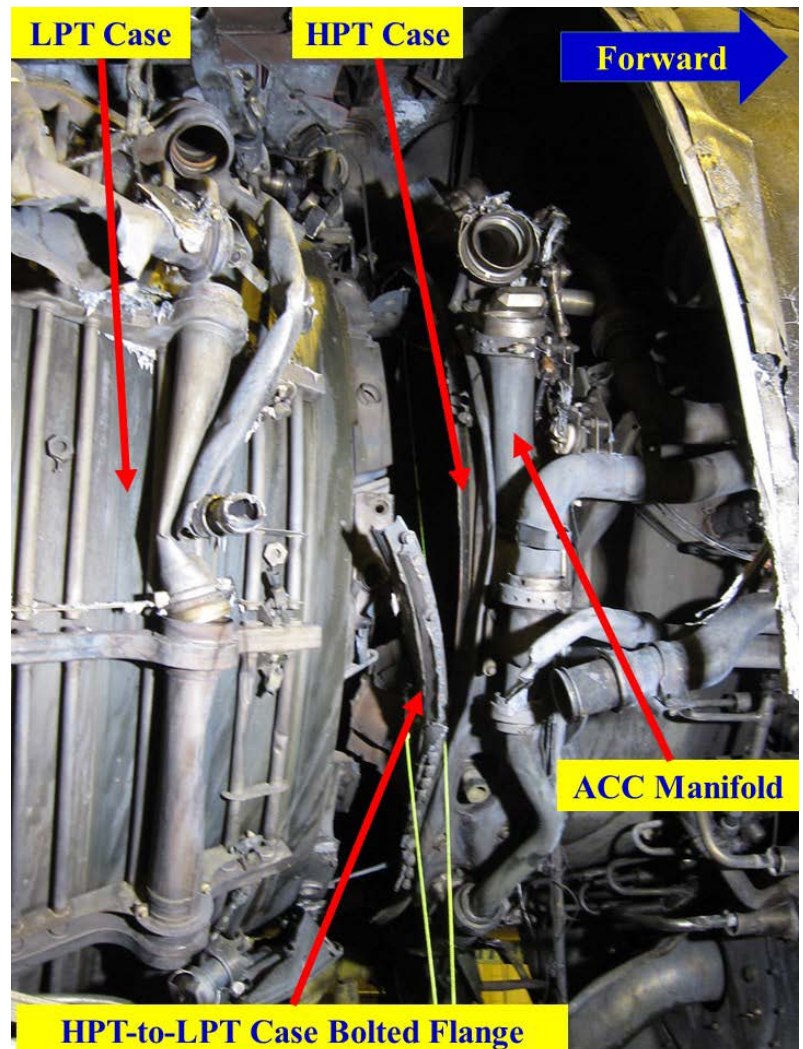
PHOTO 40: BREACH IN LOW PRESSURE TURBINE CASE

Forward of the LPT case breach, the outside of the engine core was coated with black soot and thermal distress was noted on some of the electrical cables, hoses, and hose clamps. Aft of the LPT case breach, the outside of the engine was coated with black soot as well. The external hardware forward and aft of the LPT case breached appeared to be in place and intact.

2.5.3 Internal Engine Inspection Through the Breach in the LPT Case

Looking through the breach in the LPT case, the hardware from the HPT stage 1 disk aft to the LPT stage 1 nozzle segments was visible. All eighty HPT stage 1 blades were present, full length, and exhibited TE airfoil damage. The thermal shield that attaches between the HPT stage 1 and 2 disks was missing except for the front flange that remained attached to the rear face of the HPT stage 1 disk; all the HPT stage 1 disk-to-thermal shield hook bolts were present and secured to the disk. The impeller spacer remained attached to the rear face of the HPT stage 1 disk and appeared to be intact except for the rear flange that attaches to the forward flange of the HPT stage 2 disk. All the HPT stage 1 disk-to-impeller spacer bolts were present and secure but none of the HPT stage 2 disk-to-impeller spacer bolts were present. During the collection of the debris from the runway, hardware consistent with the HPT stage 2 disk-to-impeller spacer bolts was recovered. The coupling nut and pressure tube (also referred to as the HPT pressure tube) was sheared in-line with the rear flange of the impeller spacer; the portion of the HPT pressure tube from the shear plane aft was missing. With the rear section of the HPT pressure tube missing, a portion of the fan mid shaft was visible.

PHOTO 41: HPT STAGE 1 DISK, THERMAL SHIELD, IMPELLER SPACER, AND HPT AFT AIR SEAL DAMAGE

The fan mid shaft appeared intact with no significant distress or scoring (**PHOTO 41**).

All the HPT stage 2 nozzle segments were missing (many of which were collected from the runway) except for five segments; two near the top at about the 11:00 o'clock position and three near the bottom at the 4:00 o'clock position. All the LPT stage 1 nozzle segments were present, except for 1 located at about the 10:00 o'clock position and 1 located at the 5:00 o'clock position; many of the airfoils exhibited leading edge impact damage. All the LPT stage 1 blades were present but were fractured transversely across the airfoil at different lengths. All the LPT stage 2 nozzle segments were present (**PHOTO 42**).
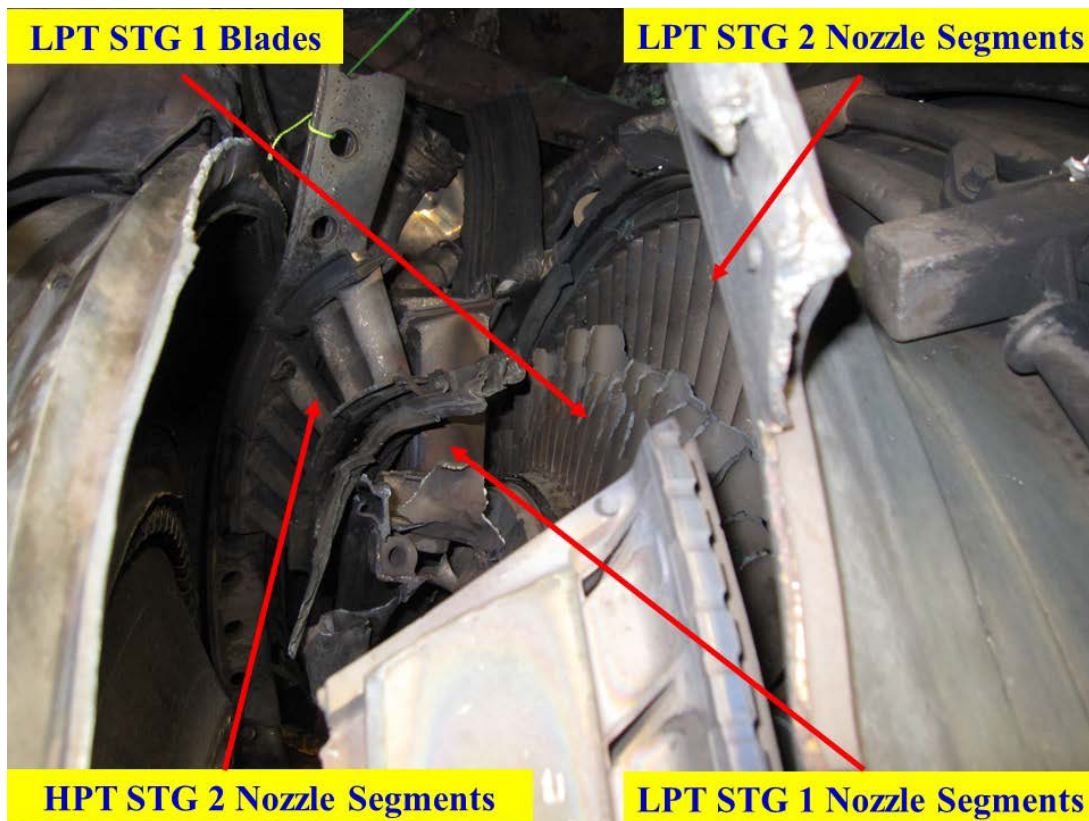
PHOTO 42: LPT STAGES 1 AND 2 HARDWARE DAMAGE

2.6   FLIGHT DECK AND FIRE SUPPRESSION DOCUMENTATION

Examination of the flight deck revealed that both thrust levers (throttles) were against the aft stops, both fuel control[9] switches were in the down and CUTOFF position (**PHOTO 43**), and the left and right engine fire suppression handles were pulled up but not rotated. The APU and cargo fire handle was found pulled up and rotated.

Toggling of the fuel control switches from RUN to CUTOFF closes the airplane spar valve and closes the engine-mounted fuel control high pressure shutoff valve (HPSOV). Pulling of the fire suppression handle performs several functions, including closing the fuel control HPSOV if not already closed and closing the spar valve if not already closed, same as the fuel control cutoff switches on the pedestal.[10]
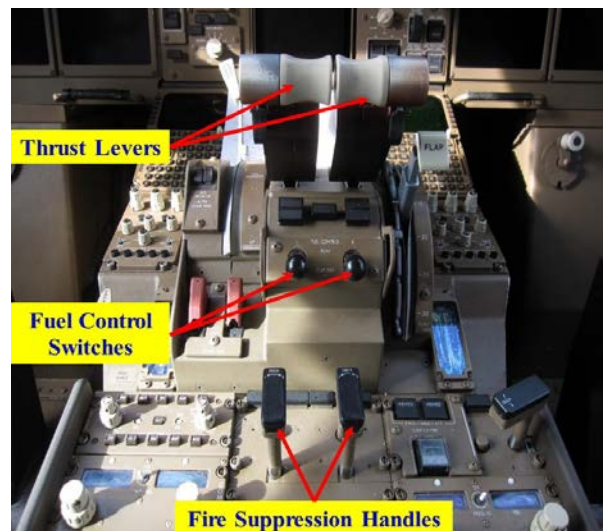
PHOTO 43: FLIGHT DECK THROTTLE AND FIRE SUPPRESSION HANDLE POSITIONS

---

[9] Although the nomenclature on the pedestal calls out 'fuel control', the GE term for this accessory is a hydromechanical unit (HMU) and it will be referenced as such during the engine exam documentation.

[10] Along with closing the fuel control shutoff valve and the spar fuel shutoff valve, pulling the fire suppression handle also performs the following actions: closes the environmental control system (ECS) pressure regulating and shutoff valve (PRSOV),

There are two fire suppression bottles for the engine – bottle 1 and bottle 2 – that are shared by both engines. Each fire suppression bottle has a dedicated discharge port for each engine. The engine fire suppression bottles are located in the forward right cargo bay. The part number for both engine fire suppression bottles is Boeing PN S332T011-24 and manufacturer (Pacific Scientific) PN 34600012-24. The SNs for bottle 1 and bottle 2 are 23046F1 and 23044F1, respectively. Visual examination of the discharge ports of each bottle revealed that the detonation device in both discharge ports in each bottle was missing the percussion cap. This is consistent with discharged fire suppression bottles. The left wing (**PHOTO 44**) and right wing (**PHOTO 45**) spar fuel shutoff valve actuators were visually confirmed in the CLOSED position as indicated by the mechanical position indicator.

PHOTO 44: LEFT ENGINE FUEL SHUTOFF VALVE IN CLOSED POSITION

PHOTO 45: RIGHT ENGINE FUEL SHUTOFF VALVE IN CLOSED POSITION

PHOTOS COURTESY OF BOEING

2.7   HPT STAGE 2 DISK FRAGMENT DOCUMENTATION

Four HPT stage 2 disk fragments, arbitrarily labeled 'A', 'B', 'C', and 'D', were recovered on the airport property (**PHOTOS 46** and **47**). This accounted for approximately the entire disk bore and approximately 93% of the disk rim (69 of 74 blade-retaining posts). While searching through the debris collected from the runway, two additional HPT stage 2 disk posts were recovered; therefore, a total of 71 of the 74 or 96 % of all the disk posts were accounted for.

A general observation was that the aft side of the disk exhibited circumferential scoring along the web area while the forward side did not. The Powerplant team labeled the HPT stage 2 disk fracture faces on-site as follows: first letter specifies the fragment in which the face is located and the second letter specifies the fragment to which the fracture face mates. For example, fracture face labeled 'A-B' indicating the fracture face is located on fragment 'A' and matches with fragment 'B'.

---

closes the ECS high pressure shut off valve, closes the hydraulic pump supply/shut-off valve, de-pressurizes the hydraulic pump, de-energize the integrated drive generator (IDG) arms the fire extinguishing system, and silences the aural warning.
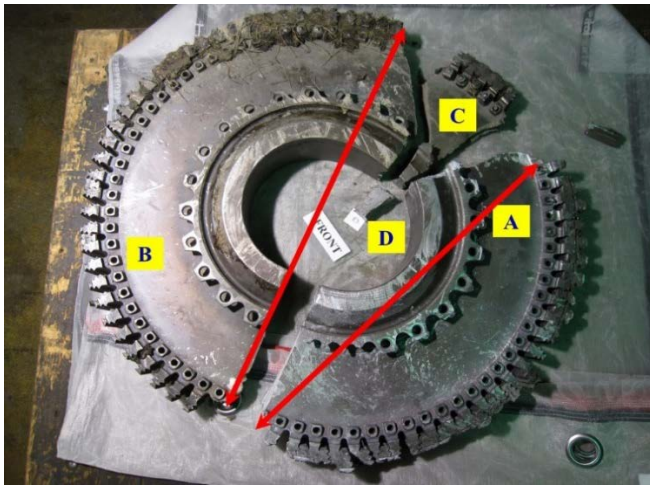
PHOTO 46: RECOVERED PIECES OF THE EVENT HPT STAGE 2 DISK – FORWARD SIDE
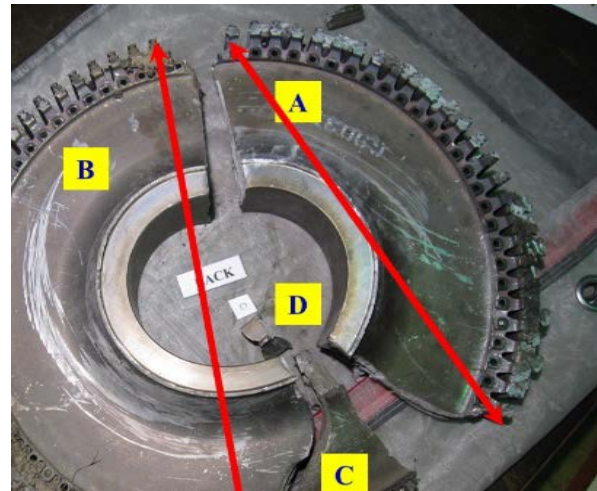
PHOTO 47: RECOVERED PIECES OF THE EVENT HPT STAGE 2 DISK – AFT SIDE

Fragment 'A' was recovered from the UPS facility and consisted of 27 blade-retaining posts (approximately 36% of the entire rim). The maximum chordal length was approximately 21.5-inches (red arrows in **FIGURES 46** and **47**). All the blades were fractured transversely across the airfoil at the platform with most of the blade shanks still present in the disk. Ten impeller spacer-to-HPT stage 2 disk attachment bolt flange holes (approximately 42% of the total) were present with seven intact and three were fractured through. All the thermal shield-to-HPT stage 2 disk bolts were fractured and only three of the bolt shanks remained in their respective holes on the HPT stage 2 disk. None of the thermal shield remained attached to fragment 'A'. Viewing the aft side of the disk, the entire spacer arm/air seal flange was fractured at the disk-to-flange radius.

Fragment 'A' fracture surface 'A-B' exhibited a discolored region near the bore of the disk towards the forward face. The discolored area exhibited a dark bluish appearance surrounded by a dark brownish appearance; away from the discolored region, the fracture surface color was fairly uniform, greyish color, and had a waffle-like appearance. The corresponding region on fragment 'B' fracture face surface 'B-A' did not show the same type or intensity of discoloration as what was seen on fragment 'A'; however, in the region that corresponded to discoloration on fragment 'A', fragment 'B' was slightly greyer than the surrounding fracture face (**PHOTOS 48** - **51**).

PHOTO 48: HPT STAGE 2 DISK FRACTURE SURFACE FOR FRAGMENT 'A' THAT MATCHES WITH FRAGMENT 'B'
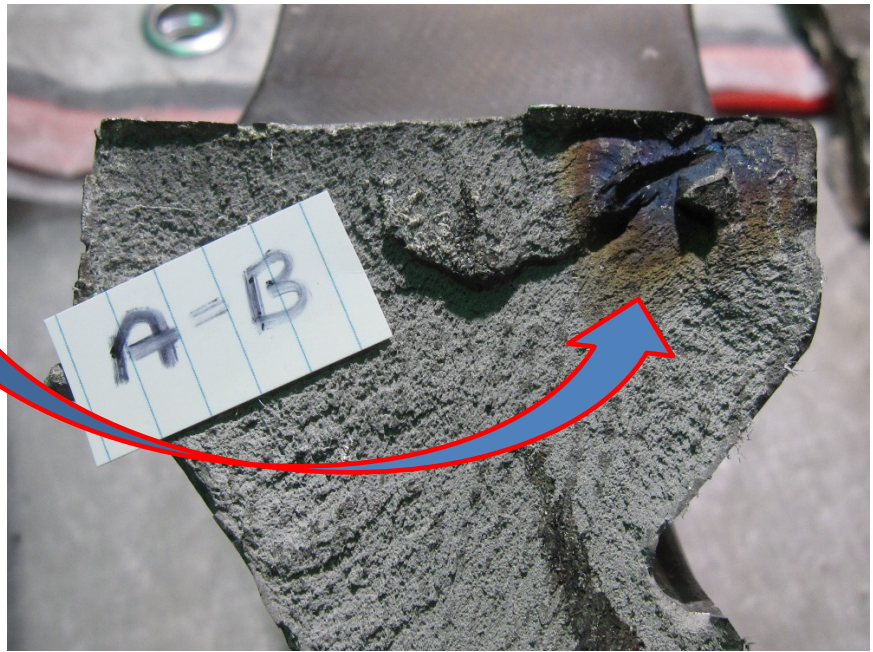
PHOTO 49: CLOSE-UP OF DISCOLORED AREA NEAR BORE TOWARDS FORWARD FACE ON FRAGMENT 'A'
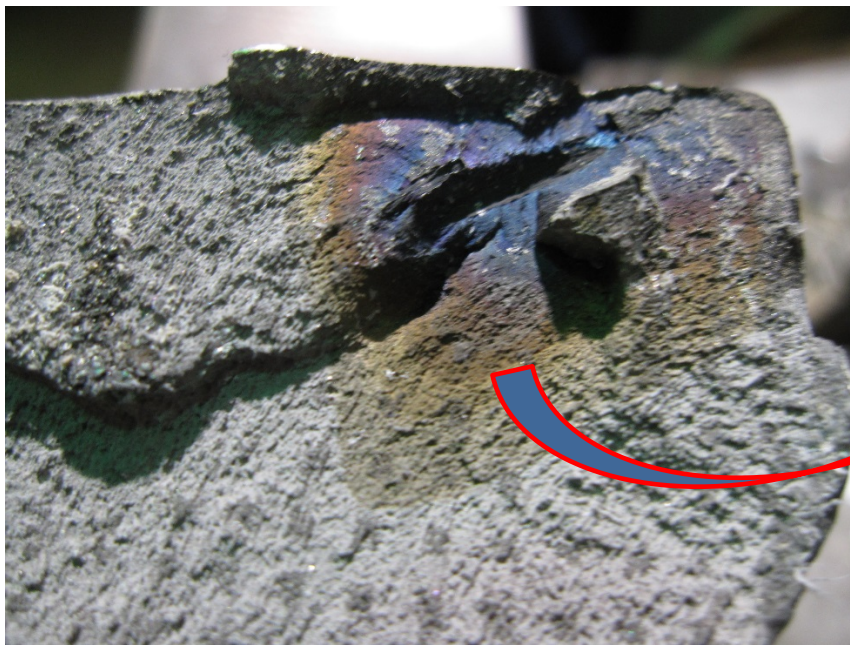
PHOTO 50: CLOSE-UP OF DISCOLORED AREA NEAR BORE TOWARDS FORWARD FACE ON FRAGMENT 'A'
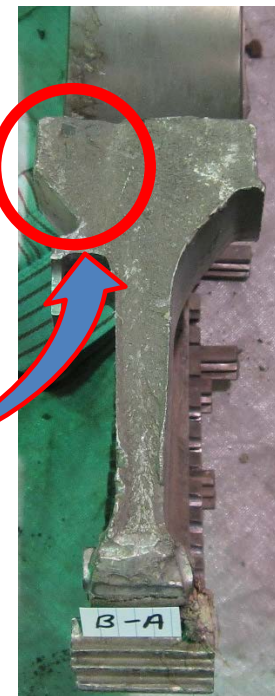
PHOTO 51: CORRESPONDING FRACTURE SURFACE ON FRAGMENT 'B'

Fragment 'B' was recovered in the grassy area near taxiway 'T10' and consisted of 37 blade-retaining posts (approximately 50% of the entire rim). The maximum chordal length was approximately 24.75-inches (red arrows in **FIGURES 46** and **47**). All the blades were fractured transversely across the airfoil at the platform with many of the blade shanks missing from the disk posts. A section of about 16 blade posts was packed with dirt while the rest were relatively dirt free. Fourteen impeller spacer attachment bolt flange holes (approximately 63% of the total) were present and intact; one was whole but cracked. All the thermal shield-to-HPT stage 2 disk bolts were fractured and only six of the bolt shanks remained in their respective holes on the HPT stage 2 disk. None of the thermal shield remained attached to fragment 'B'. The entire spacer arm/aft air seal flange was fractured at the disk-to-flange radius.

Fragment 'C' was recovered on taxiway 'A10' and consisted of five blade-retaining posts (approximately 6% of the entire rim). All the blades were fractured transversely across the airfoil at the platform with all the blade shanks still present in the disk posts. One partial impeller spacer-to-HPT stage 2 disk attachment bolt flange hole (approximately 4% of the total) was present. All the thermal shield-to-HPT stage 2 disk bolts were intact except for one where the shank was present but the bolt head was missing. None of the thermal shield remained attached to fragment 'C'. Viewing the aft side of the disk, the entire aft spacer arm/aft air seal flange was fractured at the disk-to-flange radius (See **PHOTOS 46** and **47**).

Fragment 'D' was recovered on the departure end of runway R15 overrun and consisted of no blade posts, no impeller spacer hole flange material, no thermal shield-to-HPT stage 2 disk bolt holes, and no aft spacer arm/aft air seal flange material but had features consistent with the bore. Matching fracture surfaces, fragment 'D' was identified as part of the aft side of fragment 'C' (**PHOTOS 52** - **54**).
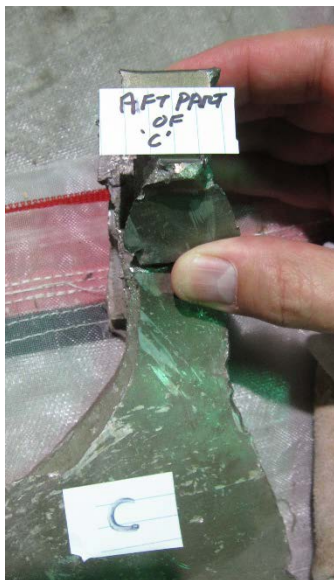
PHOTO 52: FRAGMENT 'D' MATCHED 'C'
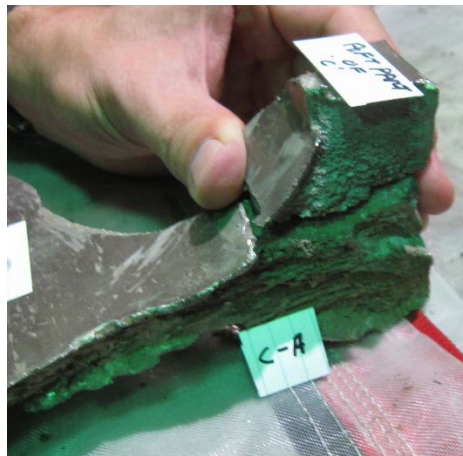
PHOTO 53: MATCHED FRACTURE SURFACES 'C'-TO-'A'
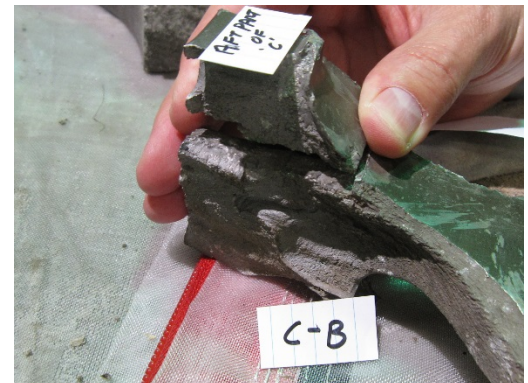
PHOTO 54: MATCHED FRACTURE SURFACES 'C'-TO-'B'

According to GE, the HPT stage 2 disk, without blades or any thermal shield attachment bolts, weighs approximately 153 pounds. Each disk fragment was weighed individually as-is and again with blade shanks and attachment bolts removed, when possible. After initial weighing, all the blade shanks and attachment bolts that could be removed were removed and weighed. The average of the blade roots when weighed was approximately 0.22 pounds and the bolts did not register on the scale so they were assumed to be negligible compared to the other hardware. Fragment 'A' weighed approximately 58 pounds

as-is with $6^1/_3$ blade shanks and three thermal shield attachment bolts; subtracting the blade shanks and attaching bolts, the fragment 'A' weighed approximately 56.6 pounds. Fragment 'B' weighed approximately 83.5 pounds as-is with two blade shanks and six thermal shield attachment bolts; subtracting the blade shanks and attaching bolts, the fragment 'B' weighed approximately 83.1 pounds. Fragment 'C' weighed approximately 7.5 pounds as-is with four blade shanks and five thermal shield attachment bolts; subtracting the blade shanks and attachment bolts, the fragment 'C' weighed approximately 6.6 pounds. Fragment 'D' weighed approximately 0.21 pounds as-is with no additional hardware. The four HPT stage 2 disk fragments together were estimated to weigh approximately 146.5 pounds representing approximately 96% of the disk by weight.

3.0 METALLURGICAL EVALUATION OF HPT STAGE 2 DISK, SN MUNBB592

The NTSB Materials Laboratory Division, Washington D.C. received all the HPT stage 2 disk fragments for fractographic and metallographic evaluation as well as striation counting. A group comprised of members from AA, Boeing, GE, FAA, and the NTSB convened at the NTSB Materials Laboratory on October 31, 2016 to commence examination of the HPT stage 2 disk fragments. See *NTSB Materials Laboratory Factual Report No. 17-034* for complete details of the metallurgical findings. After the NTSB completed its work, GE conducted their own evaluation in their GE Aviation Materials Laboratory facility in Evendale, Ohio that included bulk chemical analysis, wavelength dispersive x-ray spectroscopy (WDS) of the fracture origin, and striation counting of the fatigue region. See *NTSB Materials Laboratory Factual Report No. 17-034* Appendix B - GE *Metallurgical Investigation Report Log No. FA2016-17907* for complete details of the GE metallurgical findings.

As mentioned in Section 2.7 *HPT Stage 2 Disk Fragment Documentation*, the mating fracture faces 'A-B' and 'B-A' appeared visually different. The NTSB laboratory report identified the fracture surface differently than what was documented on-scene; **TABLE 3** provides the on-scene nomenclature to the corresponding NTSB laboratory nomenclature. Fracture surface 2 (surface 'B-A') was coated by a thin layer of particulate matter after the separation. As a result, the corresponding region on fracture surface 2 (surface 'B-A') did not show the same type or intensity of discoloration as what was seen on surface 1 (surface 'A-B'). Fracture surface 2 was then cleaned during the NTSB Materials Laboratory examination, after which it exhibited a similar appearance as fracture surface 1.

TABLE 3: HPT STAGE 2 DISK FRACTURE IDENTIFICATION	
On-Site Documentation	**NTSB Laboratory Report**
Fragment 'A'	Fragment 2
Fragment 'B'	Fragment 1
Fragment 'C'	Fragment 3
Fragment 'D'	Fragment 4
Fracture Surface 'A-B'	Fracture Surface 1
Fracture Surface 'B-A'	Fracture Surface 2

3.1 NTSB EVALUATION

Optical examination of the fragments revealed a discolored region on both fracture surfaces 1 and 2 located at the forward bore corner (**FIGURE 8** – grey area). The discolored region had a maximum depth of approximately 0.928-inches radially by 1.126-inches axially (**PHOTOS 55** and **56**). Within the discoloration region on fracture surfaces 1 and 2 was a large oblong/elliptical-shaped anomaly that was darker in appearance than the rest of the surrounding matrix (parent material) and measured approximately

0.427-inches long (major axis) and was oriented approximately 26º from the bore centerline. Higher magnification of fracture surface 1 revealed several smaller oblong/elliptical-shaped anomalies along with the large anomaly already described above (**PHOTO 57**). All the anomalies aligned with the forging flow lines. There were multiple crack origins initiating from the anomaly and the cracks propagated both inboard towards the disk bore as well as outboard towards the disk blade slots.
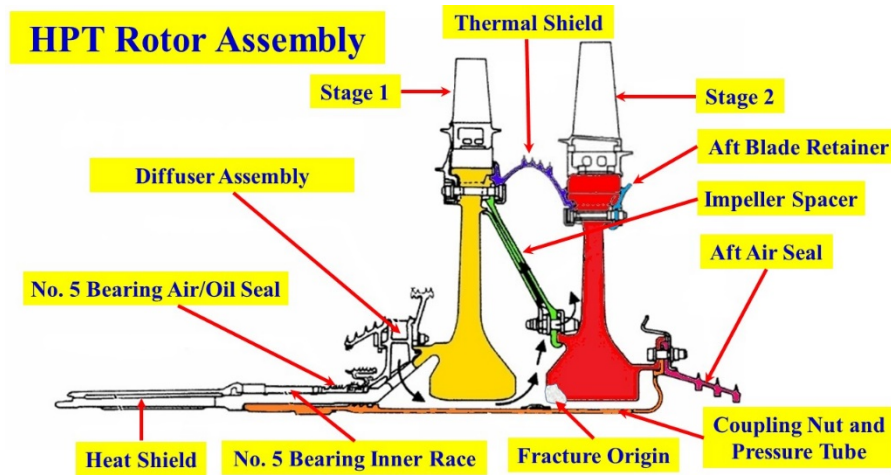
FIGURE 8: PRIMARY FRACTURE ORIGIN LOCATION ON THE EVENT HPT STAGE 2 DISK (GREYED AREA)
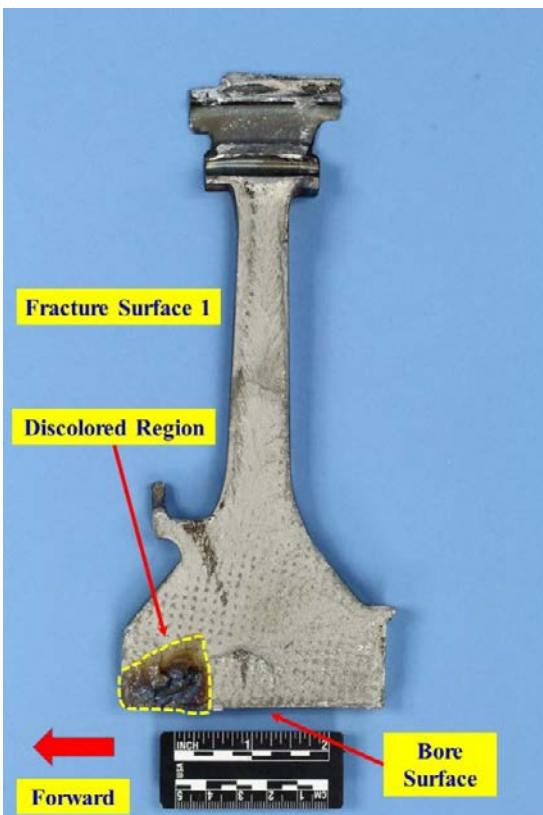
PHOTO 55: FRACTURE SURFACE 1 PRIOR TO CLEANING
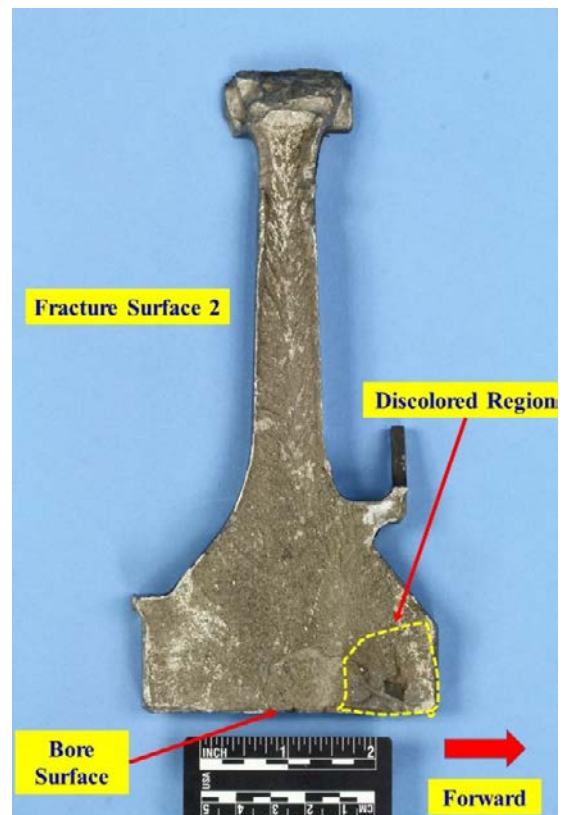
PHOTO 56: FRACTURE SURFACE 2 PRIOR TO CLEANING
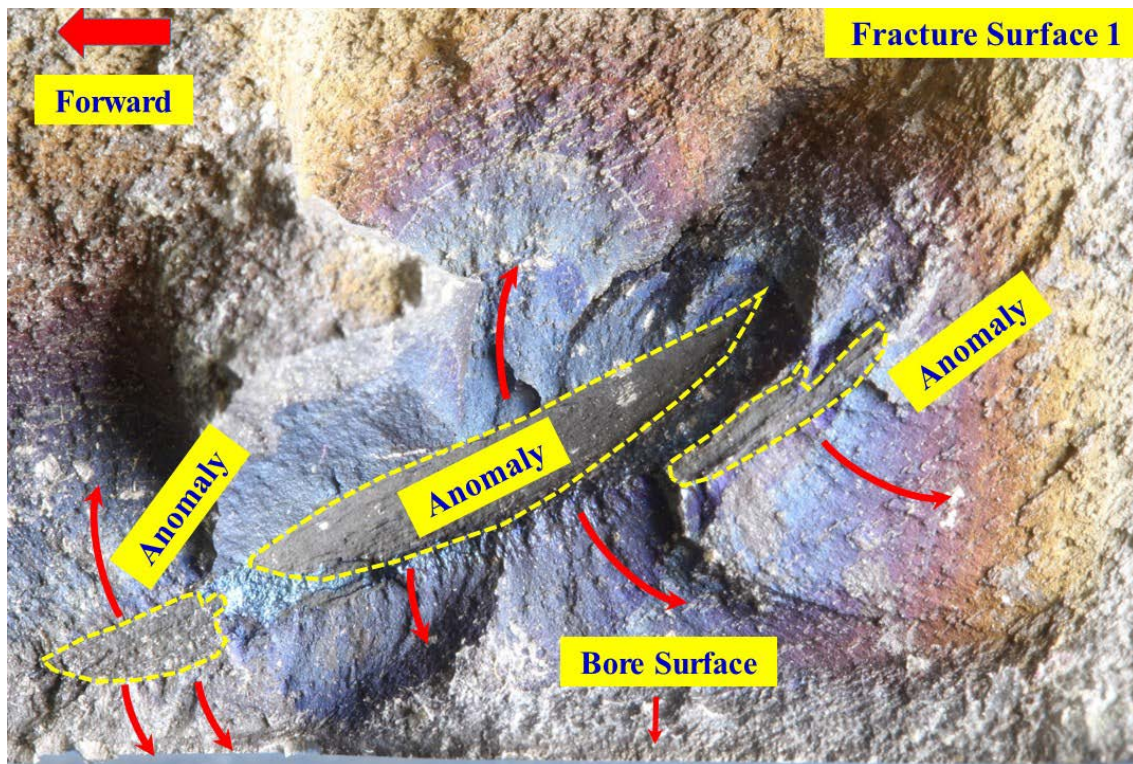
PHOTO 57: ELLIPTICAL MATERIAL ANOMALIES FOUND SUB-SURFACE NEAR BORE

A series of field emission secondary and backscatter scanning electron microscope (SEM)[11] images were taken of the material anomalies. At approximately 5,000X magnification, the anomalies were revealed to be composed of micron-sized particles embedded in a matrix material. Chemical analysis of the particles and the surrounding matrix using energy dispersive spectroscopy (EDS) revealed elevated amounts of aluminum (Al), magnesium (Mg), and the presence of oxygen (O) within the particles; the surrounding matrix had elements in the quantities consistent with the specified material - Inconel® alloy 718.[12]

---

[11] In an optical microscope, light from a source is focused on the sample and the image is formed when the sample reflects and absorbs different wavelengths of the light and the eye detects the differences to form an image. An electron microscope works in a similar manner but instead of using light, it uses electrons to bombard the sample to create images and to understand its composition. A scanning electron microscope (SEM) is one of the types of an electron microscope that offer high resolution and high magnification. The SEM focuses on the surface and composition of the sample by scanning the surface of a sample with an incident electron beam. Electrons from the sample scatter creating secondary electrons typically of low energy value or the electrons from the incident beam bounce upon impact with the sample creating backscattered electrons typically of higher energy values; both of which are collected to create three-dimensional images that are black and white. In the secondary image mode, the differences in surface topography are represented by variations in gray scale intensity while in backscatter mode, the image is mapping changes in material density. Some SEMs have an energy dispersive x-ray spectroscopy (EDS) detector that captures x-rays emitted from the sample during the creation of secondary electrons. When creating secondary electrons, x-rays are emitted as electrons from the high energy outer shells fill the void left by the ejection of lower energy electrons in order to stabilize the state of the atoms. The x-rays emitted are characteristic in energy and wavelength of the element that emitted them, so the composition of the sample can be determined. Elements that have high atomic number will have several x-ray elemental peaks while elements that have low atomic number have few x-ray elemental peaks. The various elemental peaks represent the shell that the electrons were ejected from and the shell from which the electrons were filled.

[12] Inconel® alloy 718 (also abbreviated as INCO 718) was developed by Huntington Alloys in the 1960s (Schafrik 2001) and is a wrought precipitation hardenable corrosion-resistant nickel based alloy. This material is typically made up of: Nickel plus Cobalt (Ni/Co – 50.00-55.00%) Chromium (Cr – 17.00-19.00%) Iron (Fe – Balance), Niobium plus Tantalum (Nb/Ta – 4.75-5.50%), Molybdenum (Mo – 2.80-3.30%), Titanium (Ti – 0.65-1.15%), Aluminum (Al – 0.20-0.80%), Cobalt (Co – 1.00% maximum), Carbon (C – 0.08% maximum), Manganese (Mn – 0.35% maximum), Silicon (Si – 0.35% maximum), Phosphorus

A cross-section cut was made through the center anomaly, perpendicular to the centerline of the bore, on fracture surface 2 (**PHOTOS 58**). The etched cross-section revealed a lighter area with larger grains than the darker and finer grain structure of the surrounding material. The lighter etched area measured approximately 0.15-inches along its longest (major) axis and was approximately 0.1-inches at its maximum width. The light etched area was consistent with and identified as a 'discrete white spot' (DWS). DWSs appear bright, have a distinct boundary, and the grain size may be equivalent to or larger than the matrix grain size (Jackman 1994). EDS analysis revealed that the DWS was lean in niobium (Nb) compared to the surrounding material, another characteristic of a DWS. Further examination of the light etched area revealed the presence of oxides and nitrides stringers. DWSs that are associated with clusters of oxide, nitride, and/or carbonitride particles are referred to as discrete "dirty" white spots (DDWS).[13] DDWSs form during the melt process and the stringers set up stress risers where cracks are more prone to initiate.
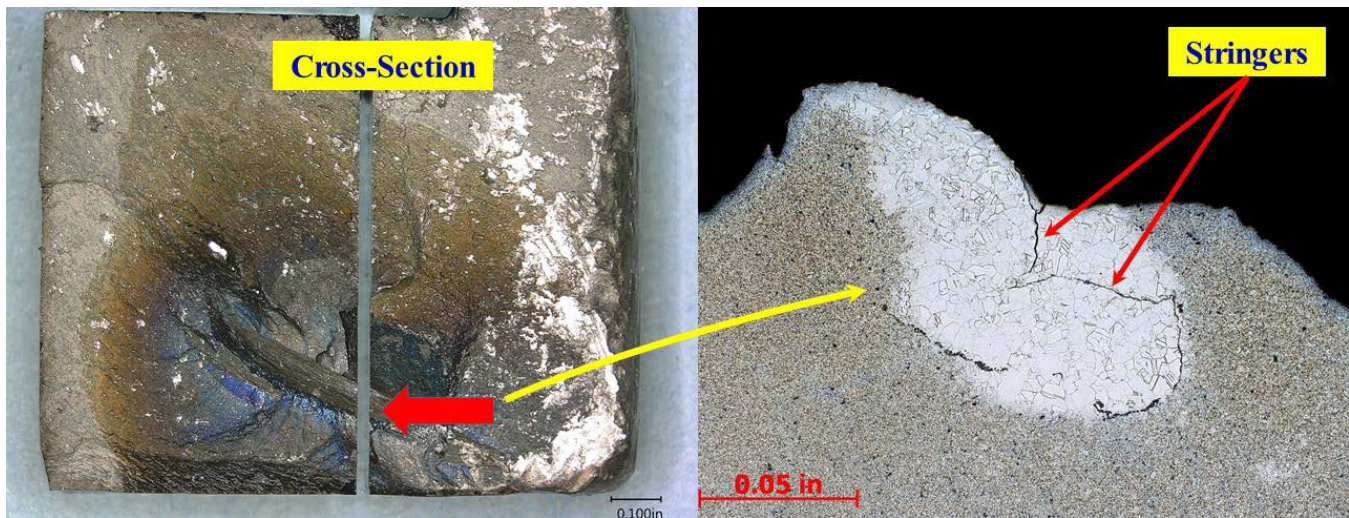
PHOTO 58: CROSS-SECTION VIEW OF ANOMALY IDENTIFIED AS A DISCRETE DIRTY WHITE SPOT

The metallurgical group identified six separate cracks initiating from the 'discrete dirty white spot'; some propagated inboard and some towards the bore. The NTSB conducted a striation density study (see Materials Laboratory Study Report 17-034S for details) on fracture surface 1 on crack Nos. 1, 2, and 6 emanating from the internal elliptical anomalies.[14] The cracks were arbitrarily numbered for documentation purposes (See **FIGURE 9** for crack locations). The purpose of striation density measurements was to estimate the number of flight cycles that elapsed between crack initiation and fracture. One striation correlates with one flight cycle where a flight cycle is assumed to include one takeoff and landing. The NTSB estimated the striation counts to be approximately 5,700 cycles, 5,600 cycles, and 3,700 cycles for cracks No. 1, No. 2, and No. 6 respectively.

Along with examining the main fracture surfaces 1 and 2, the NTSB also examined the other disk fracture surfaces; the on-scene fractures identified as between 'B' and 'C', 'C' and 'D', and 'A' and 'C'. All these fractures surfaces exhibited features consistent with overstress fractures. The overstress fractures on the disk fragments collected from the runway, fragments 'B', 'C', and 'D' are consistent with the HPT stage 2 disk initially separating into two halves, fragments 'A' and 'B'. Fragment 'A' penetrated inboard of the right wing and was recovered from the UPS building as the intact fragment 'A' while initial

---

(P – 0.015% maximum), Sulfur (S – 0.015% maximum), Boron (B – 0.006% maximum), and Copper (Cu – 0.30% maximum). Material composition is from the Special Metals Technical Bulletin for Inconel® alloy 718, copyright Sept 2007.

[13] Also referred to as 'discrete dirty white spot'. 'Discrete dirty white spot' or 'dirty discrete white spot'; both are correct.

[14] Striations are linear features on a fatigue fracture surface that indicate how far the crack advances with each stress cycle.

fragment 'B' impacted runway 28R fracturing into the three pieces later recovered and identified as fragments 'B', 'C', and 'D'.

3.2   GE EVALUATION

When the NTSB completed their examination of the HPT stage 2 disk fragments, GE performed their own fractographic and metallographic evaluation as well as striation counts. GE performed additional cross-sections through the DDWS which revealed that the exposed anomalies seen on the fracture surface were consistent with being part of a single DDWS that spanned a length of approximately 0.783-inch. GE plotted a striation curve for six cracks initiating from the DDWS as a function of the distance from the origin. Again, one striation corresponds to one flight cycle. The striation count varied from as little as about 1,700 cycles for crack No. 4 to as many as about 7,000 cycles for crack No. 6; each crack, however, had its own unique crack length and path before tensile overload (**FIGURE 9**)[15]. Striation density analysis is a calculated estimate of the total number of cycles from crack initiation (origin) to fracture; each individual cycle is **not** counted. Instead, striations (cycles) are counted/measured in discrete areas along the crack path. Differences in where the cycle count starts, ends, and the location and frequency of the individual measurements all affect the final cycle count total; therefore, variations in the cycle count number are not unexpected.

GE concluded that: "The amount of cycles for the crack to breach the disk surface could not be determined due to multiple crack fronts progressing with unknown initiation times." According to GE, the striation density steeply decreased as the crack progressed away from the origin, a behavior consistent with higher alternating stress, low-cycle fatigue (LCF) crack propagation mechanisms. Fracture morphology beyond the striated region had a dimpled morphology, consistent with tensile overload.
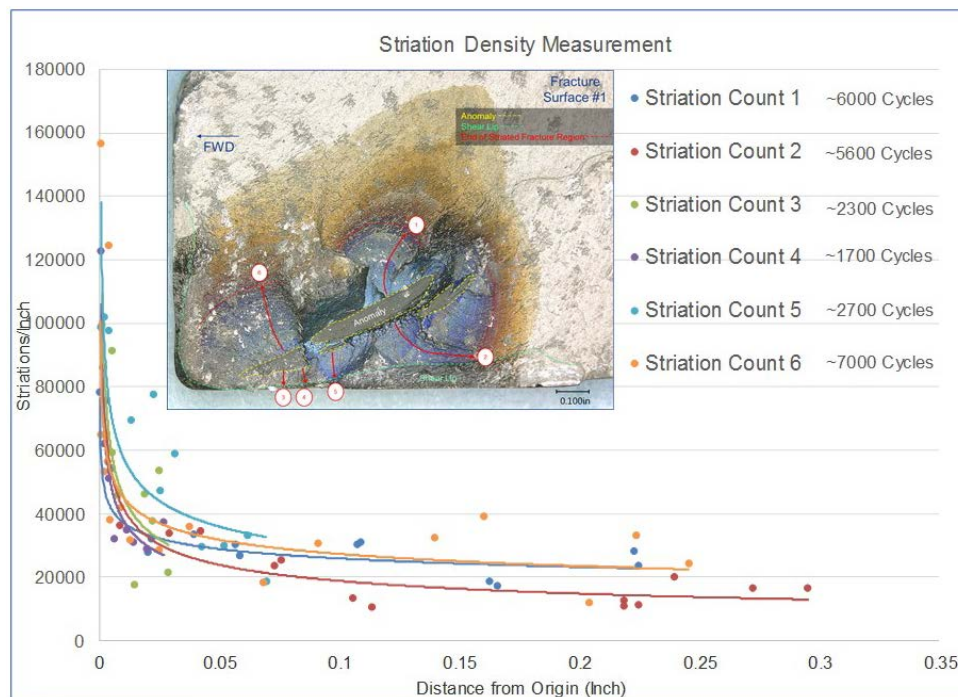
FIGURE 9: STRIATION DENSITY CURVES CREATED BY GE

FIGURE COURTESY OF GE

---

[15] Based on the GE striation evaluation, the number of cycles from initiation to failure was estimated to be about 6,000 cycles, 5,600 cycles, 2,300 cycles, 1,700 cycles; 2,700 cycles and 7,000 cycles for cracks Nos. 1 through 6, respectively.

In addition to the striation count analysis, GE conducted wavelength dispersive spectroscopy (WDS) on the DDWS. WDS is similar to EDS in that both techniques bombard the sample with electrons and the X-rays reflected off are used to identify the elemental constituents; a spectrum (energy level) of elemental peaks are created that easily identify the individual elements. The main difference is that the EDS acquires the reflective energies all at once, making it quick and simple, while the WDS acquires the energy sequentially as the full wavelength range is scanned. This means that it takes longer to perform a WDS than an EDS analysis; however, WDS provides better data resolution. According to GE, the WDS traces through the DDWS revealed the expected decrease in Nb content consistent with a DDWS and elevated Al, Mg, O, Ti, and Ni, similar to that found during EDS analysis. Bulk chemistry and hardness traverses performed on the DDWS and parent material revealed that the parent material met the requirements of chemistry and hardness; the average hardness for the DDWS was 43 Rockwell Hardness "C" Scale (HRC) which was slightly less than the typical average of 46 HRC for the parent material. There were no apparent voids/cracks between the anomaly and the rest of the parent material matrix noted during the metallographic examination.

3.3 WHITE SPOT[16]

White spots (WS) are classified into three types: 'discrete', 'dendritic', and 'solidification'. Since the event disk anomaly was characterized as a 'discrete white spot', this will be the only one described in detail. 'Discrete white spots' are areas in the material where there is a slight depletion of Niobium (Nb), a constituent of Inconel® alloy 718, and carbon, as evidenced by a reduced density of carbides, compared to the surrounding material. DWSs associated with clusters of oxide, nitride, and/or carbonitride particles are referred to as "dirty" discrete white spots (DDWS). White spots form typically when solid pieces of the original ingot melt detach ("fall-in") from the torus, shelf, or

FIGURE 10: WHITE SPOT FORMATION
FIGURE FROM (JACKMAN 1994) (MOYER 1994)

crown and sink through the molten liquid layer and become entrapped in the newly created ingot before the piece becomes completely molten (**FIGURE 10**). Heat transfer models confirm that "fall-in" solids can fail to melt completely and can subsequently be entrapped by the advancing solidification front. White spots are less likely to occur in an ESR ingot than in VAR ingots because dendrite skeletons or small broken pieces from the electrode must pass through the superheated slag giving them more time to become molten before they reach the solidification front; thus, preventing white spots[17]. It is widely accepted that white spots formation is an inherent characteristic of the VAR process. The data seems to suggest however, that the frequency of 'discrete white spot' formation (number of Ultrasonic Test Inspection (UTI) indications) using a triple-melt process is reduced versus a double-melt process.

Not all white spots are considered detrimental; it is the associated crack that can be problematic. Solidification white spots, which have not been discussed in detail, appear to have little effect

---

[16] Information in this section are cited from: (Moyer 1994) and (Jackman 1994) unless otherwise cited.
[17] (AMG - Advanced Metallurgical Group - Netherlands n.d.)

on mechanical properties. Discrete and dendritic (also not discussed in detail) may have a harmful effect based on the size, chemistry, grain size, and the presence or absence of oxide/nitride clusters. If the oxide/nitride clusters are sufficiently large, a crack can form during the forging process at either the billet or forging level. The UTI data seems to indicate that many indications in superalloys turn out to be cracks at clusters of inclusions associated with 'discrete white spots'.

3.4 "STEALTH" ANOMALIES

The FAA issued report DOT/FAA/AR-07/13 titled *Turbine Rotor Material Design-Phase II,* dated April 2008 (DOT/FAA/AR-07/13 April 2008). The report states that

> Historically, a number of rotor disk fracture and cracking events have originated from embedded anomalies, which, although they were substantial in size, were undetected by production inspections. These anomalies have been called "stealth" anomalies due to their ability to evade inspection detection; i.e., the reflected signal is small relative to the inclusion size.

The report goes on to list several types of "stealth" anomalies; however, one specific type is mentioned that is somewhat consistent with the 'discrete white spots' found on the event HPT stage 2 disk. One category of "stealth" anomaly consists of a type that is

> …ductile and well bonded, making them less likely to have cracking and voiding during ingot and billet conversion. The lack of cracking and voiding, combined with a similarity in elastic modulus and density to the parent alloy, renders them indistinguishable from the parent alloy for sonic detection. These anomalies… form a zone of material that is substantially weaker in tensile and fatigue capability than base metal.

Metallurgical evaluation found no voids or cracking at the interface between the DDWS and the parent material. The DDWS and the parent material had similar densities.

3.5 WHITE SPOT EVALUATION AND COMPARISON PERFORMED BY GE AND ATI

GE and ATI conducted a study of DWS samples that were detected by UTI and retained from billets produced during the last 30 months to better understand and categorize UTI response characteristics and to compare them with the structure and characteristics of the event DDWs. Six samples representative of typical DWS for size, shape, stringer distribution, and radial location within the billet were examined (See GE *Metallurgical Investigation Report Log No. FA2017-18058* for complete details on the evaluation process).

Of the six samples examined metallographically, five had voids/cracks while the sixth was inconclusive. Complete microstructural evaluation of the sixth sample was not possible due to sample preparation techniques used to extract the anomaly. The six samples exhibited stringers similar in morphology to what was observed on the event DDWS; however, five of the samples, unlike the event DDWS, exhibited voids/cracks. GE and ATI concluded that the voids/cracks "…may provide a reflection surface that is more conducive to ultrasonic detection." This conclusion is consistent with FAA report DOT/FAA/AR-07/13 cited in Section 3.4 *Stealth Anomalies* that stated "…lack of cracking and voiding, combined with a similarity in elastic modulus and density to the parent alloy, renders them indistinguishable from the parent alloy for sonic detection."

4.0   MANUFACTURING HISTORY OF THE EVENT HPT STAGE 2 DISK, SN MUNBB592

4.1   MANUFACTURING HISTORY

The event HPT stage 2 disk, SN MUNBB592, was made of Inconel® alloy 718 and the nickel alloy ingots/billets used to produce the disk were created and supplied by ATI Specialty Materials (for the remainder of this report ATI Specialty Materials will be referred to simply as ATI) in their Monroe, North Carolina facility in 1997. ATI used a triple-melt process - Vacuum Induction Melting (VIM), Electroslag Remelting (ESR), and Vacuum Arc Remelting (VAR) - in that order to create the event ingots/billets. After the melt/remelt processes were completed, ATI performed the billet conversion process, inspected the billets using an UTI technique, and cut the billets into the various lengths as required by the forger. ATI certified the event billets in June 1997 before shipping them to the forger, Wyman-Gordon (WG) in Houston Texas. After receiving the billets from ATI, WG cut the billets into smaller pieces of a specified length needed to produce the intended part. These smaller pieces were then press forged and rough machined into a shape close to the desired configuration of the finished part. WG certified the event forging in August 1997 and sent it to MTU for pre-machining, UTI, finished machining, shot peening, visual and dimensional inspection, and final part marking. In March 1998, MTU shipped the event disk PN 9362M43P04, SN MUNBB592, to GE for installation into ESN 690-373 in that same month-year.

FIGURE 11 provides the workflow process for the creation of the ingots and billets. From the initial Master Heat identified as FA94, five ingots/billets identified as FA94-1, FA94-2, FA94-3, FA94-4, and FA94-5 were produced. The event HPT stage 2 disk, SN MUNBB592, was produced from ingot/billet No. 2 identified as FA94-2. After the triple-melt process is completed, the ingots undergo a billet conversion process and the ingot identifier transfers to the billet; therefore, after the billet conversion process, ingot FA94-2 becomes billet FA94-2.
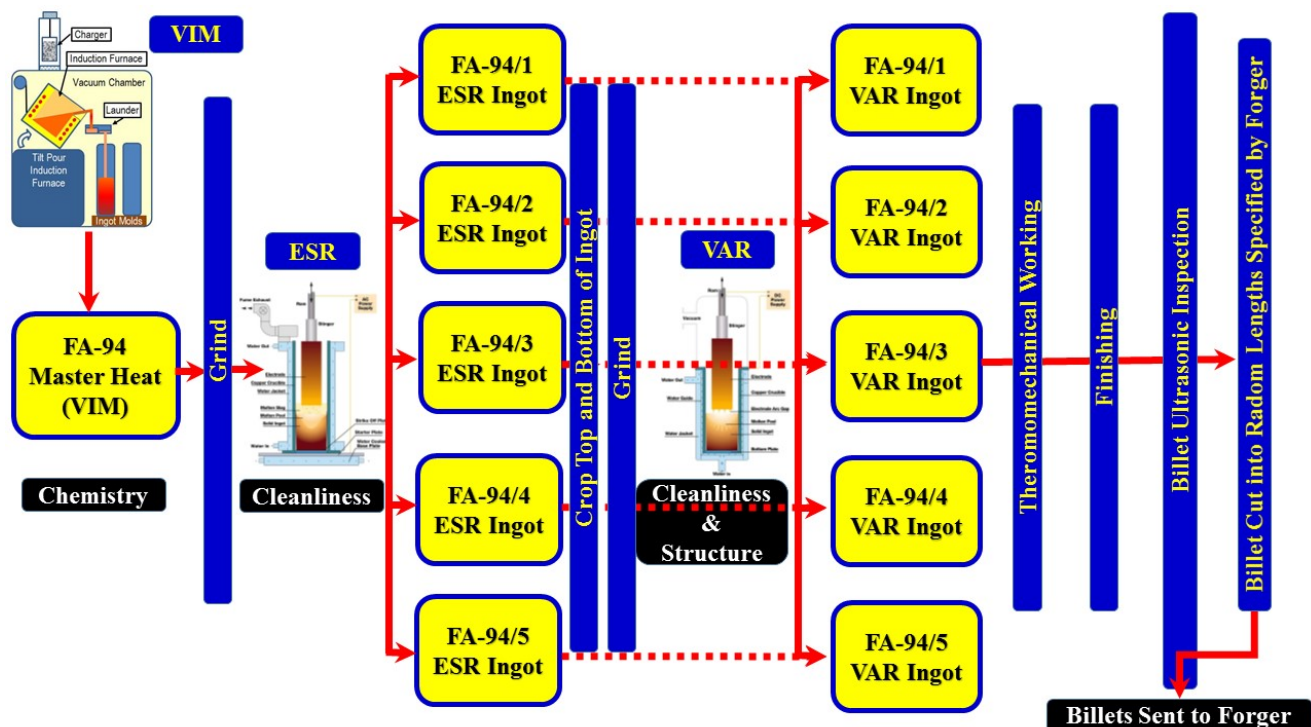
FIGURE 11: MATERIAL WORK FLOW PROGRESS – STEPS PERFORMED BY ATI

4.2 MANUFACTURING PROCESS

The Inconel® alloy 718 used to produce the event disk was created using a triple-melt process. The first melt, referred to as the Master Heat, is the Vacuum Induction Melting (VIM) process that melts, homogenizes, and refines raw material to establish the desired chemistry (**FIGURE 12**). Essentially the VIM furnace uses an electromagnetic induction-heated melting crucible inside an evacuated chamber. The primary purpose of the VIM process is to establish the desired chemistry and secondarily to refine the material by removing impurities. The raw material, referred to as 'charge', generally consists of several types of material: elemental material (in this case Ni), master alloy, scrap (revert) from previous melts or turnings/swarf, and reactive material[18] that assists in the solubility of the oxides and nitrides to help remove any impurities. All the material is not melted at once; as the initial 'charge' is melted, additional 'charges' consisting of the reactive material, scrap, etc. are added. One way to inhibit the formation of impurities is by melting the raw material in a vacuum; this reduces the oxygen and nitrogen content to inhibit the formation of oxides or nitrides. Evacuating the chamber also removes the outgas byproduct such as oxygen and nitrogen that

FIGURE 12: TYPICAL VIM PROCESS
FIGURE COURTESY OF ATI

occurs in response to the low partial pressure when the 'charge' is molten and removes unwanted contaminants with high vapor pressure; the outgas byproducts all contribute to the creation of unwanted compounds. Cleanliness of the material can be greatly enhanced by selecting the correct material of the crucible in combination with the 'charge' reactive material, and process controls for temperature, duration, and stir rate (agitation of the molten mixture) and deslagging.[19] The material can be stirred using an electromagnetic field but gas stirring can also be an option. After the material is completely melted and the material well stirred/agitated, an in-process sample is taken to ensure the correct chemistry. Essentially, a ladle is dipped into the molten material and a sample (also referred to as a 'dip') is extracted for evaluation. If the desired chemistry is not met, then additional material can be added as needed. The VIM process is the only step where the proper chemistry of the material is established and modified. Prior to the pour that creates the VIM ingots, an additional sample is extracted for final evaluation. The final step is to pour the molten material into a vertical mold creating a cast ingot that will become the electrode for the ESR process. The event Master Heat FA94 was used to create five VIM ingots designated as FA94-1, FA92-2, FA94-3, FA94-4, and FA94-5.

---

[18] (ASM Handbook, Volumne 15: Casting 2008)
[19] (ASM Handbook, Volumne 15: Casting 2008)

The second melt, referred to as the Electroslag Remelting (ESR) process, establishes the cleanliness of the material (**FIGURE 13**). The process involves continuously melting the VIM ingot (which acts like a consumable electrode) through a molten bath of electrically and metallurgical active/reactive slag and collecting the purified material in a water-cooled mold. A stub, also referred to as a 'stinger', is welded to the ingot and it serves to provide a current path to complete the electrical circuit and as a means for structurally supporting the ingot during the ESR process. The process starts by running an electrical current, typically an alternating current (AC), through the electrically conductive slag in a water-cooled mold creating a superheated slag layer. The ingot is lowered into the slag layer that acts like a refining agent and is melted creating droplets that sink through the molten slag. The density of the consumable ingot must be higher than that of the slag and the viscosity of the molten slag must be such that the ingot droplets sink to the bottom of mold instead of becoming suspended within the slag. When the droplets reach the bottom of the water-cooled mold they solidify creating a new ingot. The refined/purified ingot material builds up from the bottom of

FIGURE 13: TYPICAL ESR PROCESS
FIGURE COURTESY OF ATI

the mold moving the slag layer up in the process. As the droplets descend through the superheated slag, impurities dissolve or bind with the reactive elements within the slag and float towards the top. The floating slag layer not only serves as the melting and reactive agent, but also acts like a barrier between the consumable electrode (the VIM ingot) and the new ingot to prevent oxidation.[20] In addition, as the new ingot is created, a thin layer of slag is built up between the new ingot and the mold that also helps reduce the formation of oxides on the surface. To ensure the homogeneity and cleanliness of the new ingot and to prevent the formation of defects, it is important to select the appropriate slag material for the desired ingot composition as well as close adherence to and monitoring of the slag temperature, melt rates, and ingot (electrode) feed rates. The slag material should provide the proper electrical conductively, viscosity, and chemical reactivity and is typically composed of calcium fluoride (CaF_2), lime (CaO), and various aluminum, magnesium, and silicon oxides. The five VIM ingots were converted into five ESR ingots designated as FA94-1, FA94-2, FA94-3, FA94-4, and FA94-5. VIM ingot FA94-1 became ESR ingot FA94-1, VIM ingot FA94-2 became ESR ingot FA94-2 and so on; the ingot/billet designation stays with the piece throughout the process.

Before the ESR ingots undergo the VAR process, ATI removes any scale on the outside of the ingot. During the melting and subsequent cooling/solidification of the ESR ingot, the two transition areas, where the temperature is least stable and where resolidification material defects are most likely to form, are the top and bottom of the ingot. The bottom (referred to as the startup) and the top (referred to as the hot top) are cut and removed to reduce contamination.

---
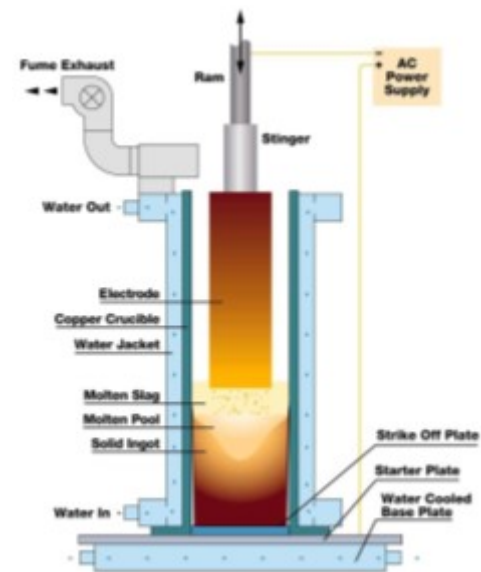
[20] (CONSARC n.d.)

The third and final melt, referred to as the Vacuum Arc Remelting (VAR) process, further refines the cleanliness of the material but the main function is to establish the desired microstructure (**FIGURE 14**). This third melt takes some of the features from the VIM and ESR melt processes and adds some additional ones. Similar to the ESR process, a 'stinger' is welded to the ingot to provide a current path to complete the electrical circuit as well as a means for structurally supporting the ingot during the VAR process. Like the VIM process, the VAR process is performed in a vacuum to promote the cleanliness of the new ingot by inhibiting the formation of oxides or nitrides by reducing the oxygen and nitrogen content while also removing outgas byproducts. Similar to the ESR, VAR melt is a continuous melt process where the original ingot is consumed and a new ingot is formed by collecting the new melted material in a water-cooled mold. Unlike the ESR process, the melting of the original ingot (consumable electrode) is not done by a molten slag mixture but instead the ingot is suspended near the newly formed ingot establishing a defined gap sometimes referred to as the "arc zone". A high power direct current (DC) is applied between the original ingot and the newly formed ingot creating a high-temperature arc that melts the original ingot.[21] As molten droplets fall through the arc gap/zone under a vacuum, the dissolved gases (outgases) are removed;

FIGURE 14: TYPICAL VAR PROCESS
FIGURE COURTESY OF ATI

unwanted or entrapped containments are vaporized; and oxide cleanliness is improved. Similar to the ESR process, the water-cooled crucible allows for a solidification of the ingot as it builds up from the bottom of the mold. Because the VAR process is in a vacuum, many of the metallurgical advantages that applied to the VIM process also apply to the VAR process as well. Close process controls on ingot feed rate, arc gap, energy input (current flow), solidification rate, and temperature gradient between the liquid and solid boundary help achieve a homogenous and directionally solidified (dendritic primary structure) structure that reduces or eliminates macro or micro-segregation.[22] The five ESR ingots were converted into VAR ingots designated again as FA94-1, FA94-2, FA94-3, FA94-4, and FA94-5.

After the VAR process, ATI performed one more operation to remove scale from the ingot before it was further processed. After the scale is removed, the ingot undergoes a billet conversion process. This step changes the non-uniform coarse microstructure of the cast ingot to a more refined and uniform billet state suitable for forging (recrystallization). Recrystallization is essentially changing the original cast coarse grain structure of the ingot by replacing it with a new and more desirable recrystallized grain structure (finer grain structure). This conversion is a two-step process. First step is a thermal heat treat process called homogenization and the second is a mechanical hot-worked forging/wrought process. During the VAR, chemical segregation of the various elements can occur reducing the mechanical properties of Inconel® alloy 718; this reduces the LCF capability of the material and can form crack initiation sites and promote crack propagation (DiConza 1991). Homogenization of the ingot is intended to dissolve and diffuse these segregation areas to create a more chemically uniform material. Furthermore, the mechanical properties of Inconel® alloy 718 can be dramatically reduced with the large precipitate and grain size that are created

---

[21] The way the DC current is applied, the original ingot acting like the (cathode (-) negative pole) and mold/crucible acting like the (anode (+) positive pole).
[22] (AMG - Advanced Metallurgical Group - Netherlands n.d.)

during the VAR remelting. Therefore, thermal and mechanical processes are used to refine the precipitates and grains to achieve the desired microstructure and uniformity. Unlike the melting process where each ingot is melted/remelted/processed individually, the homogenization was performed with multiple ingots. According to the production records, ingots FA94-1, FA94-2, and FA94-4 were all homogenized together.

The first mechanical step after homogenization heat treat is press forging, there are two steps to the press forging process: 1) "upset" (axial compression to increase the diameter) (**FIGURE 15**) and 2) "cog/drawn" (the workpiece is turned/rotated and the diameter is decreased while the length increases). During the press forging process, the coarse grains of the cast ingot are broken up and replaced by finer grains as the length of the ingot increases and the diameter decreases. Both steps are performed using an open-die; work piece constrained on two sides by each die that permit the unconstrained areas to swell/expand during the process. The dies are either flat or V-shaped, both have their advantages and disadvantages. This press forging process is repeated multiple times until the material has reached the desired size, shape, and refined microstructure. Since this process is time consuming, the ingot must be reheated often to ensure that it remains malleable and to prevent cracking if the material cools too much. According to the production records for the furnace used to heat the ingots for the press forging operation, ingots FA94-1 and FA94-2 were paired and converted using alternating press and furnace cycles to ensure the ingots remain at the desired temperature.

After the press forging process is completed, the next mechanical step performed is radial forging to the desired shape to complete conversion from ingot to billet. For the event ingot, ATI utilizes a very common radial forging machine referred to as GFM[23] (Gesellschaft für Fertigungstechnik und Maschinenbau). The GFM is a semi closed-die process comprised of four hammers that are orientated 90º (right angle) to the work piece. The word 'hammer' is a bit of a misnomer; the dies do not actually hammer on the work piece even though the high stroke rate and short stroke distance makes it appear to do so (**FIGURE 16**). Instead, each hammer presses simultaneously and only a small localized area is deformed; the workpiece is rotated and fed between compression strokes. The GFM radial process has several advantages: 1) the offsetting motion of the hammers almost eliminates all stresses and vibration to the forging machine and its foundation, 2) since only a small localized area is deformed at a time, forging forces are relatively low as compared to press forging, 3) edge cracks are dramatically reduced since the deformed area is almost entirely under compression, 4) heat losses are minimal and in some cases the workpiece temperature may increase from the deformation by the hammers, and 5) provides a more uniform shape than the open-die process (Domblesky 1994). According to the production records for the radial forging process, ingots FA94-1, FA94-2, and FA94-4 were paired together. For the event billet (FA94-2), the VAR ingot after billet conversion became a 10-inch round diameter billet.

---

[23] The basic configuration of the radial forging machine was initially developed by Dr. Bruno Kralowetz who founded **GFM** in Steyr, Austria in 1946 and the first four hammer working model of the machine was introduced in 1960 (Domblesky 1994).
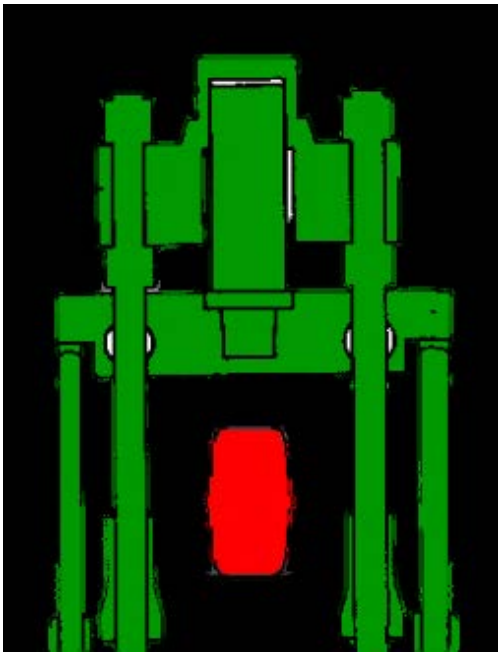
FIGURE 15: UPSET FORGING
FIGURE COURTESY OF ATI
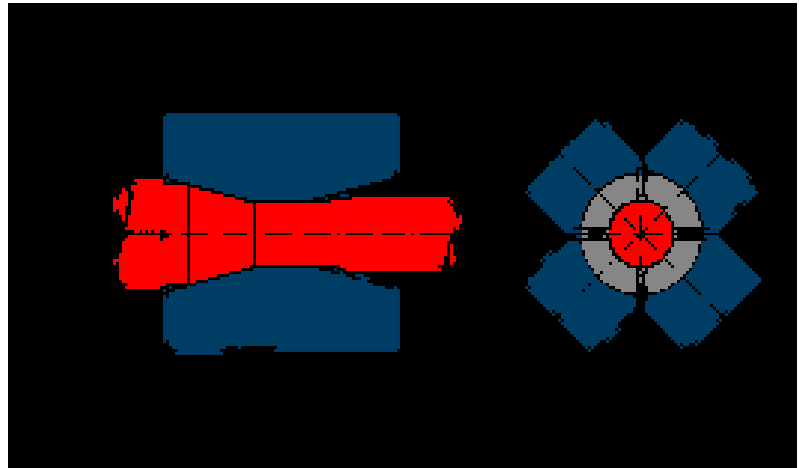
FIGURE 16: GFM FORGING
FIGURE COURTESY OF ATI

After completion of the billet conversion process, the billets were prepared for inspection. ATI first saw-cut the ends (hot top and startup bottom) because these are the areas where defects are most likely to form because the process is more transient and less stable. Additional cuts (samples) were then made at the top and bottom of the billet for visual macroscopic inspection. The final step in preparation for the UTI was a machining operation termed "peeling" and polishing to enhance the inspection effectiveness. ATI used GE specification P3TF15 titled *Ultrasonic Inspection of Billet – Immersion* UTI Class 'C' and 'E' requirements for the billets. The billets were inspected longitudinally along the full axial length as they were rotated to ensure full coverage; the process used in 1997 is the same process ATI uses currently. P3TF15 calls for a surface finish for the polishing step to be 125 micro-inches or better which "will normally ensure inspectability"; review of the ATI production records revealed that the billet was polished to 125 RMS (root mean square micro-inches) in adherence to the GE specification.

As part of the production requirement, an ultrasonic billet map is created for each billet and it provides the location of any rejectable indications, non-rejectable indications, macro-slice areas, and area cutouts where rejectable indications were cut out of the material. Review of the *Ultrasonic Billet* map sheet for FA94-2, dated June 18, 1997, revealed no found defects/rejections in billet FA94-2; (See Section 4.4.3 *UTI Performed by ATI* for additional details). Had a defect been identified, that area would have been cut, removed, and evaluated; the production records did not show any of these procedures.

Once billet FA94-2 was deemed acceptable (passed all the chemical, macro, visual inspection, UTI, dimensional inspection, etc.), ATI cut the billet to the weight or length as specified by the forger, in this case as WG had requested. Review of the ATI Certification Test sheet for billet FA94-2, dated June 17, 1997, indicated that metallography, microstructure, and grain size were acceptable per specification; UTI was performed per specification P3TF15C, S12 Amendment 1, with no defects (acceptable) found, and macro-inspection was acceptable.

WG received the event billet, FA94-2, in their Houston, Texas facility where they cut it into nine pieces; each piece to provide the exact length of material needed to create the designated parts. These stock forging pieces are commonly referred to as 'mults' (multiples). The 'mults' were press forged, heat treated, and rough-machined (**FIGURE 17**). WG completed the forging, heat treat, and rough-machining for the event disk and identified it as WG SN CBGS1293. WG shipped forging SN CBGS1293 to MTU for finish machining and final inspection.

FIGURE 17: PRESS FORGING STEPS
FIGURE COURTESY OF GE

MTU performed pre-machining and cleaning operations before the UTI of forging SN CBGS1293.[24] The pre-machining process produces what is referred to as a 'sonic shape', which is the configuration ready for the UTI. MTU has their own internal ultrasonic inspection work instructions[25], which GE approved and which meet the requirements of GE Aviation's specification P3TF1 titled *Ultrasonic Inspection* Class 'A' longitudinal and circumferential shear UTI requirements. P3TF1 states that a surface finish of 90 micro-inches[26] for longitudinal wave and circumferential shear wave "…will usually provide ultrasonic inspection with acceptable surface noise effects." The surface finish measurements were not recorded (nor were they required to be according to specification P3TF1) on the MTU router. After the UTI, additional machining, shot peening and final visual, dimensional and FPI was performed. MTU inspected the disk using a high sensitivity FPI per GE specification P3TF47 titled *Fluorescent Penetrant Inspection (FPI)*, issue number S5. Just prior to the final visual, dimensional, and FPI, the HPT stage 2 disk was stamped with the identifiers PN 9362M43P04 and SN MUNBB592. Review of the MTU Final Inspection sheet for disk SN MUNBB592, dated February 3, 1998, indicated that the disk was acceptable.

4.3   ATI SITE VISIT

The Powerplant Group, comprised of persons from GE, AA, FAA, Boeing, and the NTSB, convened at the ATI facility in Monroe, NC from February 21-22, 2017 to observe the production process and to review the production records for the Master Heat FA94 and ingot/billet FA94-2. Although the Powerplant Group did not witness the production of an individual Inconel® alloy 718 ingot/billet from start to finish (this is a lengthy process lasting weeks), each step (See **FIGURE 11**) in the process was observed; triple-melt, billet conversion, inspection, and laboratory analysis. According to ATI, the furnaces and billet conversion machines used to produce the event ingot/billet in 1997 are still in use today, as is the UTI equipment except for the individual probes, which are changed periodically (See Section 4.4.3 *UTI Performed by ATI* for details).

Review of the production records for Master Heat FA94 did not reveal or identify any anomalies or deviations from the approved process. GE reviewed the production records for Master Heat FA94 and compared it with other ingots/billets produced by ATI for them during that same time. Based on that review, GE concluded the following: 1) no practices or processing records were identified that indicate

---

[24] Review of the MTU router showed that 5 pieces were processed on one router and only one piece, forging CBGS1293, was from the event Master Heat FA94.

[25] The MTU UTI has a generic UTI inspection process specification, MTV1033 titled *Ultrasonic inspection of axisymmetric components by the immersion technique* that provides the instructions and requirements for UTI that is similar to GE UTI specification P3TF1 Class 'A'. MTU also developed a specific inspection sheet, *UT 9362M43P04-U* that specifies C50TF103 Class 'B' material (this is the GE specification for Premium quality triple-melt Inconel® alloy 718) and has the scan plan details for PN 9362M43P04 disk.

[26] For surface finishes, the higher the number the rougher the surface finish; the surface finish requirement for the billet was 125 micro-inches while for the sonic shape, which is a more refined material was 90 micro-inches.

that the Master Heat FA94 had a different potential for 'white spot' formation than other heats produced with approved practices in place at the time and 2) there were no practices or processing records identified that would indicate ingot FA94-2 had a different potential for 'white spot' formation than other ingots of the Master Heat FA94.

4.4   INSPECTIONS – EVENT BILLET AND FORGING

4.4.1   General UTI Information

UTI is an effective non-destructive inspection (NDI) method to detect surface and subsurface anomalies and can accurately determine position, size (sometimes), and shape of those anomalies. UTI uses high frequency mechanical waves (vibration), produced by a transducer(s) that propagate through the material/test specimen by means of compression and decompression (essentially forcing the atoms in the material to vibrate/oscillate) in the form of acoustic waves. The detection of discontinuities and their location is determined by interpreting the ultrasonic reflective (echoes) waves captured by the transducer(s). The acoustic waves reflect off any discontinuities/boundaries/interfaces where a change in acoustic impedance is present, such as a wall, corner, void, crack, interface (air, water, or couplant), change in material density etc. This change in impedance is referred to as an impedance mismatch and the greater the impendence mismatch the greater the amount of energy is reflected and the easier it is to detect the anomaly.

Other NDI methods, such as FPI, ECI, and x-ray, **<u>do not</u>** have the capability to detect surface and subsurface (FPI and ECI are surface (ECI also has some near surface capability[27]) inspection techniques) anomalies at the UTI sensitivity levels. However, UTI is not without its limitations. For example, the coarse material surface roughness, non-homogeneity, and coarse instead of fine grain structure can diminish the effectiveness of UTI. Furthermore, if anomalies are thin and parallel to the acoustic wave propagation direction, they may be hard to detect or may even be undetectable. The FAA issued report DOT/FAA/AR-07/13 titled *Turbine Rotor Material Design - Phase II,* dated April 2008, touched on undetectable production defects. The intent of the report was to provide the results of the FAA's effort in working with the aircraft engine industry to develop an enhanced life management process, based on probabilistic damage tolerance principles, to address the threat of material or production anomalies in high energy rotating components and to developed enhanced predictive tool capability and supplementary material/anomaly behavior characterization and modeling to support and enhance the process. The report stated that:

> Historically, a number of rotor disk fracture and cracking events have originated from embedded anomalies, which, although they were substantial in size, were undetected by production inspections. These anomalies have been called "stealth" anomalies due to their ability to evade inspection detection; i.e., the reflected signal is small relative to the inclusion size (DOT/FAA/AR-07/13 April 2008).

This reflects the FAA's and the aircraft engine industries' acknowledgement of the potential for production anomalies to go unnoticed despite the best efforts of inspections. The report goes on to list several types of "stealth" anomalies; however, one specific type is very similar to the AA event DDWS anomaly and consists of a type that is

> "…ductile and well bonded, making them less likely to have cracking and voiding during ingot and billet conversion. The lack of cracking and voiding, combined with a similarity in elastic

---

[27] The ECI for the HPT stage 2 disk inspects to a depth of approximately 0.013-inches.

modulus and density to the parent alloy, renders them indistinguishable from the parent alloy for sonic detection." and "These anomalies… form a zone of material that is substantially weaker in tensile and fatigue capability than base metal" (DOT/FAA/AR-07/13 April 2008).

There are essentially two types of UTI techniques: a pass-through transmission that requires access to both sides of the inspected material or the pulse-echo that requires access to only one side. Since ATI and MTU both employed the pulse-echo UTI technique, this will be the only one discussed here. The location, size (sometimes), and orientation of the discontinuity using pulse-echo UTI is measured as a function of the time required for the pulsed sound wave from the transducer to propagate through the test specimen and reflect/echo off the discontinuity (back surface, crack, void, etc.) back to the same transducer. The location of the discontinuity can be determined as a function of the time the echo returns to the transducer in comparison with the normal reflective wave from a known discontinuity such as a backwall, corner, etc. The size of the discontinuity can be determined by the strength (amplitude) of the echo return. Defect sizing is not solely based on the amplitude of the return signal but must be correlated with a known defect size.

Transducers come in two basic types, contact and immersion. As the names imply, a contact transducer is in physical contact with the test specimen through a thin layer of couplant while an immersion transducer utilizes water as a couplant allowing for a greater standoff distance from the test specimen. In immersion UTI, the transducer and the test specimen are submerged in a water tank and the transducer's cables are electrically sealed and made waterproof. The acoustic wave travels from the transducer through the water and into the test specimen and back to the transducer; the advantage of the immersion technique is the ease of moving the transducer and test specimen relative to one another while remaining acoustically coupled. Since ATI and MTU both use immersion echo-pulse transducers to perform the UTI, this will be the only one discussed here.

4.4.2   General UTI Equipment and Process

In its simplest form, the pulse-echo technique typically involves a pulser/receiver, a transducer(s), and a display unit. The pulser/receiver unit generates a high voltage electrical pulse that the transducer(s) convert into an acoustic wave transmitted to the test specimen. The transducer(s) then receives back the reflective signal that it electrically converts to send to the display unit for graphical representation. The transducer is typically constructed of three essential parts: 1) a backing plate, 2) the piezoelectric element (active element), and 3) matching/wear plate. The backing plate supports the piezoelectric element and dampens the acoustic wave. Matching the impedance of the backing plate and piezoelectric element increases the bandwidth thus increasing the transducer's sensitivity and resolution. Sensitivity and resolution are measures defining the effectiveness of an inspection technique and are discussed later. Bandwidth refers to the frequency range that the transducer can accommodate; highly damped transducers have high resolution but poor depth penetration while less damped transducers have greater penetration but less resolution, so selection of the damping characteristics must match the intent of the inspection criteria. The piezoelectric element is what turns the electrical signal from the pulser/receiver into a mechanical acoustic signal and vice versa. The matching layer serves to match the acoustic impedance of the piezoelectric (active) element to the medium, and in the case of the immersion transducer, to water.

The piezoelectric transducer surface does not produce a focused single point acoustic wave but rather a series of acoustic waves along the entire surface referred to as beam or front. These acoustic waves interfere and interact with one another creating a turbulent and non-uniform wave zone referred to as the "near field" (**FIGURE 18**). The interference and interaction is greatest near the transducer and dissipates as the acoustic waves propagate, combine, and spread out creating a more stable and uniform

acoustic wave zone referred to as the "far field". Anomalies are harder to distinguish in the "near field" and detection becomes better in the "far field" zone, up to a point. The best detection typically is along the centerline of the "far field" zone where the impulse and the reflective waves are the greatest. The zone where the transducer is most effective (most focused) is called the "depth of field" and is located within the "far field" (**FIGURE 18**). The natural focus point of the transducer is the "near field"-to-"far field" zone intersection point. By selecting a spherical or cylindrical focusing transducer: 1) the "far field" zone can be increased by moving the natural focus point closer to the transducer, thus increasing the opportunity for detecting anomalies and 2) focuses the energy over a smaller area, concentrating the beam over a specific area instead of the beam spreading out and dissipating, thus enhancing the capability.
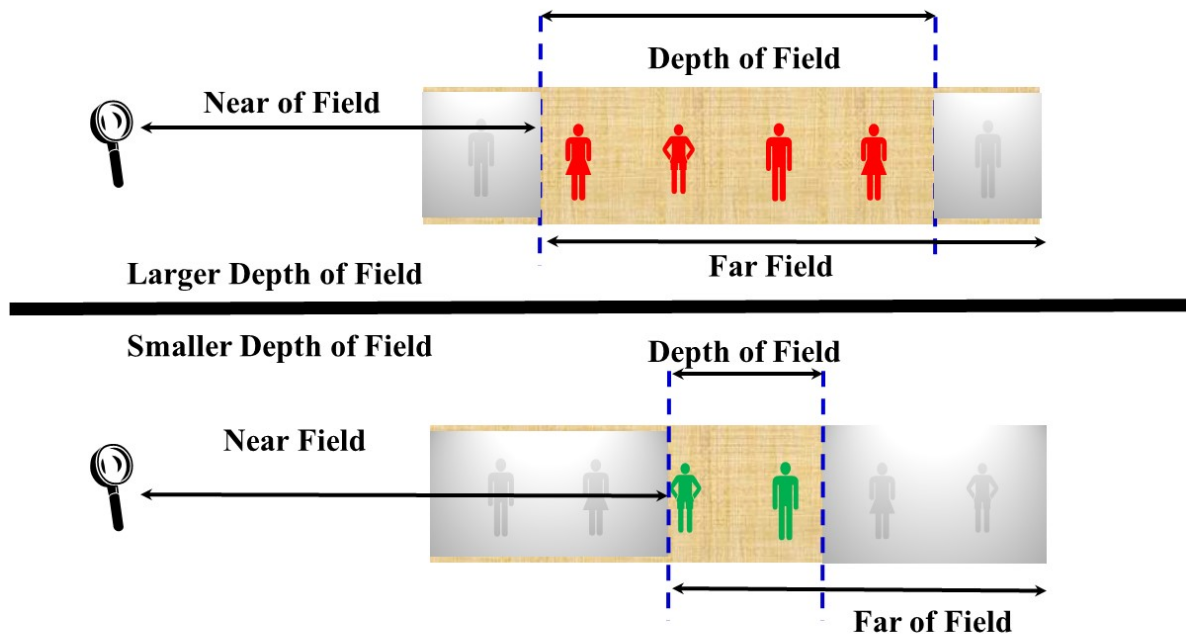
FIGURE 18: DEPTH OF FIELD AND FOCUSED AREA REPRESENTATION

The display unit graphically presents the data collected in several formats; most common of which are the A-scan, B-scan, and C-scan. The A-scan displays the raw reflective energy signal as a function of time to give depth and the discontinuity size can be determined by comparing it with a known discontinuity which was established as part of the calibration setup; this is the type of display used by ATI and MTU and is a one-dimensional representation of the data. The B-scan displays the reflective energy signal as a cross-section view of the test specimen and provides approximate depth and linear dimension/location of the discontinuity. The C-scan is a two-dimensional scan that shows the image of the feature that reflected the energy signal back as a function of depth like an A-scan, but also adds the discontinuity width. This is not done by a comparison of a known defect size as in the A-scan, but when the reflective signal starts and stops as the transducer translates across the test piece.

The probability of detection (POD) of a flaw is a function of the sensitivity and resolution of the UTI technique employed. Sensitivity relates to the flaw size and resolution relates to the spacing of those flaws between one another and/or the surface. The acoustic wave velocity through any material is constant and is independent of the force that generated the acoustic wave; each material has its own unique velocity; therefore, the frequency directly influences (inversely) the wavelength. Wavelength of the acoustic wave dictates the probability of detecting an anomaly and is the limiting factor that controls

the amount of data that the reflective wave provides back to the transducer(s); acoustic wave propagation/reflection is more efficient when the material is homogeneous, hard, and the surface finish is smooth. The energy density of the wave (amplitude) diminishes with distance due to the expansion of the wave but it also diminishes due to scattering and absorption. Attenuation is the reduction in acoustic wave energy verses distance and can affect the penetration depth of the inspection. Typically, sensitivity and resolution increases as the frequency increases; however, at higher frequencies the wave tends to scatter more, especially in coarse grained materials, which reduces the penetration depth of the inspection. Therefore, for greater penetration, lower frequencies may be more desirable and this is especially true for thick materials.

The general rule of thumb for small flaw sizes is that reflective wavelength is about half the pulse wavelength for an acceptable criteria; anything smaller, the flaw size is considered imperceptible. Therefore, the selection of the proper frequency and amplitude (energy) is important and based on the material grain structure (course vs fine), grain orientation, thickness, anticipated flaw size and location, along with other factors to optimize the inspection for the different variables. For example, if a coarse grain billet were to be UTIed, a low frequency may be more preferable due to the course crystal structure of the material. With a fine grain billet conversion process, a higher frequency may be preferable because the grain structure is finer allowing for a more sensitive inspection. However, a lower frequency may also be desirable due to the billet thickness.

Acoustic waves can travel though the material/test specimen in a variety of ways, but for the purposes of this report we will only discuss longitudinal and shear wave propagation as these are the methods employed by ATI to inspect the event billet (longitudinal wave) and MTU to inspect the forging (longitudinal and shear wave). See Sections 4.4.3 *UTI Performed by ATI* and 4.4.4 *UTI Performed by MTU* for additional details.

4.4.3   UTI Performed by ATI

ATI inspected the event billet per GE specification P3TF15 titled *Ultrasonic Inspection of Billet – Immersion*, issue number S12, Amendment 1, Class 'C' and 'E'; Class 'C' refers to Inconel 718-Fine Grain and Class 'E' refers to General Application - High Sensitivity. According to specification P3TF15:

> Ultrasonic inspection shall only be performed with personnel, equipment, and methods which meet the requirements of this specification. The qualification method shall emphasize applicable procedures on billets representative of the product to be inspected.

Specification P3TF15 provides a mix of general requirements and specific requirements (depending on inspection class designation), for the supplier performing the inspection; essentially ATI (the supplier) develops the inspection process using the guidance and requirements outlined in specification P3TF15 and GE approves that process. The following sections will compare some pertinent GE UTI requirements with those used by ATI on the event billet as they pertain to personnel, equipment, and process.

Personnel Requirement

P3TF15 specifies that personnel performing the UTI shall be qualified and certified in accordance with Aerospace Industries Association (AIA) National Aerospace Standard (NAS) 410 titled *Nondestructive Testing Personnel Qualification and Certification*, a minimum Level I or better. Level I is

the lowest qualification standard (typically there are three levels, I-III) and the inspector is qualified and capable of performing the specified tasks to include calibration, specific NDI inspection, evaluation for acceptance or rejection, and provide a written report of findings. A supervisor with a Level II or greater provides the necessary guidance and training for the Level I inspector. A Level III operator/inspector is certified by the American Society of Non-Destructive Testing (ASNT) and should have sufficient practical background to develop, establish, qualify, and approve inspection techniques and procedures and be capable of training and examination of NDT Level I and II operators/inspectors for certification in those methods. According to ATI, the inspector who performed the UTI was a Level II, originally certified as a Level II in 1992 prior to the event billet inspection in June 1997, and has successfully recertified three additional times. TABLE 4 provides the minimum requirements according to NAS 410 for a UTI inspector; the ATI inspector met those requirements.

TABLE 4: UTI MINIMUM TRAINING REQUIREMENTS			
	Level I (hours)	Level II with prior Level I (hours)	Level II without prior Level I (hours)
Minimum OJT	400	1200	1600
Minimum Classroom	40	40	80

Equipment and Process Requirement

ATI currently uses a normal beam longitudinal wave[28] immersion UTI technique employing dual pulse-echo immersion transducers with cylindrical focus and an A-scan display. The billet is immersed in a water tank and rotated about its longitudinal axis while the transducers translate along its length; thus, the billet is inspected in a helical pattern (FIGURE 19). According to ATI, this is the same set up used for the event billet back in June 1997; the transducers are the same type and style but have been replaced since 1997. Both transducers operate at the same peak frequency but their focal lengths differ to ensure that they overlap and cover slightly past centerline; the rotation of the billet ensures complete diameter coverage. The billet rotational and transducer translational speeds are set to optimize the inspection coverage. In a normal beam setup, the back surface reflective waves are always present on the A-scan display unit and are accounted for by scaling and calibration. P3TF15 specifies that for billets with a nominal diameter of 10-inches (255 millimeter (mm)) or less, the transducer(s) must operate at peak frequency of no less than 4.50-MHz and at no less than 2.25-MHz for billets with nominal diameters above 10-inches.

---

[28] Longitudinal waves oscillate the atoms in the material in the same direction the wave travels.
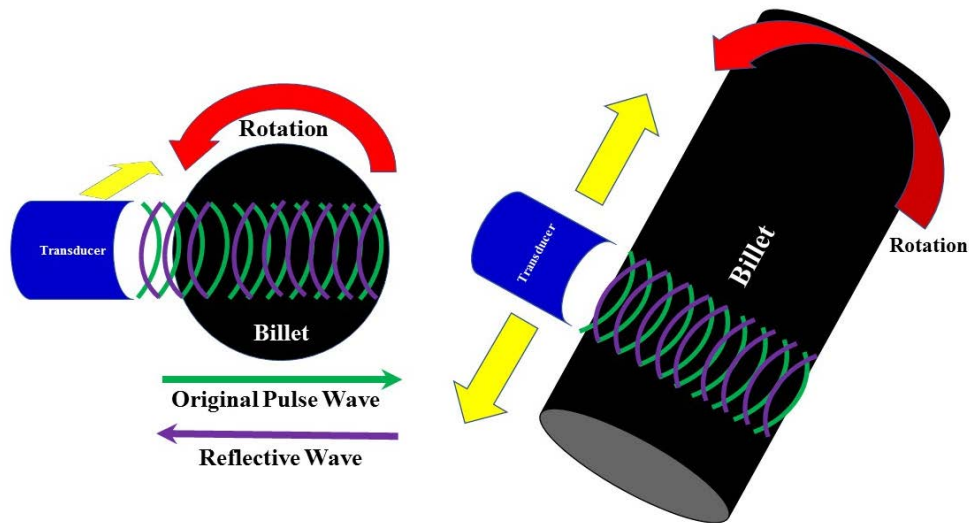
FIGURE 19: REPRESENTATION OF A NORMAL BEAM LONGITUDINAL WAVE SCAN

Specification P3TF15 provides the requirements for creating the reference/calibration standard used to set up the sensitivity of the inspection equipment; provides calibration, reject, and evaluation thresholds; how often the UTI equipment must be calibrated to ensure correct and consistent results; and how anomaly alarms and rejections are to be handled and documented.

According to specification P3TF15, the reference standard should: 1) have the same material as the base alloy type, 2) be subjected to the same thermomechanical process, and 3) have the same diameter, acoustic transmission, and surface texture. In addition, Class 'C' requires that billets with a diameter between 4.5- and 12-inches (114 to 305 mm) meet the following requirements: 1) sensitivity to detect a No. 2 flat bottom hole (FBH)[29] at 0.25-inches (6.35mm) near field depth (**FIGURE 20**), and 2) the calibration amplitude (screen height for the calibration defect referred to as the gain) of 80% full screen height (FSH), with a rejectable amplitude of 40% and the alarm threshold/evaluation limit set at 20%. ATI uses a billet reference standard made from Inconel® alloy 718 material with a series of FBHs from near surface to slightly past centerline with a known size and depth that are consistent with the GE requirements. According to the ATI UTI ultrasonic billet map test data sheet for FA94-2: 1) both transducers are the immersion type operating at a frequency greater than 4.5-MHz that satisfies the operating frequency requirement for a 10-inch round billet and 2) calibration hole size is a FBH No. 2, and 3) reject hole size set at 40% amplitude which is consistent with the calibration requirements.

---

[29] A No. 2 FBH has a diameter of $^{2}/_{64,}$ 0.031-inch, or 0.79mm.
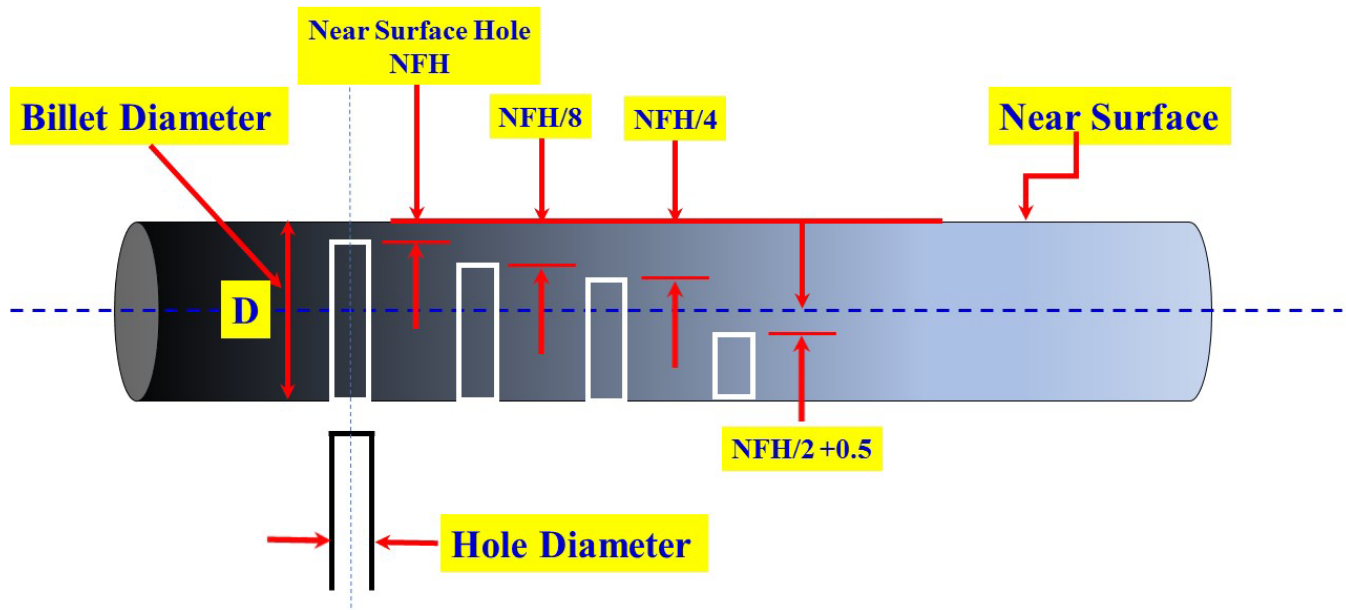
FIGURE 20: REPRESENTATIVE OF THE TYPICAL REFERENCE STANDARD WITH DESIGNATED HOLE SIZES

GE requires calibration of the transducers before and after each inspection lot or at least the start and end of each shift. According to ATI, the calibration occurs before and after each order. For billets the size of the event billet, one billet is one order. Furthermore, ATI indicated that the entire inspection instrument is calibrated every 6 months and both transducers every 3 months.

Specification P3TF15 also requires an 'Alarm and Stop-on-Indication System'; this system automatically stops the translation of the transducers when an anomaly is detected without human intervention; however, the operator/inspector makes the final determination on the acceptability or rejectability of the anomaly. While at ATI, the operator/inspector demonstrated the 'Alarm and Stop-on-Indication Systems' feature while demonstrating the uses of the reference standard.

According to specification P3TF15, all rejectable indications and all repeatable indications that are not rejectable, but exceed the alarm threshold/evaluation limit amplitude, are recorded on a billet map. Review of the ATI production records revealed that a billet map was created for each billet whether a defect was found or not. As previously mentioned, the review of the billet map for FA94-2 showed no anomalies.

For FA94-1, the billet map showed a macro-rejectable defect in the bottom of the billet so additional material was removed. For FA94-3, the billet map showed a UTI sonic-rejectable indication in the top of the billet, so additional material containing the indication was removed and the defect was located and identified. For FA94-4, the billet map showed an UTI sonic-rejectable indication in the top of the billet, so additional material containing the indication was removed. The indication could not be identified after the section was removed. For FA94-5, the billet map showed a macro-rejectable indication in the bottom of the billet, so additional material was removed.

4.4.4   UTI Performed by MTU

MTU inspected the event 'sonic shape' forging using both a longitudinal wave and a circumferential shear wave UTI per GE specification P3TF1 titled *Ultrasonic Inspection*, issue number S12 Amendment 1, Class 'A'; Class 'A' refers to Immersion Ultrasonic Inspection. Shear waves, sometimes referred to as transverse waves, oscillate the atoms in the material perpendicular (90º) to the direction the wave travels. Longitudinal waves are much stronger and travel almost twice as fast as shear waves. Shear waves are often created by using some of the energy from the longitudinal wave. The process used to inspect the 'sonic shape' forging back in 1997 is essentially the same process employed today.

Due to the geometry of the 'sonic shape' forging, a combination of longitude wave and circumferential shear wave UTI was necessary for complete and effective coverage. For example, the bore is a good candidate for a longitudinal wave since the transducer and the beam can be normal (orthogonal) to the inspection surface/area. However, longitudinal waves are not as effective in areas with radii because the geometry of the disk in that area would limit the ability of the longitudinal beam to reach all the desired areas; thus, shear waves are used. Note that at the billet UTI, ATI used only a longitudinal wave since the billet was cylindrical and symmetric about its longitudinal axis therefore easier to inspect than the 'sonic shape' forging with geometry issues.

MTU performed the UTI by immersing the 'sonic shape' forging in a water tank and performed longitudinal, circumferential shear and axial shear wave inspections using two different transducers operating at different frequencies and set for different depths. The 'sonic shape' forging was rotated about its longitudinal axis as the transducer translated across the part (**FIGURE 21**); each surface was inspected twice in this manner. The 'sonic shape' forging rotational and the transducer translational speeds were set to optimize the inspection coverage and the reflective waves were presented on an A-scan display unit similar to the billet UTI.
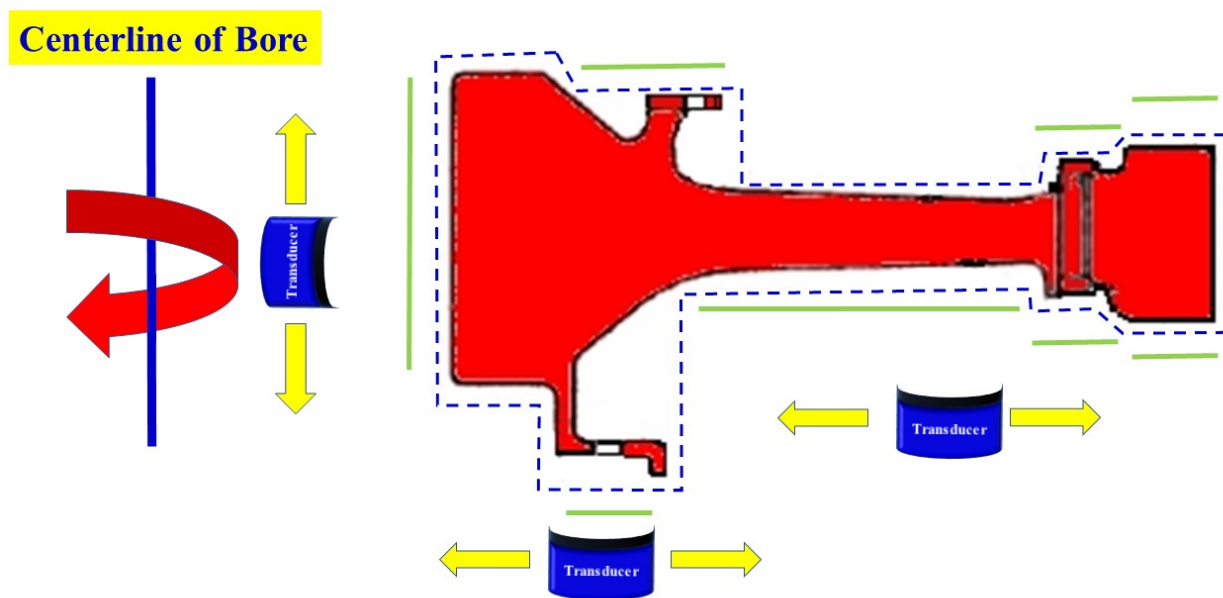
FIGURE 21: REPRESENTATION OF THE MTU UTI SCAN

Specification P3TF15 used by ATI for the billet and specification P3TF1 used by MTU for the 'sonic shape' forging are similar in many aspects. Just like specification P3TF15, specification P3TF1 calls out UTI inspector qualifications; requires the use of reference/calibration standards to set up the sensitivity of the inspection equipment; provides calibration, reject, and evaluation thresholds; how often the UTI equipment must be calibrated to ensure correct and consistent results; and how anomaly alarms and rejections are to be handled and documented.

Personnel Requirement

Inspector requirements for UTI at the billet and 'sonic shape' forging levels were comparable. Specification P3TF1 required "Personnel performing inspections to this specification shall be qualified and certified in accordance with Military Standard (MIL-STD)-410E"; MIL-STD-410E was issued in January 1991 and cancelled in August 2001. However, on June 15, 2007, the FAA issued a memorandum *Qualification Standards for Nondestructive Testing* that stated that MIL-STD-410E was rescinded and superseded by NAS410 but the FAA still considered it acceptable for inspector qualifications. Essentially the same requirements applied for the inspectors performing the billet and 'sonic shape' forging inspections.

Equipment and Process Requirement

P3TF1 specifies a peak frequency of no less than 4.75-MHz, which was slightly greater than what was required for the billet. Similar to the billet UTI, a reference standard was specified and a calibration schedule for the inspection equipment was defined. The reference standard required hole sizes from FBH No. 2 – No.5 and the calibration schedule was to be determined by the stability of the equipment calibration and "initially at the beginning and end of each work shift, whenever equipment is changed or when the material inspected is changed". At the time the event disk was inspected, MTU performed the calibration at the beginning of the shift or after new material number (different PN part) was inspected and typically, there were two shifts per day[30]. Again, similar to the billet UTI, the calibration gain for the forging was set to 80% FSH but with a slightly different rejection amplitude of 30% as opposed to the billet that was set at 40%.

According to the MTU UTI process sheet, *UT 9362M43P04-U*, and the router for SN MUNBB592: 1) the transducers used were of the immersion type with frequencies of 5.0-MHz and 10-MHz respectively, which satisfies the operating frequency requirement and 2) reject amplitude of 30% which is consistent with the calibration requirements, and 3) no defects (acceptable) found and acceptable macro-inspection results.

---

[30] Since 2016, MTU performs the calibration before and after each shift.

5.0 INCONEL® ALLOY 718 HISTORY, PROCESS ADVANCEMENTS, AND INSPECTION GUIDANCE

5.1 GE's USE AND EXPERIENCE WITH INCONEL® ALLOY 718

GE first used Inconel® alloy 718 in the 1970s and the material was processed using double-melt (VIM/VAR). In the early 1980s, GE started using Inconel® alloy 718 triple-melt (VIM/ESR/VAR) for some part applications. In the mid-1990s, GE adopted the triple-melt process for **all** its critical life limited rotating parts while some GE non-critical Inconel® alloy 718 parts may be produced using double-melt.

In GE's history with the use of Inconel® alloy 718, there have been nine manufacturing events/findings; eight manufactured using the double-melt process and one using the triple melt (**TABLE 5**). The lone triple-melt process event is the AA uncontained event in Chicago. According to the FAA, the AA event is the first and only Inconel® alloy 718 triple-melt related anomaly that has resulted in either a cracked or a fractured part in commercial aviation.

Of the eight double-melt events/findings, six were melt-related and two were forging-related. Five of the six melt-related findings were cracked parts discovered during shop inspections; the sixth was a fractured part that resulted in a subsequent failure of the engine. The one fracture event occurred in 1987 and the part was not in an aviation application, instead used in marine propulsion. Of the two forging-related events/findings, one cracked part was discovered during a shop inspection while the other was a fractured part used in an aviation application.

TABLE 5: INCONEL® ALLOY 718 IN-SERVICE CRACKS OR ROTOR BURST FINDINGS/EVENTS				
Year	Material Process DM - Double Melt TM - Triple Melt	Result	Melt Related (Y/N)	Engine Model
1971	Inconel® alloy 718 DM	Crack	Yes	Military
1977	Inconel® alloy 718 DM	Rotor Burst	No	CF6-50
1987	Inconel® alloy 718 DM	Rotor Burst	Yes	LM2500 (Marine Application)
1989	Inconel® alloy 718 DM	Crack	Yes	CF6-50
1990	Inconel® alloy 718 DM	Crack	Yes	CF6-50
1991	Inconel® alloy 718 DM	Crack	Yes	Military
1995	Inconel® alloy 718 DM	Crack	No	Military
1995	Inconel® alloy 718 DM	Crack	Yes	CF6-50
2016	Inconel® alloy 718 TM	Rotor Burst	Yes	CF6-80C2

5.2 INCONEL® ALLOY 718 PROCESS IMPROVEMENTS

5.2.1 Triple-Melt versus Double-Melt

The original method for producing Inconel® alloy 718 for aerospace or aviation applications was double-melt, either VIM/VAR or VIM/ESR. Either combination contributes to improved cleanliness but each had deficiencies. In 1994, a paper titled *Advances in Triple Melting Super Alloys 718, 706, and 720* was introduced at the Minerals, Metals & Material Society Conference (Moyer 1994). The intent of the paper was to compare the previously used double-melt process VIM/VAR or VIM/ESR to the

triple-melt process VIM/ESR/VAR. The VIM/VAR process had two major drawbacks: 1) oxide cleanliness/formation and in particular, the large size of the oxides that limits the LCF capability, and 2) the VAR tendency to produce 'white spots' that may also reduce the LCF life of the part. The ESR process, when used in combination with the VIM process (VIM/ESR), improves the oxide cleanliness but the downside is that there is a great tendency to form regions of chemical segregation especially in the center of the billet. Therefore, no matter which double melt process is chosen, there are distinctive advantages and disadvantages. Results of this study showed that the cleanliness of triple-melt was much more consistent than single- or double-melt and validated by the amount and type of UTI indications found. Triple-melt exhibited roughly an order of magnitude fewer UTI indications than double-melt; a reduction of 90% in the number of reported indications with fewer clusters of inclusions as well as fewer 'white spots'. The study concluded that even though the triple-melt added an extra melt step that increased overall production costs, it lowered the frequency of defects[31] and improved overall yield. After the AA event, GE reviewed their double-melt verses triple-melt data and even though the number of indications found in double-melt continue to trend lower, triple-melt still exhibited a significantly lower indication rate (almost 4x lower).

On February 4, 2011, the FAA issued AC 33.15-2 *Manufacturing Process for Premium Quality Nickel Alloy for Engine Rotating Parts* to provide guidance and information on the compliance with nickel materials suitability and durability requirements in §33 AIRWORTHINESS STANDARDS: AIRCRAFT ENGINES, subpart 33.15 Material[32]. The FAA concluded that triple-melt INCO 718 rotor material has significantly fewer melt-related anomalies than double-melt and recommended the triple-melt process for critical rotating components along with macroetch and UTI of billets and forgings. AC 33.15-2 had not come into existence when the event disk was produced back in 1997; however, GE had in place GE specification P1TF77 titled *MATERIAL PROCESS PLAN FOR CONTROL OF SEGREGATION AND CLEANLINESS - VIM + ESR + VAR, NICKEL BASE ALLOYS*. Comparing the FAA AC 33.15-2 with GE specification P1TF77 revealed that much of the same guidance listed in AC 33.15-2 had been present in GE specification P1TF77 with some minor differences.

5.2.2 Process and Inspection Improvements

Between the time that GE first started using the triple-melt process in limited applications in the 1980s and the shift to requiring the triple-melt process for **all** its critical rotating parts in the mid-1990s, GE instituted several process improvements. The process improvements were to enhance material cleanliness as well as to institute more stringent flaw size detection requirements at both the billet and forging levels; GE reduced the flaw rejectable limit and alarm threshold by almost half at the billet and about 20% at the forging level.

ATI also instituted some process improvements. In August of 1998, ATI switched from a 'grade 165' process to 'grade 365' process for Inconel® alloy 718 at the request of some of their forging customers. The initial change was a desulfurization step; this improved the workability during the billet conversion process in reducing voiding and tears and improved the properties of the forging itself; this also however affected surface finish. The other improvements included changes to the machining and conversion processes. GE conducted a review of sonic indications found (UTI anomalies) at ATI for 8-inch

---

[31] With triple-melt there was a 90% reduction of inclusion initiated LCF specimen failures, 80% reduction of average inclusion size, and a previously reported 50% reduction in the number of rejectable ultrasonic indications in the billet compared to VIM/VAR Inconel® alloy 718

[32] The suitability and durability of materials used in the engine must—
(a) Be established on the basis of experience or tests; and
(b) Conform to approved specifications (such as industry or military specifications) that ensure their having the strength and other properties assumed in the design data.

and 10-inch round diameter billets for the years from 1997 to 2015. After the introduction of the 'grade 365' in 1998 and the subsequent process enhancements, the sonic indication rate for both the 8-inch and 10-inch round diameter billets decreased, on average, by fivefold.

GE conducted an extensive study of the UTI indication rates at their other Inconel® alloy 718 melt suppliers as well as at their forging suppliers; the available data spanned from the mid-1990s to 2016. GE concluded that, starting around year 2000, the frequency of indications found during UTI had noticeably reduced and attributed this reduction to improved cleanliness of the material due to melt suppliers incorporating best practice process improvements over time.

The FAA, as part of the AIA Rotor Integrity Steering Committee (RISC), has also been collecting and analyzing Inconel® alloy 718 anomaly indication data[33] from various melters for both double-melt and triple-melt processes. The data (the most current data spans from 2003-2016) shows that: 1) triple-melt is about four times cleaner (fewer indications) than double-melt and has fewer false positive indications and 2) the frequency of indications has been trending lower for both double-melt and triple-melt. The FAA data seems to corroborate GE's own indication rate study.

5.3   INCONEL® ALLOY 718 INSPECTION IMPROVEMENTS – CONVENTIONAL UTI VS MULTIZONAL VS PHASED-ARRAY

Typical UTI methods for billet inspection utilize single- or dual-transducers. Improvements in sensitivity and resolution can be gained by using a focused transducer like the cylindrical-focus transducer used by ATI. The advantage of a focused transducer is that the acoustic waves, instead of spreading out from the transducer, are directed over a smaller area, either a point (spherical transducer) or a line (cylindrical transducer), at a location defined as the natural focus point which is the "near field"-to-"far field" zone intersection point (**FIGURE 22**). The disadvantage is that the focal length is fixed; a transducer cannot be focused beyond its "near field" or "far field" zones (See **FIGURE 18**). As a result, much of the material is not inspected with focused sound since it falls outside of the transducer focused zone or "depth of field". Flaws located near the billet centerline can be difficult to find with this technique; a technique called distance-amplitude correction (DAC) is employed to produce uniform target response at different depths; this greatly increases the noise at the billet center. Using a single-transducer (one zone) inspection technique severely restricts the overall effectiveness of the inspection because of the limited sensitivity imposed by the fixed-focused depth resulting in poor focusing along certain parts of the specimen's diameter and by the material noise. Adding an additional transducer with a different and overlapping focal length helps eliminate some of the deficiencies of a single-transducer (**FIGURE 23** – top part of figure).

---

[33] Data supplied by the Specialty Metal Process Consortium (SPMC), which is a group of 13 US specialty metal producers and aerospace-alloy users, collaborated to study specialty-metals production, processing, quality, and performance.
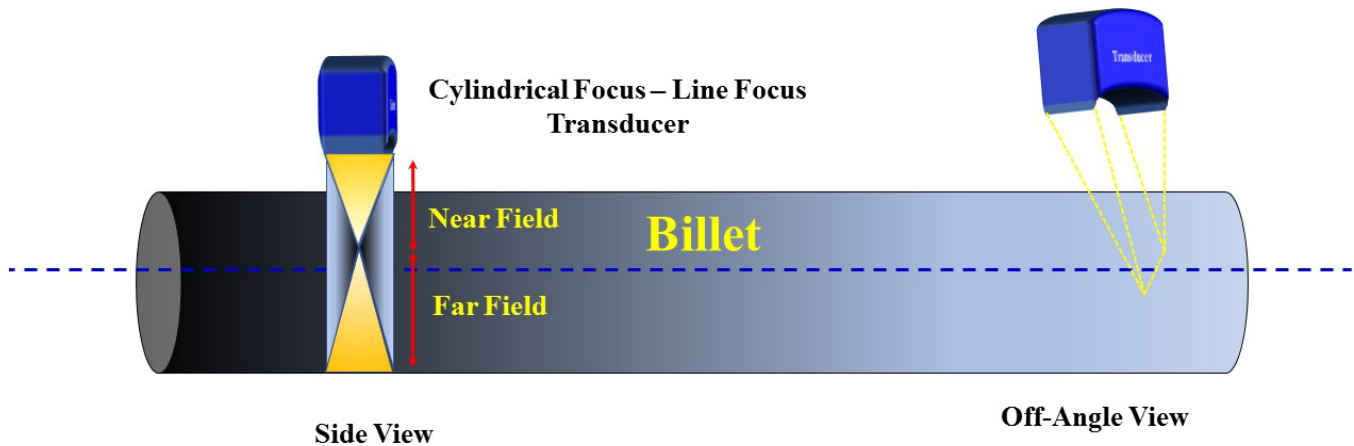
FIGURE 22: CYLINDRICAL-FOCUSED UTI TRANSDUCER REPRESENTATION

Following the July 19, 1989 United Airlines flight 232 McDonnell Douglas DC-10-10 airplane accident in Sioux City Iowa[34] that was caused by an uncontained titanium fan disk separation resulting from a manufacturing defect, the NTSB issued Safety Recommendation A-90-167 that stated:

> The NTSB recommends that the Federal Aviation Administration: intensify research in the nondestructive inspection field to identify emerging technologies that can serve to simplify, automate, or otherwise improve the reliability of the inspection process. Such research should encourage the development and implementation of redundant ("second set of eyes") inspection oversight for critical part inspections, such as for engine rotating components.

Nickel, when compared to titanium, is a much easier material to inspect, but because of some of the challenges imposed by titanium, a more sensitive inspection technique needed to be developed to detect subsurface manufacturing flaws. Based on the NTSB recommendation, there were several follow-on initiatives involving the FAA and the engine and airplane manufactures to address this issue. Two groups that considered this issue of improved inspection techniques were the AIA RISC and the Engine Titanium Consortium (ETC). The ETC, comprised of persons from Iowa State University, GE, Pratt & Whitney, and Honeywell Engines, Systems & Services, was chartered to review and improve manufacturing and in-service inspection processes for all engine titanium rotating parts.

Phase I was to develop process and inspection techniques for use on titanium based on deficiencies found during the Sioux City accident investigation and Phase II was to develop higher-sensitivity inspection methods for Ni billets that could be used to reduce the occurrences of melt-related defects in Ni forgings. Phase I focused on improvements in Ti billets using zoned inspections and Phase II was to apply those improved inspection techniques, tools, and procedures used for Ti to Ni billets. Multizonal UTI was one of the techniques developed to improve anomaly detection.

As the name implies, the multizone technique uses multiple transducers to inspect at different depths. GE developed the multizone and it is not as simple as adding additional transducers with different focal depths to the already existing inspection process but is a complicated system that requires greater time to set-up and calibrate than for a single- or dual-transducer system. Multizone is an inspection process that includes 4 to 8 5-MHz transducers each operated on a separate channel, a computer system that provides

---

[34] NTSB accident number DCA89MA063.

digital data acquisition and storage, and display a screen capable of presenting C-scan data (**FIGURE 23** – bottom part of figure). Along with the custom software that processes and images the data, one of the major features of the multizone inspection is the ability to store the data for post scan analysis as well as provides a permanent record of the inspection results; this is not possible with the current single or dual-transducer inspection technique using A-scan displays (Nieters 1995). The advantages of the multizone technique is its higher selectivity, ability to having multiple focal points along each scan, and the ability to store and retrieve data. The disadvantages are the procurement of multiple transducers, each individual transducer must be aligned which requires considerable time and specialized procedures, special fixtures to hold each transducer, and the specialized data acquisition hardware and software required.
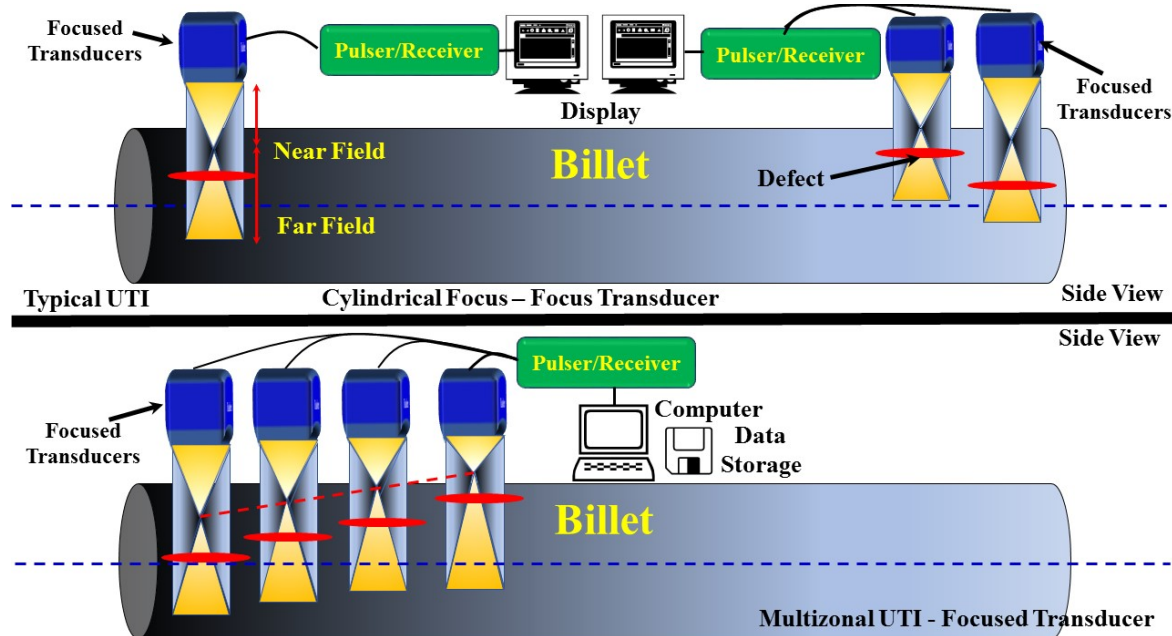
FIGURE 23: VISUAL COMPARISON OF SINGLE- AND MULTI-TRANSDUCER UTI TO MULTIZONAL UTI

An alternative method to the multizone UTI is called phased array ultrasonic inspection (PAUT). Instead of using multiple independent transducers as in the multizone technique, a single-transducer with a matrix of multiple closely packed independent elements (usually between 32 and 128 independent elements depending on the application) transmits and receives the ultrasonic pulse. Each element has its own pulser/receiver components and each element is controlled by a computer coupled encoder. Just like the multizone, the data can be permanently stored. The elements are independently excited either individually or in groups; each element can have a different depth of field and, based on the timing of the excitation of each element, the array beam can be steered/turned from its original longitudinal direction. Each element emits a spherical wave/beam and by delaying the excitation of neighboring elements, creates interference waves (waves can combine) that interact with one another resulting in the

beam having an angle of incidence to the test specimen, essentially steering the beam. In traditional UTI or multizone techniques, this steering would require several probes aligned at different angles to achieve the same result. The elements are arranged in a variety of patterns, such as linear, annular, circular or mixed; a few examples are provided in **FIGURE 24**. Advantages of the phased array is that the scanning time is much less than traditional UTI; a single probe that can focus at different depths, and the ability to steer the beam when the geometry of the specimen calls for it. Similar to the multizone, there are disadvantages as well. Phased array transducers are sensitive to misalignment errors that potentially leave the center of the billet uninspected. To address this issue, the transducer laterally sweeps multiple times over the center of the billet each revolution to ensure that the center is inspected (Iowa State University Center for Nondestructive Evaluation n.d.).

FIGURE 24: PHASED ARRAY CONFIGURATIONS

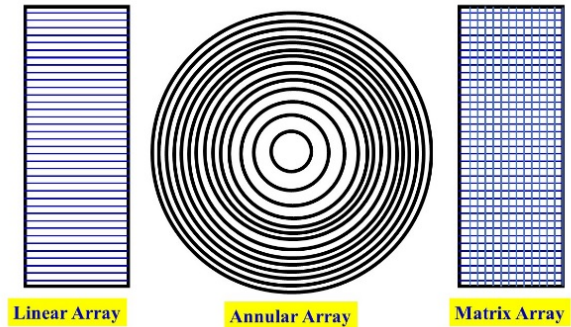As previously mentioned, the ETC first implemented inspection improvements for titanium billets (Phase I) and after that focused on transferring lessons learned from Phase I to the inspection of nickel billets (Phase II). Phase II developed calibration standards and conducted laboratory and factory assessment and demonstration for a 10-inch round diameter billet and compared UTI multizone and phased array inspection techniques to conventional UTI for a 5-inch diameter billet. In September 2005, the FAA issued the results of Phase II study in report DOT/FAA/AR-05/29 titled *Inspection Development for Nickel Billet – Engine Titanium Consortium Phase II*. The report provided the following conclusions:

1) The program goal was four times improvement over the current conventional inspection method; improvement from a #2 flat bottom hole (FBH) sensitivity to #1 FBH[35]
   a. The multizone inspection procedure and transducers[36] originally used for Ti successfully exceeded the program goal of #1 flat bottom hole (FBH) for IN718[37]
   b. For IN718, inspection sensitivity exceeded the program goal of #1 FBH at all depths in the billet.
   c. At the billet center, inspection sensitivity was approximately 31 times more sensitive than the current conventional inspection requirement [one zone]; about 3.5 times better than the program goal
2) The surface finish used for conventional inspection was adequate for the increased sensitivity of the multizone test, although the multizone test is more sensitive to surface blemishes.
3) Conclusive results showed that the multizone system can detect indications that are missed by the current conventional inspection.
4) Cost comparison revealed increase investment and operational costs for multizone compared to conventional inspection.

---

[35] A FBH is a machined hole where the bottom of the hole is perpendicular to the beam. A No. 1 FBH is a $\frac{1}{64}$-inch diameter hole and No. 2 hole is a $\frac{2}{64}$-inch diameter hole. The reflective wave height as seen on the display unit is proportional to the area of the bottom of the hole or proportional to the square of the diameter. Therefore, reducing from a No. 2 to a No. 1 equates to a four times improvement.

[36] The multizone testing used six (6) 5-MHz transducers.

[37] In the FAA's report, Inconel® alloy 718 is abbreviated as IN718.

5) Multizone and phased array[38] inspections of 5″ diameter Waspaloy® [nickel alloy] billet indicated that multizone achieved about a No. 0.5 FBH sensitivity throughout most of the billet depth while phased array achieved about a No. 0.75 FBH. The multizone inspection exceeded the conventional inspection sensitivity by about 20 times at the billet center.

6.0 CORRECTIVE ACTIONS SUMMARY OF PARTS FROM MASTER HEAT FA94

6.1 SUMMARY OF PARTS FROM MASTER HEAT FA94

Thirty-six forgings, all for either for GE or CFMI applications[39], were produced from Master Heat FA94; from which five ingots/billets were created. The ingots/billets are FA94-1, FA94-2, FA94-3, FA94-4, and FA94-5. All parts from Master Heat FA94, either in flying status or with the potential for installation into an engine/airplane, were removed from service and sent to GE for inspection. **TABLE 6** and **CHART 1** shows the status of the parts from Master Heat FA94. The "mult number" in the second column does not correspond to the forging number except for billet FA94-2. Instead the "mult number" is merely a sequential way of tracking all the forgings in that billet. For billet FA94-2 however, the WG records were reviewed and the mults sequence was matched to their respective forging SNs; therefore, the "mult number" matches the cut order.

TABLE 6: MASTER HEAT FA94 PARTS STATUS			Black – Scrapped Red – Event disk separation Green – Non-Flying, land/marine power generation Yellow – Sent to GE for Inspection	
Forging	**Heat Lot/ Mult No.**	**Configuration (Serial Number)**	**Before AA Disk Separation Event Status**	**After AA Disk Separation Event Status**
1	FA94-1/1	CFM56-5B HPT Disk	Destructively Scraped	Scrapped for end of life, scrap ticket confirmed
2	FA94-1/2	CFM56-7B HPT Disk	Destructively Scraped	Scrapped for end of life, scrap ticket confirmed
3	FA94-1/3	LM2500 HPC Aft Spool	In-Service	Not removed for inspection
4	FA94-1/4	LM2500 HPC Aft Spool	In-Service	Not removed for inspection
5	FA94-1/5	LM2500 HPC Aft Spool	In-Service	Not removed for inspection
6	FA94-1/6	LM2500 HPC Aft Spool	In-Service	Not removed for inspection
7	FA94-2/1	CF6-80C2 HPT Disk (SN MUNBB580)	Installed/In-service Engine/disk removed	Removed and sent to GE for inspection. ECI: slot bottom, bore, web, & bolt holes. UTI: circular shear (SPM 70-32-09)[40] and high resolution[41]. No anomalies
8	FA94-2/2	CF6-80C2 HPT Disk (SN MUNBB581)	Destructively Scrapped	Scrapped for end of life, scrap ticket confirmed
9	FA94-2/3	CF6-80C2 HPT Disk (SN MUNBB561)	Destructively Scrapped	Scrapped by Material Review Board (MRB), scrap ticket confirmed

---

[38] The phased array testing was conducted with a 5-MHz transducer with 113 elements laid out in a circular pattern with the elements connected such that asymmetrical elements were fired at the same time.

[39] CFMI is a partnership between General Electric in the USA and Safran (formerly Snecma *(Société Nationale d'Etude et de Construction de Moteurs d'Aviation)* Moteurs) of France. CFM is not an acronym; however, the company (CFMI) and product line (CFM56) receive their names by a combination of the two parent companies' commercial engine designations: GE's CF6 and Snecma's M56. Snecma changed its name to Safran Aircraft Group, a subsidiary of the Safran Group, in May 2016.

[40] SPM 70-32-09 titled *Immersion Ultrasonic Inspection of Engine Run Hardware* describes the equipment, technique, and procedures for conducting component level immersion ultrasonic inspections of engine run titanium and nickel alloy hardware. This document provides general inspection guidance applicable to all parts identified in the document but also provides specific inspection scan plans for the parts. The HPT stage 2 disk is not specified in SPM 70-32-09; therefore, it was used as general inspection instructions and a unique inspection scan plan was developed for this part. The HPT stage 1 disk is called out specifically in SPM70-32-09 and a scan plan already exists.

[41] According to GE, the UTI high resolution scans were performed at enhanced sensitivity beyond current product levels; a multizone process was used (See Section 6.3 for details on multizone).

TABLE 6: MASTER HEAT FA94 PARTS STATUS			Black – Scrapped Red – Event disk separation Green – Non-Flying, land/marine power generation Yellow – Sent to GE for Inspection	
Forging	**Heat Lot/ Mult No.**	**Configuration (Serial Number)**	**Before AA Disk Separation Event Status**	**After AA Disk Separation Event Status**
10	FA94-2/4	CF6-80C2 HPT Disk (SN MUNBB637)	Not In-Service; engine/disk at shop visit	Disk quarantined and returned to GE. ECI: slot bottom, bore, web, & bolt holes. UTI: circular shear and high resolution. No anomalies
11	FA94-2/5	CF6-80C2 HPT Disk (SN MUNBB592)	In-Service	Disk Separation
12	FA94-2/6	CF6-80C2 HPT Disk (SN MUNBB571)	Installed/In-service Engine/disk removed	Part removed and inspected by operator: FPI, visual and ECI bore/web (SPM 70-32-10) – No anomalies in bore/web. ECI blade slot bottom (SPM 70-32-23) and ECI bolt holes (SPM 70-32-07) not performed. Sent to GE for additional inspections: ECI slot bottom, bore, web, and bolt holes. UTI circular shear & high resolution - No Anomalies
13	FA94-2/7	CF6-80C2 HPT Disk (SN MUNBB562)	Destructively Scrapped	Scrapped at new make due to damage at production, scrap ticket confirmed
14	FA94-2/8	CFM56-5A HPT Disk (SN GWNGR682)	Destructively Scrapped	Scrapped for end of life, scrap ticket confirmed
15	FA94-2/9	CFM56-5A HPT Disk (SN GWNGR683)	Destructively Scrapped	Scrapped for end of life, scrap ticket confirmed
16	FA94-3/1	CFM56 HPT Disk	Destructively Scrapped	Scrapped for end of life, scrap ticket confirmed
17	FA94-3/2	CFM56-7B HPT Disk (SN GWNGR535)	Scrapped but not destroyed yet	Sent to GE for inspection. ECI: slot bottom, bore, and web. ECI boltholes - not applicable (NA). UTI: circular shear and high resolution. No anomalies
18	FA94-3/3	CFM56-5C HPT Disk	Destructively Scraped	Scrap ticket confirmed, scrapped for end of life
19	FA94-3/4	CFM56-7B HPT Disk (SN GWNGR537)	Scrapped but not destroyed yet	Sent to GE for inspection. ECI: slot bottom, bore, and web. ECI boltholes - NA. UTI: circular shear and high resolution. No anomalies
20	FA94-3/5	CFM56-7B HPT Disk	Destructively Scraped	Scrap ticket confirmed, scrapped for end of life
21	FA94-3/6	CFM56-5B HPT Disk (SN GWNGR539)	Installed/In-service Engine/disk removed	Removed and sent to GE for inspection. ECI: slot bottom, bore, & web. ECI bolt holes - NA. UTI: circular shear and high resolution. No anomalies
22	FA94-3/7	CFM56-5C HPT Disk	Destructively Scraped	Scrap ticket confirmed, scrapped for end of life
23	FA94-4/1	CFM56-5C HPT Disk (SN GWNGR541)	On the shelf as a spare	Sent to GE for inspection. ECI: slot bottom, bore, and web. ECI boltholes - NA. UTI: circular shear and high resolution. No anomalies
24	FA94-4/2	CFM56-7B HPT Disk	Destructively Scrapped	Scrapped for end of life, scrap ticket confirmed
25	FA94-4/3	CFM56-7B HPT Disk	Destructively Scrapped	Scrapped for end of life, scrap ticket confirmed
26	FA94-4/4	CFM56-5B HPT Disk	Destructively Scrapped	Scrapped for end of life, scrap ticket confirmed
27	FA94-4/5	CFM56-5B HPT Disk	Believed Scrapped	Scrap ticket NOT found, will be added to CFM SB 72-0088 ENGINE - General - (72-00-00) Accident Involved Hardware Service Bulletin for critical parts that are no longer serviceable.
28	FA94-4/6	CFM56-5B HPT Disk	Destructively Scraped	Scrapped for end of life, scrap ticket confirmed
29	FA94-4/7	CFM56-5B HPT Disk	Destructively Scraped	Scrapped for end of life, scrap ticket confirmed
30	FA94-4/8	CFM56-5B HPT Disk	Destructively Scraped	Scrapped for end of life, scrap ticket confirmed
31	FA94-5/1	CF6-80C2 Spool Aft Shaft (SN GWNBJ275)	Installed/In-service Engine/disk removed	Part Removed and sent to GE for inspection. ECI slot bottom & boltholes - NA. ECI bore/web, and UTI circular shear and high resolution. No anomalies
32	FA94-5/2	CF6-80C2 LPT Disk	Believed Scrapped	Operator records show that this disk was retired for life limit & was sold to a reputable aviation scrap metal dealer for destructive reclamation. The dealer was subsequently acquired by another company who was contacted but could not produce the scrap tag. Scrap ticket NOT found. Note that this is a low energy LPT disk. This part will be added to GE SB 72-0785 ENGINE - General - (72-00-00) Accident

TABLE 6: MASTER HEAT FA94 PARTS STATUS				▮ Black – Scrapped ▮ Red – Event disk separation ▮ Green – Non-Flying, land/marine power generation ▮ Yellow – Sent to GE for Inspection
Forging	Heat Lot/ Mult No.	Configuration (Serial Number)	Before AA Disk Separation Event Status	After AA Disk Separation Event Status
				Involved Hardware for critical parts that are no longer serviceable.
33	FA94-5/3	LM2500 HPC Aft Spool		Not removed for inspection
34	FA94-5/4	LM2500 HPC Aft Spool		Not removed for inspection
35	FA94-5/5	LM2500 HPC Aft Spool		Not removed for inspection
36	FA94-5/6	LM6000 HPC Aft Spool		Not removed for inspection

CHART 1: MASTER HEAT FA94 PARTS STATUS

6.2   MAINTENANCE MANUAL CHANGES

GE will add enhanced UTI to the CF6-80C ESM GEK92451 for both the HPT stage 1 and stage 2 disks; Chapter/Section/Subject 72-53-02 for the HPT stage 1 disk and 72-53-06 for the HPT stage 2 disk. The inspection is to be performed when the HPT disks are at the piece part level. The incremental change to the ESM is planned for release by the end of June 2017 and will be immediately available electronically on the GE Customer Web Center after issuance.

HPT stage 1 and 2 disk scan plans call for using a 45º and 65º shear wave scan for the bore, forward and aft faces, the forward and aft transition faces, and the aft web (web thickness is sufficient to allow for full penetration from one side); the bore would get an additional radial longitudinal scan. GE developed the scan plan for the HPT stage 2 disk while inspecting disk SN MUNBB571 from Master Heat FA94; this disk was returned to GE for inspection. The scan plan for the HPT stage 1 disk already existed as part of SPM 70-32-09 titled *Immersion Ultrasonic Inspection of Engine Run Hardware* (See **FOOTNOTE 40** for additional details).

6.3   ALL OPERATORS WIRES/LETTERS

On October 28, 2016, the same day as the event, Boeing issued a Multi-Operator Message (MOM) Message number: MOM-MOM-16-0726-01B, informing all customers, field service bases, regional directors, customer resident representatives, and other selected organizations of the event. The MOM stated that the airplane had caught fire during the takeoff sequence, was stopped on the runway, all persons on board were evacuated with some injuries, and that the NTSB was leading the investigation and support was dispatched from GE, Boeing, and the FAA to assist.

On November 4, 2016, GE issued an All Operators Wire (AOW) to all CF6-80C2 operators informing them of the turbine disk uncontainment on October 28, 2016 at the O'Hare International Airport. The AOW informed operators that much of the HPT stage 2 disk was recovered, examination of the disk fracture surface revealed a material anomaly, additional work was ongoing to understand the anomaly, a related pool of potential suspect parts was being identified, and the NTSB was leading the investigation with support of GE, Boeing, and the operator. The AOW was immediately available electronically on the GE Customer Web Center after issuance.

6.4   SERVICE BULLETINS AND AIRWORTHINESS DIRECTIVES

GE is coordinating with the FAA to issue Category 5[42] SB 72-1562 for a specific subpopulation of CF6-80C2 HPT stage 1 and 2 disks. As previously mentioned, GE performed an extensive study on UTI indication rates from the mid-1990s to 2016 of their Inconel® alloy 718 suppliers. GE concluded that noticeable improvements in product cleanliness (fewer UTI indications) in the year 2000 and later were due to process improvements implemented prior to that time. Therefore, GE determined CF6-80C2 HPT disks produced from Inconel® alloy 718 prior to 2000 were deemed candidates for the UTI. Although **all** Inconel® alloy 718 triple-melt parts would have exhibited this same benefit in product cleanliness in the year 2000 and later, based on stress/volume and Continued Airworthiness Assessment Methodologies (CAAM)[43] assessments, the CF6-80C2 was the initial engine type from the CF6 series

---

[42] According to GE, a Category 5 means "Do as soon as the affected part is removed from the engine"; this does not drive engines off-wing or parts from engines.

[43] The FAA issued AC 39-8 titled *CONTINUED AIRWORTHINESS ASSESSMENTS OF POWERPLANT AND AUXILIARY POWER UNIT INSTALLATIONS OF TRANSPORT CATEGORY AIRPLANES* to establish guidance for estimating the risks associated with identified unsafe conditions; defining, prioritizing, and selecting suitable corrective actions for all identified

designated for UTI. Since HPT stage 2 disks used in the CF6-80C2 engine can also be used on the CF6-80A (dual certificated), GE plans to issue Category 5 SB 72-0869 with the same inspection requirements (UTI) and subpopulation (disks produced before the year 2000) as planned for SB 72-1562 to capture the entire populations of HPT stage 2 disks. GE anticipates that SBs 72-1562 and 72-0869 will be released by the end of June 2017 and August 2017, respectively. The SBs will be immediately available electronically on the GE Customer Web Center after issuance. The FAA is evaluating issuing ADs mandating the intent of the GE SB 72-1562 and SB 72-0869, to ultrasonically inspect all CF6-80C2 HPT stage 1 and 2 disks produced before the year 2000 and all CF6-80A HPT stage 2 disks produced before the year 2000.

Parts for the CFM56 engine are also made from Inconel® alloy 718 but since CFM56 engines tend to accumulate cycles at a much higher rate than the CF6 engine, there are considerably fewer potential CFM56 disks produced prior to the year 2000 that are still in service compared to the CF6. GE is working with the FAA Engine Certification Office (ECO) to determine the appropriateness of additional inspections for the CFM56 fleet and the fleets of other GE and CFM engine models; other original equipment manufacturer (OEM) engine models with Inconel® alloy 718 may also be candidates for inspection. Further agency and industry study is required to determine the best path forward for the engine models of all OEMs.

7.0   TRAJECTORY ANALYSIS

Uncontained engine failures can never be totally eliminated; therefore, the FAA provides regulations and guidance on how engine and airframe manufacturers should try to prevent, mitigate, and address engine uncontained failures when they occur. When considering an uncontained engine event, the failure event is divided into two major phases/categories; the first being the actual failure event, internal engine debris that can be released from the engine, and the second being the effect that the released debris has on the engine, airframe, and occupants on board and the ability for a safe landing.

14 *CFR* Part 33-AIRWORTHINESS STANDARDS: AIRCRAFT ENGINES address the issue of uncontained engine debris in two separate sections §33.19 (*Durability*) and §33.94 (*Blade containment and rotor unbalance tests*); however, the engine regulations pertain mainly to a blade release and not to rotor burst. The engine casings are incapable of containing a rotor burst due to the large amount of energy involved with this type of event. Therefore, to address rotor burst events, the FAA looks to the airframer, in this case Boeing, to design the aircraft to minimize the hazards to the airplane and the occupants on board.

According to the airplane's FAA Type Certificate Data Sheet (TCDS) A1NM, Revision 35, dated June 20, 2016, the Boeing Model 767-300 was certified on September 22, 1986. Uncontained engine debris at that time was addressed in 14 *CFR* Part 25-AIRWORTHINESS STANDARDS: TRANSPORT CATEGORY AIRPLANES section §25.903 (*Engines*) subsection §25.903(d)(1) that stated: "*Design precautions must be taken to minimize the hazards to the airplane in the event of an engine rotor failure or of a fire originating within the engine which burns through the engine case*". The FAA issued ACs[44] to:

> Provides guidance such as methods, procedures, and practices acceptable to the Administrator for complying with regulations and grant requirements. ACs may also contain explanations of regulations, other guidance material, best practices, or information useful to the aviation community. They do not create or change a regulatory requirement.

unsafe conditions; and verifying that the corrective actions were effective. The AC is intended to present a tangible means of logically assessing and responding to the safety risks posed by unsafe conditions.

[44] The AC system became effective in 1962. It provides a single, uniform, agency-wide system that the FAA uses to deliver advisory material to FAA customers, industry, the aviation community, and the public.

However, at the time that the Boeing 767-300 was type certificated in 1986, no AC existed to provide guidance on how to comply with §25.903(d)(1). Instead FAA Order 8110.11, *Design Considerations for Minimizing Damage Caused by Uncontained Aircraft Turbine Engine Rotor Failures*, published in 1975, was in effect (FAA Order 8110.11 has been subsequently cancelled) and outlines some of the means found acceptable for minimizing effects of damage caused by uncontained rotor failures. Sections 5 and 6 of the order provide design considerations for critical systems (including fuel systems) to minimize the damage that can be caused by uncontained engine debris (See Airworthiness Group Chairman's' Factual Report for this accident for additional information on the airplane certification requirements).

On March 9, 1988, after certification of the Boeing 767-300, the FAA issued AC 20-128 titled *Design Considerations for Minimizing Hazards Caused by Uncontained Turbine Engine and Auxiliary Power Unit Rotor Failure.* AC 20-128 provided guidance on the methods for compliance "…pertaining to design precautions taken to minimize hazards to the airplane and persons on board in the event of an uncontained[45] engine failure…" and defines fragment spread angles (**FIGURE 25**), based on historical engine failure events, that the designer should mitigate hazards within the defined impact damage zone. Following the 1989 United Airlines DC-10-10 airplane accident in Sioux City Iowa, the NTSB issued Safety Recommendation A-90-170 that states:

> The NTSB recommends that the Federal Aviation Administration: analyze the dispersion pattern, fragment size and energy level of released engine rotating parts from the July 19, 1989, Sioux City, Iowa, DC-10 accident and include the results of this analysis, and any other peripheral data available, in a revision of AC 20-128 for future aircraft certification.

Based on that NTSB Safety Recommendation, the FAA revised AC 20-128 and on March 25, 1997 issued AC 20-128A; the fragment spread angles (**FIGURE 25**) remained the same from AC 20-128. For a rotor burst event, the expectation is for the airframer to account for large disk fragments, such as fragments 'A' and 'B' in **PHOTO 46,** to exit the engine at a ±3° angle fore and aft from the center of the plane of rotation and for smaller disk fragments, such as fragments 'C' and 'D' in **PHOTO 46,** to exit the engine at a ±5° fore and aft from the center of the plane of rotation. These are the same fragment exit trajectories that were specified in FAA Order 8110.11. The AC also provides allowance for an "alternate engine failure model" to be used to assess the single large one-third piece of disk having a fragment spread angle of ±5°. Boeing has used this alternate, more conservative, model for their rotor burst assessment.

---

[45] According to AC 20-128 and 20-128A, uncontained failure is defined as: "For the purpose of airplane evaluations in accordance with this AC, uncontained failure of a turbine engine is any failure which results in the escape of rotor fragments from the engine or APU that could result in a hazard. Rotor failures which are of concern are those where released fragments have sufficient energy to create a hazard to the airplane."
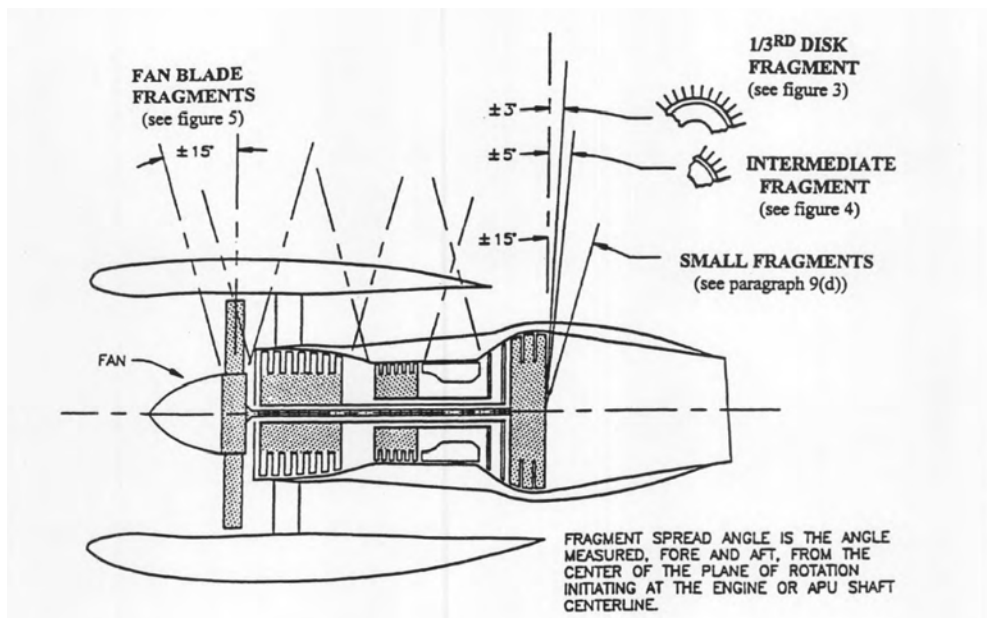
FIGURE 25: FRAGMENT SPREAD ANGLE EXCERPTED FROM FAA AC 20-128A

Boeing performed a trajectory analysis to estimate the exit angle for the disk fragment that departed the engine inboard and penetrated through the right wing (**FIGURES 26** and **27**). The result of the analysis estimated that the disk fragment exited the engine at about 4.3° aft of the HPT stage 2 disk rotation plane and that the fragment passed over the fuselage.
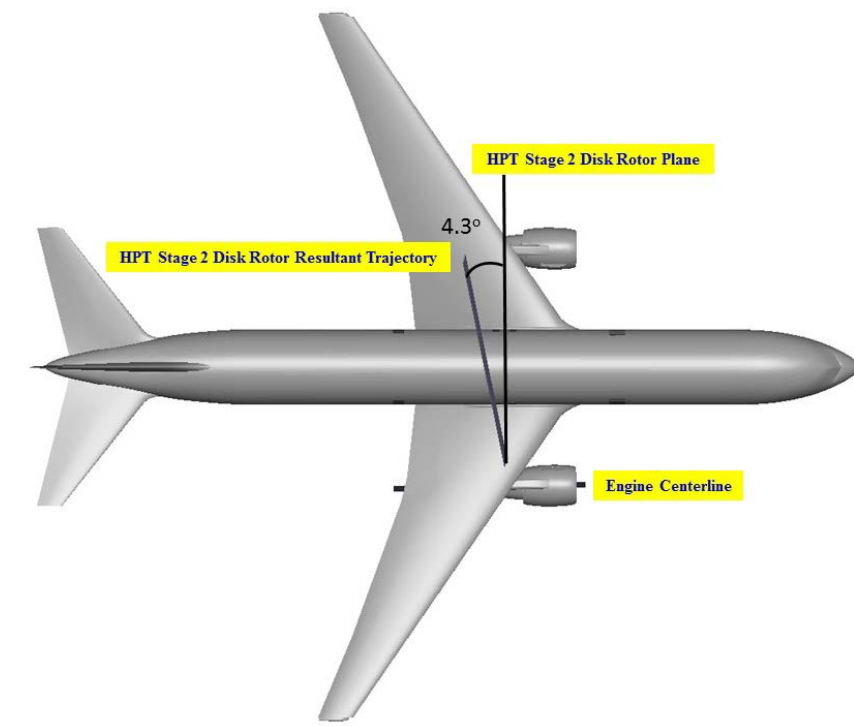

FIGURE 26: HPT STAGE 2 DISK FRAGMENT EXIT TRAJECTORY THROUGH INBOARD RIGHT WING
(TOP VIEW)

FIGURE COURTESY OF BOEING

FIGURE 27: HPT STAGE 2 DISK FRAGMENT EXIT TRAJECTORY THROUGH INBOARD RIGHT WING
(FORWARD LOOKING AFT)

FIGURE COURTESY OF BOEING

Jean-Pierre Scarfo
Aerospace Engineer
Powerplant Lead

REFERENCES

Aerospace Industries Association Rotor Manufacturing Project (RoMan) Report. October 24, 2002. *Guidelines to Minimize Manufacturing Induced Anomolies in Critical Rotating Parts.* Washington, DC: Office of Aviation Research and Development.

AMG - Advanced Metallurgical Group - Netherlands. n.d. "Electroslag Remelting (ESR)." *http://web.ald-vt.de/cms/vakuum-technologie/anlagen/electroslag-remelting-esr/.*

AMG - Advanced Metallurgical Group - Netherlands. n.d. "Vacuum Arc Remelting (VAR)." *http://web.ald-vt.de/cms/vakuum-technologie/anlagen/vacuum-arc-remelting-var/.*

ASM Handbook, Volumne 15: Casting. 2008. "Vacuum Induction Melting." In *Volume 15 Handbook Committee*, 1-8. ASM International.

CONSARC. n.d. "Electroslag Remelting Furnaces." *www.consarc.com/wp-content/uploads/sites/11/2014/12/esr.pdf.*

DiConza, Paul J., Ronald R. Biederman, and Rishi P. Singh. 1991. "Homogenization and Thermomechanical Process of Cast Alloy 718." *Superalloys 718,625,706 and Various Derivatives.* The Minerals, Metals & Materials Society, 1991. 161-171.

Domblesky, Joseph P., Rajiv Shivpuri, Taylan Altan. 1994. *A REVIEW OF RADIAL FORGING TECHNOLOGY INCLUDING PREFORM DESIGN FOR PROCESS OPTIMIZATION.* Contract Report from NSF Engineering Research Center for Net Shape Manufacturing, Ohio State University, Waterliet, New York: US Army Arment Research Dvelopment and Engineering Center.

DOT/FAA/AR-05/29. September 2005. *Inspection Development for Nickel Billet – Engine Titanium Consortium Phase II.* Washington, DC: Office of Aviation Research and Development.

DOT/FAA/AR-06/3. February 2006. *Guidelines to Minimize Manufacturing Induced Anomolies in Critical Rotating Parts.* Washington, DC: Office of Aviation Research and Development.

DOT/FAA/AR-07/13. April 2008. *Turbine Rotor Material Design - Phase II.* Washington, DC: Office of Aviation Research.

Iowa State University Center for Nondestructive Evaluation. n.d. "Phased Arrays." *https://www.cnde.iastate.edu/research/ultrasonic/phased-arrays/.*

Jackman, Laurence A, Gernant E. Maurer, Sunil Widge. 1994. "White Spots in Superalloys." *Superalloys 718,625,706 and Various Derivatives.* The Minerals, Metals & Materials Society, 1994. 153-166.

Moyer, J.M, L. A. Jackman, C. B. Adasczik, R. M. Davis, and R. Forbes-Jones. 1994. "Advances in Triple Melting Superalloys 718, 706 and 720." *Superalloys 718,625,706 and Various Derivatives.* The Mineals, Metal & Materials Society, 1994. 39-48.

Nieters, Edward J., Robert S. Gilmore, Robert C. Trzaskos, John D. Young, David C. Copley, Patrick J. Howard, Michael E. Keller, and William J. Leach. 1995. "A Multizone Technique for Billet Inspection." *Review of Progress in Quantitative Nondestructive Evaluation, Vol 14.* New York: Plenum Press. 2137-2144.

Schafrik, Robert E., Douglas D. Ward, and Jon R. Groh. 2001. "Application of Alloy 718 in GE Aircraft Engines: Past, Present and Next Five Years." *Superalloys 718,625,706 and Various Derivatives.* TMS (The Minerals, Metals & Materials Society), 2001. 1-11.

Schirra, John J., Robert H. Caless, and Robert W. Hatala. 1991. "The Effects of Laves Phase on the Mechanical Properities of Wrought and Cast + HIP Inconel 718." *Superalloys 718,625,706 and Various Derivatives.* The Minerals, Metals & Materials Society, 1991. 375-388.